Online ISSN : 2249-4626
Print ISSN : 0975-5896
DOI : 10.17406/GJSFR

Global Journal

of Science Frontier Research: F

Mathematics and Decision Science

Some Bicomplex Modules

Improved Korteweg De Vries

Highlights

Propagation of Gravity Waves

Symmetric Metric S-Connection

Discovering Thoughts, Inventing Future

VOLUME 16 ISSUE 3 VERSION 1.0

Global Journal of Science Frontier Research: F
Mathematics & Decision Sciences

Global Journal of Science Frontier Research: F
Mathematics & Decision Sciences

Volume 16 Issue 3 (Ver. 1.0)

Open Association of Research Society

Incorporation No.: 0423089
License No.: 42125/022010/1186
Registration No.: 430374
Import-Export Code: 1109007027
Employer Identification Number (EIN):
USA Tax ID: 98-0673427

Global Journals Inc.

*(A Delaware USA Incorporation with "Good Standing"; **Reg. Number: 0423089**)*

Sponsors: Open Association of Research Society
Open Scientific Standards

Publisher's Headquarters office

Global Journals® Headquarters
945th Concord Streets,
Framingham Massachusetts Pin: 01701,
United States of America
USA Toll Free: +001-888-839-7392
USA Toll Free Fax: +001-888-839-7392

Offset Typesetting

Global Journals Incorporated
2nd, Lansdowne, Lansdowne Rd., Croydon-Surrey,
Pin: CR9 2ER, United Kingdom

Packaging & Continental Dispatching

Global Journals
E-3130 Sudama Nagar, Near Gopur Square,
Indore, M.P., Pin:452009, India

Find a correspondence nodal officer near you

To find nodal officer of your country, please email us at *local@globaljournals.org*

eContacts

Press Inquiries: *press@globaljournals.org*
Investor Inquiries: *investors@globaljournals.org*
Technical Support: *technology@globaljournals.org*
Media & Releases: *media@globaljournals.org*

Pricing (Including by Air Parcel Charges):

For Authors:
22 USD (B/W) & 50 USD (Color)
Yearly Subscription (Personal & Institutional):
200 USD (B/W) & 250 USD (Color)

Integrated Editorial Board
(Computer Science, Engineering, Medical, Management, Natural Science, Social Science)

Dr. Bart Lambrecht
Director of Research in Accounting and Finance Professor of Finance
Lancaster University Management School
BA (Antwerp); MPhil, MA, PhD (Cambridge)

Dr. Carlos García Pont
Associate Professor of Marketing
IESE Business School, University of Navarra
Doctor of Philosophy (Management), Massachusetts Institute of Technology (MIT)
Master in Business Administration, IESE, University of Navarra
Degree in Industrial Engineering, Universitat Politècnica de Catalunya

Dr. Fotini Labropulu
Mathematics - Luther College
University of Regina Ph.D., M.Sc. in Mathematics
B.A. (Honors) in Mathematics
University of Windso

Dr. Lynn Lim
Reader in Business and Marketing
Roehampton University, London
BCom, PGDip, MBA (Distinction), PhD, FHEA

Dr. Mihaly Mezei
ASSOCIATE PROFESSOR
Department of Structural and Chemical Biology, Mount Sinai School of Medical Center
Ph.D., Etvs Lornd University
Postdoctoral Training,
New York University

Dr. Söhnke M. Bartram
Department of Accounting and Finance Lancaster University Management School Ph.D. (WHU Koblenz)
MBA/BBA (University of Saarbrücken)

Dr. Miguel Angel Ariño
Professor of Decision Sciences
IESE Business School
Barcelona, Spain (Universidad de Navarra)
CEIBS (China Europe International Business School).
Beijing, Shanghai and Shenzhen
Ph.D. in Mathematics
University of Barcelona
BA in Mathematics (Licenciatura)
University of Barcelona

Philip G. Moscoso
Technology and Operations Management
IESE Business School, University of Navarra
Ph.D in Industrial Engineering and Management, ETH Zurich
M.Sc. in Chemical Engineering, ETH Zurich

Dr. Sanjay Dixit, M.D.
Director, EP Laboratories, Philadelphia VA Medical Center
Cardiovascular Medicine - Cardiac Arrhythmia
Univ of Penn School of Medicine

Dr. Han-Xiang Deng
MD., Ph.D
Associate Professor and Research Department Division of Neuromuscular Medicine
Davee Department of Neurology and Clinical Neuroscience Northwestern University Feinberg School of Medicine

Dr. Pina C. Sanelli
Associate Professor of Public Health
Weill Cornell Medical College
Associate Attending Radiologist
NewYork-Presbyterian Hospital
MRI, MRA, CT, and CTA
Neuroradiology and Diagnostic Radiology
M.D., State University of New York at Buffalo,School of Medicine and Biomedical Sciences

Dr. Roberto Sanchez
Associate Professor
Department of Structural and Chemical Biology
Mount Sinai School of Medicine
Ph.D., The Rockefeller University

Dr. Wen-Yih Sun
Professor of Earth and Atmospheric Sciences Purdue University Director National Center for Typhoon and Flooding Research, Taiwan
University Chair Professor
Department of Atmospheric Sciences, National Central University, Chung-Li, TaiwanUniversity Chair Professor
Institute of Environmental Engineering, National Chiao Tung University, Hsin-chu, Taiwan.Ph.D., MS The University of Chicago, Geophysical Sciences
BS National Taiwan University, Atmospheric Sciences
Associate Professor of Radiology

Dr. Michael R. Rudnick
M.D., FACP
Associate Professor of Medicine
Chief, Renal Electrolyte and Hypertension Division (PMC)
Penn Medicine, University of Pennsylvania
Presbyterian Medical Center, Philadelphia
Nephrology and Internal Medicine
Certified by the American Board of Internal Medicine

Dr. Bassey Benjamin Esu
B.Sc. Marketing; MBA Marketing; Ph.D Marketing
Lecturer, Department of Marketing, University of Calabar
Tourism Consultant, Cross River State Tourism Development Department
Co-ordinator, Sustainable Tourism Initiative, Calabar, Nigeria

Dr. Aziz M. Barbar, Ph.D.
IEEE Senior Member
Chairperson, Department of Computer Science
AUST - American University of Science & Technology
Alfred Naccash Avenue – Ashrafieh

Contents of the Issue

Global Journal of Science Frontier Research: F
Mathematics and Decision Sciences
Volume 16 Issue 3 Version 1.0 Year 2016
Type : Double Blind Peer Reviewed International Research Journal
Publisher: Global Journals Inc. (USA)
Online ISSN: 2249-4626 & Print ISSN: 0975-5896

Effects of Nonisothermality and Wind-Shears on the Propagation of Gravity Waves (I): Comparison between *Hines*' Model and WKB Approach

By J. Z. G. Ma
California Institute of Integral Studies, United States

Abstract- In the presence of the vertical temperature & wind-speed gradients, we extend *Hines*' isothermal and shear-free model to calculate the vertical wavenumber (m_r) and growth rate (m_i) of gravity waves propagating in a stratified, non-isothermal, and wind-shear atmosphere. The profiles obtained from the extended Hines' model are compared with those from the Wentzel-Kramers-Brillouin (WKB) approach up to 300 km altitude. The empirical neutral atmospheric and wind models (NRLMSISE-00 and HWM93) are used to obtain the vertical profiles of the mean-field properties and the zonal/meridional winds.

GJSFR-F Classification : *MSC 2010: 76B15*

Strictly as per the compliance and regulations of :

Notes

Effects of Nonisothermality and Wind-Shears on the Propagation of Gravity Waves (I): Comparison between *Hines*' Model and WKB Approach

J. Z. G. Ma

Abstract- In the presence of the vertical temperature & wind-speed gradients, we extend *Hines'* isothermal and shear-free model to calculate the vertical wavenumber (m_r) and growth rate (m_i) of gravity waves propagating in a stratified, non-isothermal, and wind-shear atmosphere. The profiles obtained from the extended *Hines'* model are compared with those from the Wentzel-Kramers-Brillouin (WKB) approach up to 300 km altitude. The empirical neutral atmospheric and wind models (NRLMSISE-00 and HWM93) are used to obtain the vertical profiles of the mean-field properties and the zonal/meridional winds. Results show that (1) relative to the WKB model, extended *Hines'* m_i -profile deviates further away from *Hines'* model due to the lack of the non-isothermal effect; (2) the m_r-profiles obtained from both the extended *Hines'* and WKB models superimpose upon each other, and amplify *Hines'* m_r- magnitude; (3) the extended *Hines'* model provides identical perturbations for all physical quantities (i.e., pressure, density, temperature, wind components) which diverge the most from *Hines'* model in the 100-150 km layer; while the WKB model presents respective growths for different parameters, however, with the same vertical wavelengths which is not constant; and, (4) with the increase of phase speed (C_{ph}), while Hines' m_i - profile kee ps constant, the m_i-profiles of the extended Hines' and WKB models drop down and soars up, respectively; by contrast, the m_r-profiles of the three models fall off monotonously when C_{ph}/C (where C is sound speed) is no more than 0.75, but the profiles of the extended *Hines'* and WKB models overlap upon each other below 0.6, which shift away from *Hines'* model.

I. Introduction

Atmospheric thermal structure and background winds substantially influence the propagation of gravity waves in regions where thermal and/or Doppler ducting is confirmed either theoretically (e.g., *Pitteway & Hines* 1965; *Wang & Tuan*, 1988; Hickey 2001; *Walterscheid et al.* 2001; *Snively & Pasko* 2003; *Yu & Hickey* 2007a,b,c) or experimentally (e.g., *Hines & Tarasick* 1994; *Taylor et al.* 1995; *Isler et al.* 1997; *Walterscheid et al.* 1999; *Hecht et al.* 2001; *Liu & Swenson* 2003; *She et al.* 2004; *Snively et al.* 2007; *She et al.* 2009). The vertical variations in temperature and zonal/medidional wind shears have therefore become the two dominant factors and received increasing attentions in the transport, reflection, refraction, dissipation, and evanescence of gravity waves propagating in atmosphere. Accordingly, *Hines* (1960)'s locally isothermal, shear-free gravity wave theory with the WKB approximation has been extended by previous authors to ob-

Author: California Institute of Integral Studies, San Francisco, CA, USA. e-mail: zma@mymail.ciis.edu

tain generalized dispersion relations for accommodating to more complicated atmospheric situations.

Einaudi & *Hines* (1971) formulated an anelastic dispersion relation that includes the thermal and homogeneous wind effects, nevertheless in the absence of vertical wind shears, with the same growth rate (m_i) but an updated vertical wave number square (m_r^2) from *Hines'* formula ($m_{r\text{Hines}}^2$), expressed by

$$m_i = -\frac{1}{2H} \; ; \quad m_{r\text{Hines}}^2 = \frac{\Omega^2 - \omega_a^2}{C^2} + k_h^2 \frac{\omega_b^2 - \Omega^2}{\Omega^2} \quad \Rightarrow \quad m_r^2 = \frac{\Omega^2 - \omega_a^2}{C^2} + k_h^2 \frac{\omega_B^2 - \Omega^2}{\Omega^2} \quad (1)$$

where $\Omega = \omega - \mathbf{k}_h \cdot \mathbf{v}_0$ is the intrinsic (or, Doppler-shifted) angular frequency, ω is the extrinsic (ground-based) frequency, $\mathbf{k}_h$ is the horizontal wavenumber vector, $\mathbf{v}_0$ is the horizontal mean-field wind vector, $C = \sqrt{\gamma g H}$ is the sound speed in which γ is the adiabatic index, g is the gravitational acceleration, and, H is Hines' scale-height, ω_B is the non-isothermal Brunt-Väisälä buoyancy frequency, and ω_a is the isothermal acoustic-cutoff frequency. The thermal effect is given in the definition of ω_B with $\omega_B^2 = \omega_b^2 + g k_T$ [in which $\omega_b^2 = (1-1/\gamma)(g/H)$ is Hines' isothermal buoyancy frequency, and $k_T = (\mathrm{d}H/\mathrm{d}z)/H$ is the thermal inhomogeneous number], and the wind effect is implicitly involved in Ω. Note that Eq.(1) is an extended *Hines* (1960)' expression which recovers his original windless result for $k_T = 0$ and $\mathbf{v}_0 = 0$. The last $\Omega - m_r$ dispersion equation in Eq.(1) is widely used in gravity wave studies as *Hines'* locally isothermal and shear-free model.

Later, *Gossard* & *Hooke* (1975) introduced the structure and behavior of the highest-frequency gravity waves in the mesosphere. The result was the same as Eq.(1) but without the first term. By considering the Coriolis parameter (*Eckart* 1960), Marks & Eckermann (1995) and *Eckermann* (1997) updated Eq.(1) to expose the effect of the Earth's rotation effect, as well as wave refraction, saturation, and turbulent damping via ray-tracing mapping. *Vadas* & *Fritts* (2004,2005) adopted Hines' isothermal model to examine the influence of dissipation terms, like kinematic viscosity and thermal diffusivity, and derived a complex dispersion relation and GW damping rate arising from mesoscale convective complexes in the thermosphere. Note that in the last formula of Eq.(1), the thermal effect is present in ω_B, but missing in ω_a. Besides, these studies did not take into consideration the wind-shear effect (i.e., $\omega_{\mathrm{v}} = |\mathrm{d}\mathbf{v}_0/\mathrm{d}z|$), but assuming a uniform background horizontal wind.

The role played by shears in gravity wave propagation was dominantly recognized at first through discussions of linear instabilities in a 2D, stably-stratified, horizontal shear flows of an ideal Boussinesq fluid (*Miles* 1961; *Howard* 1961), as well as of the onset of atmospheric turbulence (e.g., *Hines* 1971; *Dutton* 1986). It was found that the isothermal (gradient) Richardson number, $Ri = \omega_b^2/\omega_{\mathrm{v}}^2$, has a critical value, $Ri_c = 1/4$. If $Ri > Ri_c$, flows are stable everywhere; however, this criterion may not rigorously apply for all scenarios, but as a necessary, not sufficient condition for instabilities (*Stone* 1966; *Miles* 1986), particularly when, e.g., the shear is tilted from zenith (*Sonmor* & *Klaassen* 1997), or, when the molecular viscosity is important (*Liu* 2007). Even for all arbitrarily large values of Ri, a family of explicit, elementary, stably-stratified, time-dependent, and non-parallel

flows was verified to be unstable (*Majda* & *Shefter* 1998). A growing body of experimental and observational data also indicated that turbulence survives $Ri \gg 1$ (*Galperin et al.* 2007). Notwithstanding the above, there has been no such a dispersion relation of gravity waves which is derived to get Ri and Ri_c directly by solving the linear fluid equations under the WKB approximation.

Notes

Fortunately, sheared atmosphere had already been studied for tens of years before *Hines* (1960)'s WKB work. A special treatment was adopted to the perturbation of fluid equations in an incompressible atmosphere ($\gamma \to \infty$): linear wavelike solutions are assumed in time and horizontal coordinates, with ω, k_h, and the mean-field state varying neither in time nor in the horizontal plane. As such the perturbed vertical profiles of bulk properties are obtained in view of the vertical variation in the background temperature and horizontal velocity (*Taylor* 1931; *Goldstein* 1931; see a review by *Fritts* & *Alexander* 2003). This approach has now been developed fully numerically as a generalized full-wave model (FWM) to treat the propagation of non-hydrostatic, linear gravity waves in a realistic compressible, inhomogeneous atmosphere which is dissipative due to not only the eddy processes in the lower atmosphere but also the molecular processes (viscosity, thermal conduction and ion drag) in atmosphere, in addition to the altitude-dependent mean-field temperature and horizontal winds, as well as Coriolis force (Hickey 2011; Hickey et al. 1997,1998,2000,2001,2009,2010; *Walterscheid* & *Hickey* 2001,2005,2012; *Schubert et al.* 2003,2005). Importantly, the WKB approach has been employed to yield a Taylor-Goldstein equation or a more generalized quadratic equation and the non-isothermal and shearing effects can be obtained in the presence of the height-varying temperature and wind shears (see, e.g., *Beer* 1974; Nappo 2002; *Sutherland* 2010). The most recent contribution was performed by *Zhou* & *Morton* (2007). Upon the background gradient properties of the atmosphere, the authors found that the vertical wavenumber depends only on the intrinsic horizontal phase speed ($C_{ph} = \Omega/k_h$). Unfortunately, the generalized dispersion equation is unable to restore Eq.(1) due to some algebra inconsistencies.

we are inspired to concentrate on the exact expressions of the dispersion relation obtained by extending *Hines'* model and by adopting the WKB approximation. The purpose lies in describing the features of gravity wave propagation in a compressible and non-isothermal atmosphere in the presence of atmospheric wind shears. The motivation to tackle this subject is the necessity to find an accurate gravity wave model in data-fit modeling to demonstrate the modulation of waves excited by natural hazards (like, tsunami/vocano events, nuclear explosion, etc.) in realistic atmosphere. The region concerned is from the sea level to ∼200 km altitude within which the atmosphere is non-dissipative (negligible viscosity and heat conductivity) and the ion drag and Coriolis force can be reasonably omitted (*Harris* & *Priester* 1962; *Pitteway* & *Hines* 1963; *Volland* 1969a,b). The structure of the paper is as follows: Section 2 extends *Hines'* model, Eq.(1), by involving the nonthermaility and wind-shears in the dispersion relation. Section 3 gives a generalized dispersion relation by employing the WKB approach. Section 4 compares the two models and illustrates their deviations from *Hines'* isothermal and shear-free model. Section 5 offers a summary and conclusion. In the study, the mean-field properties up to 300 km

altitude are obtained from the empirical neutral atmospheric model (NRLMSISE-00; *Picone et al.* 2002) and the horizontal wind model (HWM93; *Hedin et al.* 1996). We choose a Cartesian frame, $\{\hat{\mathbf{e}}_x, \hat{\mathbf{e}}_y, \hat{\mathbf{e}}_z\}$, where $\hat{\mathbf{e}}_x$ is horizontally due east, $\hat{\mathbf{e}}_y$ due north, and $\hat{\mathbf{e}}_z$ vertically upward.

II. Extended Hines' Model: Dispersion Relation

Up to ∼200 km altitude, the neutral atmosphere can be considered non-dissipative with negligible eddy process, molecular viscosity and thermal conduction, ion-drag, and Coriolis effect (*Harris & Priester* 1962; *Pitteway & Hines* 1963; *Volland* 1969a,b). The governing non-hydrostatic and compressible equations to describe gravity waves are based on conservation laws in mass, momentum, and energy, as well as the equation of state (e.g., *Beer* 1974; *Fritts & Alexander* 2003; *Zhou & Morton* 2007; for a complete set of equations including dissipative terms, see, e.g., *Landau & Lifshitz* 1959; *Volland* 1969a; *Francis* 1973; *Hickey & Cole* 1987; *Vadas & Fritts* 2005; *Liu et al.* 2013):

$$\frac{D\rho}{Dt} = -\rho\nabla\cdot\mathbf{v}, \quad \frac{D\mathbf{v}}{Dt} = -\frac{1}{\rho}\nabla p + \mathbf{g}, \quad \frac{Dp}{Dt} = -\gamma p\nabla\cdot\mathbf{v}, \quad p = \rho R_s T \tag{2}$$

in which $\mathbf{v}$, ρ, p, and T are the atmospheric velocity, density, pressure, and temperature, respectively; $D/Dt = \partial/\partial t + \mathbf{v}\cdot\nabla$ is the substantial derivative over time t; $\mathbf{g} = \{0, 0, -g\}$ is the gravitational acceleration; and γ and R_s are the adiabatic index and gas constant, respectively. The vertical profiles of Hines' scale height H, and these three input parameters, γ, g, and R_s, are given in Fig.1, where two additional scale heights, H_ρ (in density) and H_p (in pressure), are also shown for comparisons with H, the definitions of which are given below in Eq.(4).

Acoustic-gravity waves originate from the small perturbations away from their mean-field properties and propagate in a stratified atmosphere (*Gossard & Hooke* 1975). We linearize Eq.(2) by employing

$$\left.\begin{array}{l} \rho = \rho_0 + \rho_1, T = T_0 + T_1, p = p_0 + p_1 \\ \mathbf{v} = \mathbf{v}_0 + \mathbf{v}_1 = \{U, V, 0\} + \{u, v, w\} \\ \left(\frac{\rho_1}{\rho_0}, \frac{p_1}{p_0}, \frac{T_1}{T_0}, \frac{u}{U}, \frac{v}{V}, w\right) \propto e^{i(\mathbf{k}\cdot\mathbf{r}-\omega t)} \end{array}\right\} \tag{3}$$

where parameters attached by subscript "$_0$" are ambient mean-field components and those with subscript "$_1$" are the linearized quantities; U and V are the zonal (eastward) and meridional (northward) components of the mean-field wind velocity (note that the wind is horizontal and thus the vertical component W is zero), respectively; (u, v, w) are the three components of the perturbed velocity, respectively; $\mathbf{k} = \{k, l, m\}$ in which k and l are the two horizontal wavenumbers which are constants, constituting a horizontal wave vector $\mathbf{k}_h = \{k, l\} = k_h\mathbf{k}_{h0}$ with $k_h = \sqrt{k^2 + l^2}$ and $\mathbf{k}_{h0} = \mathbf{k}_h/k_h$, and, $m = m_r + im_i$ is the vertical wave vector which is a complex; and, ω is the extrinsic angular wave frequency which is a constant. The inhomogeneities of the mean-field properties bring about following altitude-dependent parameters:

$$k_\rho = \frac{1}{H_\rho} = \frac{\mathrm{d}(\ln\rho_0)}{\mathrm{d}z},\ k_p = \frac{1}{H_p} = \frac{\mathrm{d}(\ln p_0)}{\mathrm{d}z},\ k_T = \frac{\mathrm{d}(\ln T_0)}{\mathrm{d}z},\ \omega_\mathrm{v} = \sqrt{\left(\frac{\mathrm{d}U}{\mathrm{d}z}\right)^2 + \left(\frac{\mathrm{d}V}{\mathrm{d}z}\right)^2} \quad (4)$$

in which k_ρ, k_p, and k_T are the density, pressure, and temperature scale numbers, respectively, satisfying $k_T = k_p - k_\rho$ from the equation of state. Note that ω_v is the shear-related parameter in the unit of angular frequency, rad/s.

Notes

The linearization of Eq.(2) yields following set of perturbed equations:

$$\left.\begin{array}{l} \frac{\partial\rho_1}{\partial t} + \mathbf{v}_0\cdot\nabla\rho_1 + \mathbf{v}_1\cdot\nabla\rho_0 + \rho_0\nabla\cdot\mathbf{v}_1 + \rho_1\nabla\cdot\mathbf{v}_0 = 0 \\ \frac{\partial\mathbf{v}_1}{\partial t} + \mathbf{v}_1\cdot\nabla\mathbf{v}_0 + \mathbf{v}_0\cdot\nabla\mathbf{v}_1 = -\frac{1}{\rho_0}\nabla p_1 + \frac{\rho_1}{\rho_0}\mathbf{g} \\ \frac{\partial p_1}{\partial t} + \mathbf{v}_0\cdot\nabla p_1 + \mathbf{v}_1\cdot\nabla p_0 = -\gamma p_0\nabla\cdot\mathbf{v}_1 - \gamma p_1\nabla\cdot\mathbf{v}_0 \\ \frac{p_1}{p_0} = \frac{\rho_1}{\rho_0} + \frac{T_1}{T_0} \end{array}\right\} \quad (5)$$

which provides following dispersion equation:

$$\begin{bmatrix} \omega & k & l & m - ik_\rho & 0 \\ 0 & \omega & 0 & i\frac{\mathrm{d}U}{\mathrm{d}z} & k \\ 0 & 0 & \omega & i\frac{\mathrm{d}V}{\mathrm{d}z} & l \\ -ig & 0 & 0 & \omega & m - ik_p \\ 0 & k & l & m - i\frac{k_p}{\gamma} & \frac{\omega}{C^2} \end{bmatrix} \begin{bmatrix} \frac{\rho_1}{\rho_0} \\ u \\ v \\ w \\ \frac{p_1}{p_0} \end{bmatrix} = 0 \quad (6)$$

from which a generalized, complex dispersion relation of gravity waves is derived in the presence of non-isothermality and wind shears, if and only if the determinant of the coefficient matrix is zero:

$$\Omega^4 - \left(C^2K^2 + gk_T\right)\Omega^2 - (\gamma-1)gk_h\Omega V_{k1} + C^2k_h^2\omega_B^2 = i\gamma gm\Omega\left(\Omega - k_hHV_{k1}\right) \quad (7)$$

in which $\Omega = \omega - \mathbf{k}_h\cdot\mathbf{v}_0 = \omega - (kU + lV) = \omega - k_hV_k$ is the intrinsic (or, Doppler-shifted) angular frequency, $K^2 = k_h^2 + m^2$, $V_k = \mathbf{k}_{h0}\cdot\mathbf{v}_0 = \sqrt{U^2+V^2}\cos\theta$, and $V_{k1} = \mathbf{k}_{h0}\cdot(d\mathbf{v}_0/dz) = \omega_\mathrm{v}\cos\theta'$, where θ and θ' are the angles between the horizontal wave vector $\mathbf{k}_h$ and (1) the mean-field wind velocity $\mathbf{v}_0$, (2) the wind velocity gradient, respectively. Note that $\theta = \theta'$ if θ' is independent of z.

Because m is a complex, using $(m_r + im_i)$ instead of m in Eq.(7) produces the solutions of the dispersion relation:

$$m_i = \left(-\frac{1}{2}\quad \frac{1}{H} - \frac{V_{k1}}{C_{ph}}\right) \quad (8)$$

and

$$\Omega^4 - \left[C^2 \quad k_h^2 + m_r^2 - \frac{2-\gamma}{2\gamma}\frac{1}{H}\frac{V_{k1}}{C_{ph}}\right) + \omega_A^2\Big]\Omega^2 + C^2 k_h^2 \omega_B^2 \left(1 - \frac{\cos^2\theta'}{4R_I}\right) = 0 \qquad (9)$$

which can be expressed alternatively as follows:

$$m_r^2 = \frac{\Omega^2 - \omega_A^2}{C^2} + k_h^2 \frac{\omega_B^2 - \Omega^2}{\Omega^2} + \frac{1}{2}\frac{V_{k1}}{C_{ph}}\left(\frac{2-\gamma}{\gamma H} - \frac{1}{2}\frac{V_{k1}}{C_{ph}}\right) \qquad (10)$$

in which $C_{ph} = \Omega/k_h$ is the intrinsic horizontal phase speed, $\omega_A^2 = \omega_a^2 + gk_T$ is the nonisothermal acoustic-cutoff frequency, and $R_I = R_i + gk_T/\omega_{\rm v}^2$ is the nonisothermal (gradient) Richardson number.

The last equation in Eq.(3) reveals that the amplitude (denoted by A^* as follows) of all the perturbations grows exponentially by following the same growth:

$$A^* \propto e^{-m_i z} \text{ for } m_i \text{ independent of } z; A^* \propto e^{-\int m_i \mathrm{d}z} \text{ for } m_i \text{ dependent of } z \qquad (11)$$

Under shear-free conditions ($V_{k1} = 0$), Eq.(11) recovers the growth, $A(0)e^{z/2H}$, of Hines' classical result. Note that the temperature gradient, as represented by k_T, does not influence the amplitude growth; and, only in the presence of the shear can the horizontal phase speed (C_{ph}) come into play to modulate the growth.

Eq.(9) is a quadratic equation of Ω^2. It is easy to see that for small shear ($V_{k1}/HC_{ph} \ll m_r^2$) there exists a critical value of $R_{Ic} = \cos^2\theta'/4$. Note that the inclusion of θ' is consistent with the result shown in Hines (1971). If $R_I < R_{Ic}$, one solution of Ω^2 is negative and thus turbulence can be completely excluded; otherwise, if $R_I > R_{Ic}$, the two roots of Ω^2 are always positive and any turbulence is suppressed. Under isothermal condition, this nonisothermal result recovers the conclusion introduced by *Hines* (1971) and *Dutton* (1986) with $\theta' = 0$. However, if the shear is large enough, the coefficient of Ω^2 in Eq.(9) may be positive. On the one hand in this case, $R_I > R_{Ic}$ always leads to negative Ω^2 and turbulence is inevitably excited; on the other hand, $R_I < R_{Ic}$ gives one negative root of Ω^2, meaning turbulence can be developed. As a result, from our WKB dispersion relation, we confirm that the criterion of $R_{Ic} = 1/4$ is merely as a necessary but not sufficient condition for instabilities (*Stone* 1966; *Miles* 1986).

Eq.(10) makes us easier to identify the effects of nonisothermality and wind shear on the propagation of gravity waves by comparison with previous dispersion relations introduced in literature. First of all, by assuming $k_T = 0$ and $\mathbf{v}_0 = 0$, Hines (1960)'s dispersion relation for an isothermal and windless atmosphere is recovered, with $\omega_A \to \omega_a$, $\omega_B \to \omega_b$, and $V_{k1} \to 0$. Secondly, for a nonisothermal and windless atmosphere, *Einaudi* & *Hines* (1971)'s result as shown in Eq.(1) is produced, certainly after the correction of the erroneous isothermal cutoff frequency ω_a replaced by the nonisothermal ω_A. We stress here that, although Eq.(1) is widely used as the dispersion relation for nonisothermal atmosphere by almost all the previous authors in both theoretical modeling and data

analysis, the formula is not accurate because it has a wrong expression of the cutoff frequency, which leads to absurd result that buoyancy frequency can be larger than the cutoff frequency. We point out the buoyancy frequency can never be larger than the cutoff frequency for either an isothermal or nonisothermal case, and the accurate nonisothermal dispersion relation in an windless atmosphere is not Eq.(1), but as follows:

$$m_r^2 = \frac{\Omega^2 - \omega_A^2}{C^2} + k_h^2 \frac{\omega_B^2 - \Omega^2}{\Omega^2} \tag{12}$$

Notes

Lastly, Eq.(10) exposes that wind shear (V_{k1}) influences the vertical wave propagation always in combination with the intrinsic phase speed (C_{ph}), the same feature as that affecting the vertical amplitude growth rate in Eq.(8). Due to the fact that the inclusion of wind shear term in the dispersion relation of gravity waves has not been found in literature, we thus make use of the FWM approach to validate the wind-shear effect, as to be given in the next section.

III. WKB Approach

In the WKB approach, linear wavelike solutions are assumed in time and horizontal coordinates, however, not in the vertical direction; by contrast, the mean-field properties are supposed to vary only in the vertical direction. As a result, we follow Eq.(3) to linearize Eq.(2) by adopting

$$\left(\frac{\rho_1}{\rho_0},\ \frac{p_1}{p_0},\ \frac{T_1}{T_0},\ \frac{u}{U},\ \frac{v}{V}, w\right) \propto A(z) e^{i(\mathbf{k}_h \cdot \mathbf{r} - \omega t)} \tag{13}$$

in which $A(z)$ represents respective amplitude of all the perturbations. The resultant set of linearized equations is as follows:

$$\left.\begin{array}{l} i\left(ku + lv\right) + \frac{\partial w}{\partial z} + k_\rho w = i\Omega \frac{\rho_1}{\rho_0},\ i\left(ku + lv\right) + \frac{\partial w}{\partial z} + \frac{k_p}{\gamma} w = i\frac{\Omega}{\gamma}\frac{p_1}{p_0},\ \frac{p_1}{p_0} = \frac{\rho_1}{\rho_0} + \frac{T_1}{T_0} \\ i\Omega u - \frac{\partial U}{\partial z} w = ik\frac{C^2}{\gamma}\frac{p_1}{p_0},\ i\Omega v - \frac{\partial V}{\partial z} w = il\frac{C^2}{\gamma}\frac{p_1}{p_0},\ i\Omega w = g\frac{\rho_1}{\rho_0} + \frac{C^2}{\gamma}\left[\frac{\partial}{\partial z}\left(\frac{p_1}{p_0}\right) + k_p \frac{p_1}{p_0}\right] \end{array}\right\} \tag{14}$$

in which the reduction of variables yields following two coupled equations between w and p_1/p_0:

$$\left.\begin{array}{l} \gamma\Omega\frac{\partial w}{\partial z} + \left(\gamma \mathbf{k}_h \cdot \frac{d\mathbf{v}_0}{dz} - \frac{\Omega}{H}\right) w - i\left(\Omega^2 - C^2 k_h^2\right)\frac{p_1}{p_0} = 0 \\ i\left[\gamma\left(\Omega^2 - g k_T\right) H - g\left(\gamma - 1\right)\right] w - C^2 \Omega H \frac{\partial}{\partial z}\left(\frac{p_1}{p_0}\right) + g\left(\gamma - 1\right)\Omega H \frac{p_1}{p_0} = 0 \end{array}\right\} \tag{15}$$

This set of equations corrects Eq.(4) of *Zhou & Morton* (2007; hereafter ZM07) by

(1) updating ZM07's term of $\mathbf{k}_h \cdot (d\mathbf{v}_0/dz)$ with $\gamma \mathbf{k}_h \cdot (d\mathbf{v}_0/dz)$;

(2) updating ZM07's term of $i\left(\Omega^2 - C^2 k_h^2\right)$ with $-i\left(\Omega^2 - C^2 k_h^2\right)$;

(3) updating ZM07's term of $(p_1/p_0)\Omega H g + C^2 \Omega H (1/p_0)\partial p_1/\partial z$ with $(p_1/p_0)\Omega H g(\gamma - 1) - C^2 \Omega H \partial(p_1/p_0)/\partial z$.

Eqs.(14,15) provide a full set of governing equations for gravity wave propagation:

$$\frac{\partial^2 w}{\partial z^2} + f(z)\frac{\partial w}{\partial z} + g(z)w = 0, \quad \text{or,} \quad \frac{\partial^2 \tilde{w}}{\partial z^2} + q^2(z)\tilde{w} = 0 \tag{16}$$

together with

$$\left.\begin{aligned}
i\Omega\tfrac{p_1}{p_0} &= -(\beta-1)\left[\gamma\tfrac{\partial w}{\partial z} + \left(\gamma\tfrac{V_{k1}}{\Omega} + \tfrac{k_p}{k_h}\right)k_h w\right]\\
i\Omega\tfrac{\rho_1}{\rho_0} &= -(\beta-1)\left[\tfrac{\partial w}{\partial z} + \left(\tfrac{V_{k1}}{\Omega} + \tfrac{k_\rho}{k_h} + \tfrac{\beta}{\beta-1}\tfrac{k_p-\gamma k_\rho}{\gamma k_h}\right)k_h w\right]\\
i\Omega\tfrac{T_1}{T_0} &= -(\beta-1)\left\{(\gamma-1)\tfrac{\partial w}{\partial z} + \left[(\gamma-1)\tfrac{V_{k1}}{\Omega} + \tfrac{k_T}{k_h} - \tfrac{\beta}{\beta-1}\tfrac{k_p-\gamma k_\rho}{\gamma k_h}\right]k_h w\right\}\\
iku &= -\beta\tfrac{k^2}{k_h^2}\tfrac{\partial w}{\partial z} + \left[\tfrac{k}{\Omega}\tfrac{\partial U}{\partial z} - \beta\tfrac{k^2}{k_h^2}\left(k_h\tfrac{V_{k1}}{\Omega} - \tfrac{1}{\gamma H}\right)\right]w\\
il\upsilon &= -\beta\tfrac{l^2}{k_h^2}\tfrac{\partial w}{\partial z} + \left[\tfrac{l}{\Omega}\tfrac{\partial V}{\partial z} - \beta\tfrac{l^2}{k_h^2}\left(k_h\tfrac{V_{k1}}{\Omega} - \tfrac{1}{\gamma H}\right)\right]w
\end{aligned}\right\} \tag{17}$$

In the above, following functions are defined:

$$\left.\begin{aligned}
f(z) &= -\tfrac{1}{H} - \tfrac{d\left(\ln C_d^2\right)}{dz} = -\tfrac{1}{H} + \beta k_T + 2(\beta-1)\tfrac{V_{k1}}{C_{ph}}\\
g(z) &= \tfrac{1}{C_d^2}\left(\tfrac{1}{\beta-1}\omega_b^2 - 2V_{k1}^2\right) - \tfrac{1}{\beta}k_h^2 + \tfrac{\beta^2}{\beta-1}\tfrac{k_T}{\gamma H} + \tfrac{1}{C_{ph}}\left\{V_{k2} - \left[1+\beta\left(k_T H - \tfrac{2}{\gamma}\right)\right]\tfrac{V_{k1}}{H}\right\}\\
q^2(z) &= g(z) - \tfrac{1}{4}f^2(z) - \tfrac{1}{2}\tfrac{df}{dz} =\\
&= \tfrac{\Omega^2-\Omega_A^2}{C^2} + k_h^2\tfrac{\Omega_B^2-\Omega^2}{\Omega^2} + \beta\tfrac{V_{k1}}{C_{ph}}\left[\tfrac{2-\gamma}{\gamma H} - (3\beta-2)k_T - 3(\beta-1)\tfrac{V_{k1}}{C_{ph}} + \tfrac{V_{k2}}{V_{k1}}\right]
\end{aligned}\right\} \tag{18}$$

and following notations are applied:

$$\left.\begin{aligned}
&\omega = c_{ph}k_h,\ C_{ph} = c_{ph} - V_k,\ C^2 = C_{ph}^2 + C_d^2,\ k_{kT} = \tfrac{1}{k_T}\tfrac{dk_T}{dz}\\
&\beta = \tfrac{C^2}{C_d^2},\ \alpha = \tfrac{\gamma}{2}\left\{1+\beta\left[1+\tfrac{k_T}{k_p}\left(1+\tfrac{k_{kT}}{k_T} - \tfrac{3}{2}\beta\right)\right]\right\}\\
&V_{k2} = \mathbf{k}_{h0}\cdot\tfrac{d^2\mathbf{v}_0}{dz^2} = \tfrac{k}{k_h}\tfrac{d^2U}{dz^2} + \tfrac{l}{k_h}\tfrac{d^2V}{dz^2}\\
&\omega_b^2 = \tfrac{\gamma-1}{\gamma}\tfrac{g}{H},\ \Omega_B^2 = \omega_B^2 + (\beta-1)gk_T;\ \omega_a^2 = \tfrac{C^2}{4H^2},\ \Omega_A^2 = \omega_A^2 + (\alpha-1)gk_T
\end{aligned}\right\} \tag{19}$$

where c_{ph} is the extrinsic horizontal phase speed; C_d is the complementary phase speed introduced for mathematical convenience; k_{kT} is the inhomogeneous number of k_T; α and β are altitude-dependent coefficients determined by atmospheric inhomogeneities irrelevant of wind shears; V_{k2} is another input parameter, in addition to V_{k1}, contributed by wind shears. Note that the two newly introduced pseudo-frequencies, Ω_A and Ω_B, are contributed by wave-independent frequencies, ω_A and ω_B, and wave-dependent components, $(\alpha-1)gk_T$ and $(\beta-1)gk_T$, respectively.

As ZM07 pointed out, Eq.(16) reduces to the traditional Taylor-Goldstein equation if there is no temperature variation and $\gamma \to \infty$ (e.g., *Nappo* 2002); the $q^2(z)$ recovers Hines (1960)' dispersion relation in a windless isothermal atmosphere; and, $w(z)$ yields Beer (1974)'s result under z-independent wind and non-isothermal conditions. However, we argue that ZM07's another claim, the signs of V_{k1}^2 [or, $(\mathbf{k}_h \cdot d\mathbf{v}_0/dz)^2$ in that paper] and k_T^2 [or, $(dH/dz)^2$ in that paper] in $q^2(z)$ are all negative which is "consistent with the fact

that gravity waves cannot propagate freely at discontinuous boundaries", is invalid due to the fact that the process is also determined by V_{k2}, while k_T^2 does not appear in $q^2(z)$ but k_{kT} occurs in α; more important, the buoyancy frequency ω_b and the cut-off frequency ω_a in ZM07's $q^2(z)$ must be replaced by ω_B and ω_A, respectively, due to the presence of k_T.

Notes

In the cumbersome Eq.(18), $q^2(z)$ could be either positive to describe freely upward/downward propagating waves in atmosphere, or negative to demonstrate evanescent "waves" (in fact "nonwaves" with infinite vertical wavelength) which are simply exponentially growing or decaying in amplitude. The choice of growing versus decaying is usually determined by things such as boundary conditions, or the finiteness of, e.g., energy. In its propagation, a wave can have $q^2(z) > 0$ at some altitudes in one region, and becomes evanescent with $q^2(z) < 0$ in a different region. At the boundary between two such regions where $q^2(z) = 0$, wave reflection and transmission occur. Interestingly, in the case of $q^2(z) > 0$, Eq.(18) provides the vertical wavenumber $m = m_r + im_i$ of the plane-wave solution with

$$m_i = \frac{1}{2}f(z) = -\frac{1}{2H} + \frac{\beta}{2}k_T + (\beta - 1)\frac{V_{k1}}{C_{ph}} \tag{20}$$

and

$$m_r^2 = q^2(z) \tag{21}$$

Notice that the above FWM solutions are not exactly the same as the WKB results given in Eq.(8) and Eq.(10), respectively, but with extra terms in addition to modifications.

IV. Comparison and Validation

a) Mean-field atmospheric properties

The unperturbed mean-field atmospheric properties and related gravity-wave parameters are calculated from two empirical, neutral atmospheric models: (1) NRLMSISE-00, developed by Mike Picone, Alan Hedin, and Doug Drob (*Picone et al.* 2002); and (2) the horizontal wind model, HWM93, developed by *Hedin et al.* (1996). We arbitrarily choose a position at 60° latitude and -70° longitude for a local apparent solar time of 1600 hour on the 172th day of a year, with daily solar $F_{10.7}$ flux index and its 81-day average of 150. The daily geomagnetic index is 4. Fig.2 demonstrates the results. The upper two panels illustrate the vertical profiles of mean-field mass density (ρ_0), pressure (p_0), temperature (T_0), sound speed (C), zonal (eastward) wind (U), and meridional (northward) wind (V), while the lower two ones present those of wave-relevant inhomogeneous scale numbers (k_ρ, k_p, and k_T), and atmospheric cut-off frequencies (ω_a under isothermal condition and ω_A under non-isothermal condition) as well as buoyancy frequencies (ω_b under isothermal condition and ω_B under non-isothermal condition).

The upper left panel gives ρ_0 (solid blue), p_0 (dash blue), C (solid red), and T_0 (dash red). The magnitude of ρ_0 decreases all the way up from 1.225 kg/m^3 (or, 2.55×10^{25} $1/m^3$) at the sea level to only 2.38×10^{-11} kg/m^3 (4.95×10^{14} /m^3) at 300 km altitude.

The value of p_0 has a similar tendency to ρ_0. It reduces from 10^5 Pa at the sea level to 8.27×10^{-6} Pa finally. T_0 is 281 °K at the sea level. It decreases linearly to 224 °K at 13 km, and then returns to 281 °K at 47 km, followed by a reduction again to 146 °K at 88 km. Above this height, the temperature goes up continuously and reaches a stable exospheric value of ∼1200 °K above 300 km height. At 194 km it is 1000 °K. Parameter C follows the variation of $T_0^{1/2}$. At the sea level, it is 336 m/s; at 300 km altitude, it is 697 m/s. The upper right panel exposes U (solid blue) and V (dash pink). Both of the horizontal wind components oscillate twice dramatically in altitude within ±51 m/s in amplitude below 200 km altitude, and above this height they grow roughly proportionally to the height.

In the lower left panel, three curves are illustrated: density scale number k_ρ (solid blue), pressure scale number k_p (dash red), and temperature scale number k_T (solid black). Clearly, up to 200 km altitude, $k_\rho \neq k_p$ always holds and thus the isothermal condition $k_T = 0$ is broken in atmosphere, except at three heights: 13.1 km, 47.2 km, and 87.9 km. However, above 100 km altitude, k_T eventually keeps its positive polarization after two times of adjustment from negative to positive values. Above 200 km altitude, $k_T = 0$ can be considered valid. Note that the scale height H is equal to $-1/k_p$. At the sea level, H is calculated as 8.44 km and then soaring to as high as 75.6 km when approaching to about 200 km altitude and beyond.

The lower right panel draws two pairs of frequencies of gravity waves: ω_A (solid red) & ω_a (dash red), and ω_B (solid blue) & ω_b (dash blue). At all altitudes, ω_a and ω_A are always larger than ω_b and ω_B, respectively. That is, $\omega_a > \omega_b$ and $\omega_A > \omega_B$ are guaranteed for all altitudes. Thus, the buoyancy frequencies can never be larger than the corresponding cut-off frequencies in either the isothermal case or the non-isothermal one. Nevertheless, this result does not exclude at some altitudes, when we compare the difference of the isothermal and nonisothermal cases, $\omega_a < \omega_B$ (say, 100-180 km) or $\omega_A < \omega_b$ (e.g., 70-80 km). This warns us to be cautious in applications about which thermal conditions are used, isothermal or non-isothermal? It is not accurate to use isothermal cutoff frequency and nonisothermal buoyancy frequency together, nor nonisothermal cutoff frequency and isothermal buoyancy frequency together. The two sets of frequencies under isothermal and nonisothermal conditions, respectively, should not be confused and mixing up, especially in wave analysis and data-fit modeling.

Compared with the vertical profiles of atmospheric properties, NRLMSISE-00 and HWM93 also provide the horizontal gradients of ρ_0, T_0, p_0, U, and V. These inhomogeneities are always at least $10^{2\sim3}$ smaller than the vertical gradients. It is reasonable to assume, as most authors did, that the mean-field parameters are uniform and stratified in the horizontal plane, free of any inhomogeneities compared to that in the vertical direction, i.e., $\partial/\partial x \simeq 0$, $\partial/\partial y \simeq 0$ and $\nabla \cong (\partial/\partial z)\hat{\mathbf{e}}_z$. Besides, we assume an intrinsic wave-frequency Ω and a horizontal wave-number k_h equivalent to a period of 30 minutes and a wavelength of ∼50 km, respectively, based on the data of the relations between horizontal wavelength and wave periods during the SpreadFEx campaign (*Taylor et al.* 2009).

Notes

Notes

b) Profiles of m_r and m_i in different models

To manifest the nonisothermal and wind-shear effects on the propagation of gravity waves, we compare the vertical profiles of growth rate m_i and vertical wavenumber m_r calculated from the three dispersion relations of (1) Eq.(1), which is from *Hines* (1960)'s classical isothermal and windless model; (2) Eqs.(8,10) of extended Hines's model in the presence of nonisothermality (namely, vertical temperature gradient) and wind shears (namely, vertical zonal and meridional wind gradients) as described in Section 2; and, (3) Eqs.(20,21) of the WKB approach as discussed in Section 3. The result is depicted in Fig.3. The LHS panel plots m_i and the RHS one symbolizes $\pm m_r$. In the panels, solid black lines, dotted red lines, and dash blue lines represent Hines', extended Hines', and WKB models, respectively.

The LHS panel let us be aware that above ∼200 km altitude the three growth rates converge to one profile. Below this height there appears the divergence. See the *Hines'* growth rate first of all. This is the classical result in gravity wave studies. According to Eq.(1), the rate is only determined by temperature T_0: $m_i = -1/(2H) = -g/(2R_sT_0)$. Thus, its vertical profile is correlated directly to the change of T_0 shown in the upper left panel of Fig.2. At the sea level, *Hines'* rate is -0.3 per 10 km. It reduces to -0.4 per 10 km at 13 km altitude, and then recovers to -0.3 per 10 km at 47 km. It falls down again to -0.6 per 10 km till 88 km, followed by an increase continuously in altitude to saturate at roughly -0.06 per 10 km above 200 km. Relative to *Hines'* model, the extended Hines' model is appreciably modulated, with a singularity at around 100±20 km altitude, where m_i soars up to $+\infty$ from below the altitude, and tends sharply down to $-\infty$ from above the altitude. This is caused by the zero phase speed $C_{ph} = 0$. Checking Eq.(8 leads us to confirm that the modulation comes from the wind-shear term, V_{k1}/C_{ph}. Below the 80 km altitude the shear modulation is much smaller. By contrast, above 120 km the growth rate fluctuates a complete cycle around *Hines'* profile. Concerning the WKB growth rate, although Eq.(20) includes both an additional nonisothermal term, k_T, and a coefficient, β, attached to the wind-shear term, its vertical profile keeps impressively away from the complicated extended Hines' model, but follows *Hines'* isothermal/shear-free model, except a little departure below 200 km altitude. We thus suggest that the extended Hines' model may exaggerate the shear effect due to the absence of the nonisothermal term in m_i; whileas the WKB model involves both nonisothermal and wind-shear effects and thus is able to provide a more realistic m_i-profile, which is surprisingly much closer to Hines' result after avoiding the nonisothermal deficiency in the extended Hines' model. This confirms *Hickey* (2011)'s argument that the WKB approach offers a more accurate picture for gravity waves propagating in realistic atmosphere by focusing on the vertical properties of perturbations.

In the RHS panel the three vertical wavenumbers (m_r) calculated from the three models reveal a more interesting result. As given in Eq.(1), *Hines'* model is only determined by the temperature profile T_0. By contrast, the extended Hines's model and the WKB one are dependent of not only T_0 but also its gradient (k_T) and wind shears (V_{k1}/C_{ph}), as given in both Eq.(10) and Eq.(21). The two profiles superimpose upon each other, and deviate from *Hines'*s model, though not significant. Similar to the LHS panel, there exists a discontinuity in the 80–120 km layer, contributed by $C_{ph} = 0$. Towards 300 km altitude

and beyond, the difference among the three models are increasingly disappearing with height. We notice that, although Eq.(10) and Eq.(21) are cogently discrepant due to the difference in shear-related terms (V_{k1}/C_{ph}):

$$\frac{1}{2}\left(\frac{2-\gamma}{\gamma H}-\frac{1}{2}\frac{V_{k1}}{C_{ph}}\right) \quad \text{versus} \quad \beta\left[\frac{2-\gamma}{\gamma H}-(3\beta-2)\,k_T-3(\beta-1)\frac{V_{k1}}{C_{ph}}+\frac{V_{k2}}{V_{k1}}\right] \tag{22}$$

there are α and β coefficients attached to ω_A and ω_B, respectively, in the WKB approach. The existence of these two coefficients make the complicated WKB expressions to produce an identical profile to that of the extended Hines' model. We thus suppose that, with a simpler mathematical expression but a complete recovery of the WKB result, the extended Hines' model is convenient and sufficient to account for the features of the vertical wavenumber in dealing with the propagation of gravity waves, particularly in ray-tracing mapping and its data-fit simulations.

c) Profiles of wave amplitudes in different models

Nonisothermality and wind-shears influence the vertical growth of gravity wave amplitudes. Fig.4 delineates the vertical profiles of atmospheric wave growth from (1) Hines' model (top left panel); (2) extended Hines' model (top right panel); and (3) the WKB approach (lower six panels) under initial conditions of $w_0 = 1.17\times10^{-4}$ m/s and $\mathrm{d}w_0/\mathrm{d}z = 0$ for wave-period $T = 33.3$ minutes. In the top two panels, the horizontal axis is the dimension-free amplitude growth, $A^* = A(z)/A(0)$, calculated from Eq.(11). The WKB results are produced by Eqs.(16,17).

The top LHS panel discloses the vertical profile of A^* calculated from *Hines'* model. First of all, the A^*-magnitude has an exact exponential growth in altitude, which reaches 7 at the 300 km altitude, reproducing *Hines* (1960)'s result. Secondly, the two envelops produced by $\exp(\int \mathrm{d}z/2H)$ and $\exp(z/2H_{400})$, respectively, are identical above 200 km altitude but with a little divergence (no more than 15%) in the 80-140 km layer, where $H_{400} = 67.1$ km is the scale height at the 400 km altitude. It is therefore reliable to use 67.1 km as the altitude-independent scale height under 300 km, particularly above 150 km altitude. Thirdly, between 200 km and 300 km, there are 6.5 cycles in the oscillation of the perturbed amplitude. This is consistent with the m_r-profile in Fig.4: above 200 km altitude $m_r \sim 0.4$ km^{-1}, corresponding to a wavelength of ~16 km in the vertical perturbation; this wavelength gives rise to 6.5 cycles within a 100 km layer. After including the effects of non-isothermality and windshears, the above features have discernable modifications, respectively, as exposed in the top RHS panel calculated from the extended *Hines'* model. At first, the exponential increase is now damped from 7 to 6 at the 300 km altitude due to the appearance of the damping factor $\kappa = 1 - HV_{k1}/C_{ph}$. In addition, the extended profile has a bulge which modifies the exponentially-growing envelop within the 100-150 km layer. From the U/V profiles in Fig.2 we suggest that this abnormality is related to the violent shears of the neutral wind. Finally, there are 7.5 cycles above the 200 km altitude, indicating that realistic atmosphere has a little shorter vertical wavelength, ~14 km, than *Hines'* idealized model due to the presence of the temperature & horizontal wind gradients. Note that based on Eq.(3) the amplitudes of all the six atmospheric

perturbations, i.e., p_1/p_0, ρ_1/ρ_0, T_1/T_0, u/U, v/V, and w, follow the same rule versus altitude in *Hines*' and extended *Hines*' models. It is seen that gravity waves propagate upward with an amplitude amplified exponentially or slightly damped, with an oscillation the frequency of which is determined by or a little modified from $m_r(z)$.

Notes

The lower six panels in Fig.4 demonstrate the perturbations of the six perturbed parameters under the WKB approach. The simulations use the adaptive-step, 4th-order Runge-Kutta method to calculate Eq.(16) under the initial conditions w_0 and $\mathrm{d}w_0/\mathrm{d}z$. At each step, after solving $w(z)$ and $\mathrm{d}w/\mathrm{d}z$, Eq.(17) is applied to obtain the perturbations of $p_1/p_0, \rho_1/\rho_0, T_1/T_0$ and u, v. Notice that the initial conditions of these 5 perturbations are all determined by w_0 and $\mathrm{d}w_0/\mathrm{d}z$. Firstly, all the perturbations have a same vertical wavelength. For example, above the 200 km altitude, there are 8.5 cycles, presenting a further shorter vertical wavelength, 12.5 km, than the previous *Hines*' model and the extended *Hines*' model. Secondly, unlike the identical profile of the amplitude growths for all the perturbations in *Hines*' two models, the WKB model gives different envelops of the atmospheric parameters to present distinct characteristics. For instance, the maximal amplitude of p_1/p_0 is smaller than that of both ρ_1/ρ_0 and T_1/T_0, while the phases of the last two are opposite. In addition, the perturbed components in velocity, u, v, w, evolve differently versus altitude. Take their amplitudes at the 300 km altitude as an example: their amplitudes are of 90 m/s, 550 m/s, and 140 m/s, respectively. In view of the vertically growing envelops, all the profiles have much smaller magnitudes than that of Hines' model, as shown in the middle right panel (in pink), above 100 km altitude, while below ∼80 km altitude all the perturbations appear to be zero. Notice that the three perturbations in pressure, density, and temperature satisfy the perturbed equation of state, $p_1/p_0 = \rho_1/\rho_0 + T_1/T_0$.

d) Inuence of phase speed in different models

The intrinsic phase speed, C_{ph}, affects the propagation of gravity waves in the three models introduced above. The relations are given by Eq.(1) in *Hines*' model, by Eqs.(8,10) in the extended *Hines*' model, and Eqs.(20,21) in the WKB approach. Fig.5 delineates the influence of dimension-free parameter, C_{ph}/C, on amplitude A^* in the two Hines' models (top panel), and on m_i (lower left) as well as m_r (lower right) of the three models at 100 km altitude where $C = 293$ m/s. Assume C_{ph}/C changes from 0 to 1.

In the top panel, *Hines*' A^* (in blue) flies up from 1 at $C_{ph}/C = 0$ to 2350 at $C_{ph}/C = 1$. By contrast, the extended *Hines*' A^* (in pink) experiences a sharp drop to nearly 0.1 within $C_{ph}/C < 0.1$ and then climbs up gradually to 33 at $C_{ph}/C = 1$. The ratio between the two values of A^* (in black) increases from 1 at $C_{ph}/C = 0$ and reaches to 72 at $C_{ph}/C = 1$. Review the top right panel of Fig.4. At the 106 km altitude, the ratio is 69, corresponding to $C_{ph} = 0.93C = 272$ m/s.

In the lower left panel, the dependence of m_i on C_{ph}/C has different features among the three models. In *Hines*' model (in blue), m_i keeps constant versus C_{ph}/C. In the extended *Hines*' model (in pink), m_i drops rapidly from infinity to about -0.7 $(10\mathrm{km})^{-1}$

with the increase of C_{ph}/C, and $m_i = 0$ at $C_{ph}/C = 0.074$. On the contrary, in the WKB case, m_i builds all the way up with C_{ph}/C from -0.58 $(10\text{km})^{-1}$ to infinity, with $m_i = 0$ at $C_{ph}/C = 0.791$. Similar to m_i, the dependence of m_r on C_{ph}/C in the lower right panel also exposes differences among the three models. *Hines*' case decreases continuously from infinity at $C_{ph}/C = 0$ to 0 at $C_{ph}/C = 0.9$. For the extended *Hines*' model and the WKB approach, both curves superimpose upon each other for $C_{ph}/C < 0.5$, falling down from infinity to $m_r = \pm 0.2$; they keep dropping but with different rates: the former reach zero at $C_{ph}/C = 0.97$ while the latter is at a smaller value of $C_{ph}/C = 0.75$. Beyond these two phase speeds, respectively, the former increases a little to ± 0.02 km^{-1}, while the latter rises rapidly to infinity.

V. Summary and Discussion

Gravity waves were extensively studied in the 1950s-1960s, when rudimentary theories and a myriad of effects were investigated (e.g., *Gossard* & *Munk* 1954; *Eckart* 1960; *Tolstoy* 1963; *Journal of Atmospheric and Terrestrial Physics* 1968; *Georges* 1968; and *AGARD* 1972). Since then, the understandings of the wave physics and its role played in the interactions between atmosphere and ionosphere have gained considerable progress (see details in, e.g., *Fritts* & *Alexander* 2003; *Fritts* & *Lund* 2011). The advance is dominantly achieved with a couple of approaches: (1) linear wave analysis under WKB-approximation (e.g., *Pitteway* & *Hines* 1963; *Einaudi* & *Hines* 1971; *Hines* 1971; *Gill* 1982; *Hickey* & *Cole* 1987,1988; *Nappo* 2002; *Vadas* 2007); (2) FWM formalism of vertical perturbation (e.g., *Lindzen* & *Tung* 1976; *Hickey et al.* 1997, 1998, 2000, 2001; *Liang et al.* 1998; *Walterscheid* & *Hickey* 2001; *Schubert et al.* 2003, 2005).

Realistic atmosphere is not isothermal and shear-free. It is featured by large temperature and wind-speed gradients especially in the vertical direction. Experiments demonstrated that the gradients can reach up to 100° K per km and 100 m/s per km, respectively (see, e.g., *Liu* & *Swenson* 2003; *She et al.* 2009). It is thus necessary to take into account these factors in theoretical modeling and data-fit studies. In this paper, we extended *Hines*' locally isothermal and shear-free model by including the nonisothermal and wind-shear effects, and derive dispersion relation of gravity waves by applying the WKB approximation. Exact analytical expressions of growth rate (m_i) and vertical wavenumber (m_r) are obtained. The nonisothermality is found to influence wave propagation through the vertical temperature gradient, as denoted by the temperature inhomogeneous number k_T, which extends the isothermal buoyancy and cut-off frequencies to their nonisothermal counterparts. In the WKB approach, k_T also contributes to a coefficient α. By contrast, the wind-shear exerts its impact through the combined effect of the vertical wind gradient (V_{k1}) and the intrinsic horizontal phase speed (C_{ph}).

We compare the extended *Hines*' model with the WKB results within 300 km altitude (note that the non-dissipation condition satisfies below 200 km altitude) with an arbitrary 50-km horizontal wavelength and 33.3-minute wave period. The vertical profiles of the background atmospheric properties and the horizontal winds are calculated from the empirical neutral atmospheric models NRLMSISE-00 and HWM93. Simulations expose

Notes

Notes

that the extended *Hines'* m_i-profile deviates away from *Hines'* model further than the WKB one due to the lack of the non-isothermal effect. In addition, the two m_r curves obtained from the extended *Hines'* and the WKB models superimpose upon each other, both of which amplify *Hines'* m_r magnitudes in the vertical direction. What is more, all the perturbations in the extended *Hines'* model has an identical profile in the growth of amplitude. This profile has a slight modification to the *Hines'* classical model except the 100-150 km layer. By contrast, the WKB model provides respective profiles of perturbations in pressure, density, temperature, zonal wind, meridional wind, and vertical wind. Finally, the propagation of gravity waves is related to the phase speed (C_{ph}): when it increases, the *Hines'* m_i-profile keeps constant, but the extended *Hines'* m_i drops down continuously while the WKB one soars up monotonously; at the same time, the three m_r profiles fall off together when C_{ph} is no more than $0.75C$, the two profiles obtained from the extended Hines' & the WKB models overlap upon each other which shift away from Hines' model.

VI. Acknowledgments

This work was done at the Embry-Riddle Aeronautical University (ERAU), Daytona Beach, FL. J. Ma thanks Professor M.P. Hickey, J.B. Snively, and M.D. Zettergren for the financial supports. Copies of the simulation runs and figures can be obtained by emailing to zma@mymail.ciis.edu.

References Références Referencias

1. AGARD (1972), Effects of atmospheric acoustic gravity waves on electromagnetic wave propagation, *Conf. Proc., 115*, Harford House, London.
2. Beer, T. (1974), Atmospheric Waves, John Wiley, New York.
3. Dutton, J. A. (1986), The Ceaseless Wind, Dover, New York.
4. Eckart, C. (1960), Hydrodynamics of oceans and atmospheres, Pergamon, New York.
5. Eckermann, S. D. (1997), Inuence of wave propagation on the Doppler spreading of atmospheric gravity waves, *J. Atmos. Sci., 54*, 2554-2573.
6. Einaudi, F., and C. O. Hines (1971), WKB approximation in application to acousticgravity waves, *Can. J. Phys., 48*, 14581471.
7. Francis, S. H. (1973), Acoustic-gravity modes and large-scale traveling ionospheric disturbances of a realistic, dissipative atmosphere, *J. Geophys. Res., 78*, 2278-2301.
8. Fritts, D. C., and M. J. Alexander (2003), Gravity wave dynamics and effects in the middle atmosphere, *Rev. Geophys., 41*, 1003, doi:10.1029/2001RG000106.
9. Fritts, D. C., and T. S. Lund (2011), Gravity wave inuences in the thermosphere and ionosphere: Observations and recent modeling, in: *Aeronomy of the Earths Atmosphere and Ionosphere*, ed.: Abdu, M. A., Pancheva, D., and Bhattacharyya, A., Springer, 109130.
10. Galperin, B., S. Sukoriansky, and P. S. Anderson (2007), On the critical Richardson number in stably stratified turbulence, *Atmos. Sci. Let., 8*, 6569.
11. Georges, T. M. (1968), Acoustic-gravity waves in the atmosphere, Symposium Proceedings, U.S. Government Printing Office, Washinton, D. C.
12. Gill, A. E. (1982), Atmosphere-ocean dynamics. Academic Press, Orlando, FL, International Geophysics Series.

13. Goldstein, S. (1931), On the instability of superposed streams of fluids of different densities, *Proc. R. Soc. London, Ser. A, 132*, 524-548.
14. Gossard, E. E., and W. H. Hooke (1975), Waves in the Atmosphere, Elsevier, New York.
15. Gossard, E. E., and W. H. Munk (1954), On gravity waves in the atmosphere, *J. Meteorol., 11*, 259-269.
16. Harris, I. and W. Priester (1962), Time dependent structure of the upper atmosphere, *J. Atmos. Sci., 19*, 286-301.
17. Hecht, J. H., R. L. Walterscheid, M. P. Hickey, and S. J. Franke (2001), Climatology and modeling of quasi-monochromatic atmospheric gravity waves observed over Urbana Illinois, *J. Geophys. Res., 106*, 51815196.
18. Hedin, A. E., E. L. Fleming, A. H. Manson, F. J. Schmidlin, S. K. Avery, R. R. Clark, S. J. Franke, G. J. Fraser, T. Tsuda, F. Vial, and R. A. Vincent (1996), Empirical wind model for the upper, middle and lower atmosphere, *J. Atmos. Terr. Phys.* 58, 1421-1447.
19. Hickey, M. P. (2001), Airglow variations associated with nonideal ducting of gravity waves in the lower thermosphere region, *J. Geophys. Res.*, 106, 17,90717,918.
20. Hickey, M. P. (2011), Atmospheric gravity waves and effects in the upper atmosphere associated with tsunamis, in: The Tsunami Threat – Research and Technology, ed.: Nils-Axel MArner, ISBN: 978-953-307-552-5, In Tech, Croatia and Shanghai.
21. Hickey M. P., and K. D. Cole (1987), A quantic dispersion equation for internal gravity waves in the thermosphere, *J. Atmos. Terr. Phys., 49*, 889-899.
22. Hickey M. P., and K. D. Cole (1988), A numerical model for gravity wave dissipation in the thermosphere, *J. Atmos. Terr. Phys.*, *50*, 689697.
23. Hickey, M. P., Richard L. Walterscheid, Michael J. Taylor, William Ward, Gerald Schubert, Qihou Zhou, Francisco Garcia, Michael C. Kelly, and G. G. Shepherd (1997), Numerical simulations of gravity waves imaged over Arecibo during the 10-day January 1993 campaign, *J. Geophys. Res., 102*, 11,475-11,489.
24. Hickey, M. P., M. J. Taylor, C. S. Gardner, and C. R. Gibbons (1998), Full-wave modeling of small-scale gravity waves using Airborne Lidar and Observations of the Hawaiian Airglow (ALOHA-93) O(^{1}S) images and coincident Na wind/temperature lidar mea- surements. *J. Geophys. Res.*, *103*, 6439-6453.
25. Hickey, M. P., R. L. Walterscheid, and G. Schubert (2000), Gravity wave heating and cooling in Jupiters thermosphere, *Icarus, 148*, 266–281.
26. Hickey, M. P., G. Schubert, and R. L. Walterscheid (2001), Acoustic wave heating of the thermosphere, *J. Geophys. Res., 106*, 2154321548.
27. Hickey, M. P., G. Schubert, and R. L. Walterscheid (2009), Propagation of tsunami-driven gravity waves into the thermosphere and ionosphere, *J. Geophys. Res., 114*, A08304, doi:10.1029/2009JA014105.
28. Hickey, M. P., G. Schubert, and R. L. Walterscheid (2010), Atmospheric airglow uctuations due to a tsunami-driven gravity wave disturbance, *J. Geophys. Res., 115*, A06308, doi:10.1029/2009JA014977.
29. Hines, C. O. (1960), Internal atmospheric gravity waves at ionospheric heights, *Can. J. Phys., 38*, 1441-1481.
30. Hines, C. O. (1971), Generalization of the Richardson criterion for the onset of atmospheric turbulence, *Q. J. R. Met Soc., 97*, 429-439.
31. Howard, L. (1961), Note on a paper of John W. Miles, *J. Fluid Mech., 10*, 509512.

Notes

32. Isler, J. R., M. J. Taylor, and D. C. Fritts (1997), Observational evidence of wave ducting and evanescence in the mesosphere, *J. Geophys. Res., 102*, 26,30126,313.
33. Journal of Atmospheric and Terrestrial Physics (1968), Symposium on upper atmospheric winds, waves and ionospheric drift, *J. Atmos. Terr. Phys.* (Spec. Issue), 30 (5).
34. Landau, L. D., and E. M. Lifshitz (1959), Fluid mechanics, Pergamon, New York.
35. Liang, J., W. Wan, and H. Yuan (1998), Ducting of acoustic-gravity waves in a nonisothermal atmosphere around a spherical globe, *J. Geophys. Res., 103*, 11,22911,234.
36. Lindzen, R. S., and K.-K. Tung (1976), Banded convective activity and ducted gravity waves, *Mon. Wea. Rev., 104*, 16021617.
37. Liu, H.-L. (2007), On the large wind shear and fast meridional transport above the mesopause, *Geophys. Res. Lett., 34*, L08815, doi:10.1029/2006GL028789.
38. Liu, A. Z., and G. R. Swenson (2003), A modeling study of O_2 and OH airglow perturbations induced by atmospheric gravity waves, *J. Geophys. Res., 108*, 4151, doi:10.1029/2002JD002474, D4.
39. Liu, X., J. Xu, J. Yue, and S. L. Vadas (2013), Numerical modeling study of the momentum deposition of small amplitude gravity waves in the thermosphere, *Ann. Geophys., 31*, 114.
40. Majda, A., and M. Shefter (1998), Elementary stratified ows with instability at large Richardson number, *J. Fluid Mech., 376*, 319350.
41. Marks, C. J., and S. D. Eckermann (1995), A three-dimensional nonhydrostatic raytracing model for gravity waves: Formulation and preliminary results for the middle atmosphere, *J. Atmos. Sci., 52*, 1959-1984.
42. Miles, J. (1961), On the stability of heterogeneous shear ows, *J. Fluid Mech., 10*, 496508.
43. Miles, J. (1986), Richardsons criterion for the stability of stratified shear ow, *Phys. Fluids, 29*, 3470.
44. Nappo, C. J. (2002), An Introduction to Atmospheric Gravity Waves, Academic, San Diego, California.
45. Picone, J. M., A. E. Hedin, D. P. Drob, and A. C. Aikin (2002), NRLMSISE-00 empirical model of the atmosphere: Statistical comparisons and scientific issues, *J. Geophys. Res.*, 107(A12), 1468, doi:10.1029/2002JA009430.
46. Pitteway, M. L. V., and C. O. Hines (1963), The viscous damping of atmospheric gravity waves, *Can. J. Phys., 41*, 19351948.
47. Pitteway, M. L. V., and C. O. Hines (1965), The reection and ducting of atmospheric acoustic-gravity waves, *Can. J. Phys., 43*, 22222243.
48. Schubert, G., M. P. Hickey, and R. L. Walterscheid (2003), Heating of Jupiters thermosphere by the dissipation of upward propagating acoustic waves, *ICARUS, 163*, 398-413.
49. Schubert, G., M. P. Hickey, and R. L. Walterscheid (2005), Physical processes in acoustic wave heating of the thermosphere, *J. Geophys. Res., 110*, DOI:10.1029/2004JD005488.
50. Snively, J. B., and V. P. Pasko (2003), Breaking of thunderstorm-generated gravity waves as a source of short-period ducted waves at mesopause altitudes, *Geophys. Res. Lett., 30*, 2254, doi:10.1029/2003GL018436.
51. She, C. Y., T. Li, B. P. Williams, T. Yuan, and R. H. Picard (2004), Concurrent OH imager and sodium temperature/wind lidar observation of a mesopause region

Notes

undular bore event over Fort Collins/Platteville, Colorado, *J. Geophys. Res., 109*, D22107, doi:10.1029/2004JD004742

52. She, C. Y., D. A. Krueger, R. Akmaev, H. Schmidt, E. Talaat, and S. Yee (2009), Longterm variability in mesopause region temperatures over Fort Collins, Colorado (41N, 105W) based on lidar observations from 1990 through 2007, *J. Terr. Sol. Atmos. Phys.*, 71, 15581564.
53. Snively, J. B., V. P. Pasko, M. J. Taylor, and W. K. Hocking (2007), Doppler ducting of short-period gravity waves by midlatitude tidal wind structure, *J. Geophys. Res., 112*, A03304, doi:10.1029/2006JA011895.
54. Sonmor, L. J., and G. P. Klaassen (1997), Toward a unified theory of gravity wave breaking, *J. Atmos. Sci., 54*, 26552680.
55. Stone, P. H. (1966), On non-geostrophic baroclinic stability, *J. Atmos. Sci., 23*, 390-400.
56. Sutherland, B. R. (2010), Internal gravity waves, Cambridge University Press, Cambridge.
57. Taylor, G. I. (1931), Effect of variation in density on the stability of superposed streams of fluid, *Proc. R. Soc. London, Ser. A, 132*, 499-523.
58. Taylor, M. J., D. N. Turnbull, and R. P. Lowe (1995), Spectrometric and imaging measurements of a spectacular gravity wave event observed during the ALOHA-93 campaign, *Geophys. Res. Lett., 22*, 28492852.
59. Taylor, M. J., P.-D. Pautet, A. F. Medeiros, R. Buriti, J. Fechine, D. C. Fritts, S. L. Vadas, H. Takahashi, and F. T. Sao Sabbas (2009), Characteristics of mesospheric gravity waves near the magnetic equator, Brazil, during the SpreadFEx campaign, *Ann. Geophys., 27*, 461472.
60. Tolstoy, I. (1963), The theory of waves in stratified uids including the effects of gravity and rotation, *Rev. Mod. Phys., 35*, 207-230.
61. Vadas, S. L. (2007), Horizontal and vertical propagation and dissipation of gravity waves in the thermosphere from lower atmospheric and thermospheric sources, *J. Geophys. Res., 112*, A06305, doi:10.1029/2006JA011845.
62. Vadas, S. L., and D. C. Fritts (2004), Thermospheric responses to gravity waves arising from mesoscale convective complexes, *J. Atmos. Sol. Terr. Phys., 66*, 781-804.
63. Vadas, S. L., and D. C. Fritts (2005), Thermospheric responses to gravity waves: Inuences of increasing viscosity and thermal diffusivity, *J. Geophys. Res., 110*, D15103, doi:10.1029/2004JD005574.
64. Volland, H. (1969a), Full wave calculations of gravity wave propagation through the thermosphere, *J. Geophys. Res., 74*, 17861795.
65. Volland, H. (1969b), The upper atmosphere as a multiple refractive medium for neutral air motions, *J. Atmos. Terr. Phys., 31*, 491-514.
66. Walterscheid, R. L., J. H. Hecht, R. A. Vincent, I. M. Reid, J. Woithe, and M. P. Hickey (1999), Analysis and interpretation of airglow and radar observations of quasimonochromatic gravity waves in the upper mesosphere and lower thermosphere over Adelaide, Australia (35S, 138E), *J. Atmos. Sol. Terr. Phys., 61*, 461478.
67. Walterscheid, R. L., and M. P. Hickey (2001), One-gas models with height-dependent mean molecular weight: Effects on gravity wave propagation, *J. Geophys. Res., 106*, 28,831-28,839.
68. Walterscheid, R. L., and M. P. Hickey (2005), Acoustic waves generated by gusty ow over hilly terrain, *J. Geophys. Res., 110*, DOI: 10.1029/2005JA011166.

Notes

69. Walterscheid, R. L., and M. P. Hickey (2012), Gravity wave propagation in a diffusively separated gas: Effects on the total gas, *J. Geophys. Res., 117*, A05303, doi:10.1029/2011JA017451.
70. Walterscheid, R. L., G. Schubert, and D. G. Brinkman (2001), Small-scale gravity waves in the upper mesosphere and lower thermosphere generated by deep tropical convection, *J. Geophys. Res., 106*, 31,82531,832.
71. Wang, D. Y., and T. F. Tuan (1988), Brunt-Doppler ducting of small period gravity waves, *J. Geophys. Res., 93*, 9916-9926.
72. Yu, Y., and M. P. Hickey (2007a), Time-resolved ducting of atmospheric acousticgravity waves by analysis of the vertical energy ux, *Geophys. Res. Lett., 34*, L02821, doi:10.1029/2006GL028299.
73. Yu, Y., and M. P. Hickey (2007b), Numerical modeling of a gravity wave packet ducted by the thermal structure of the atmosphere, *J. Geophys. Res., 12*, A06308, doi:10.1029/2006JA012092.
74. Yu, Y., and M. P. Hickey (2007c), Simulated ducting of high-frequency atmospheric gravity waves in the presence of background winds, *Geophys. Res. Lett., 34*, L11103, doi:10.1029/2007GL029591.
75. Zhou, Q. and Y. T. Morton (2007), Gravity wave propagation in a nonisothermal atmosphere with height varying background wind, *Geophys. Res. Lett., 34*, L23803, doi:10.1029/2007GL031061.

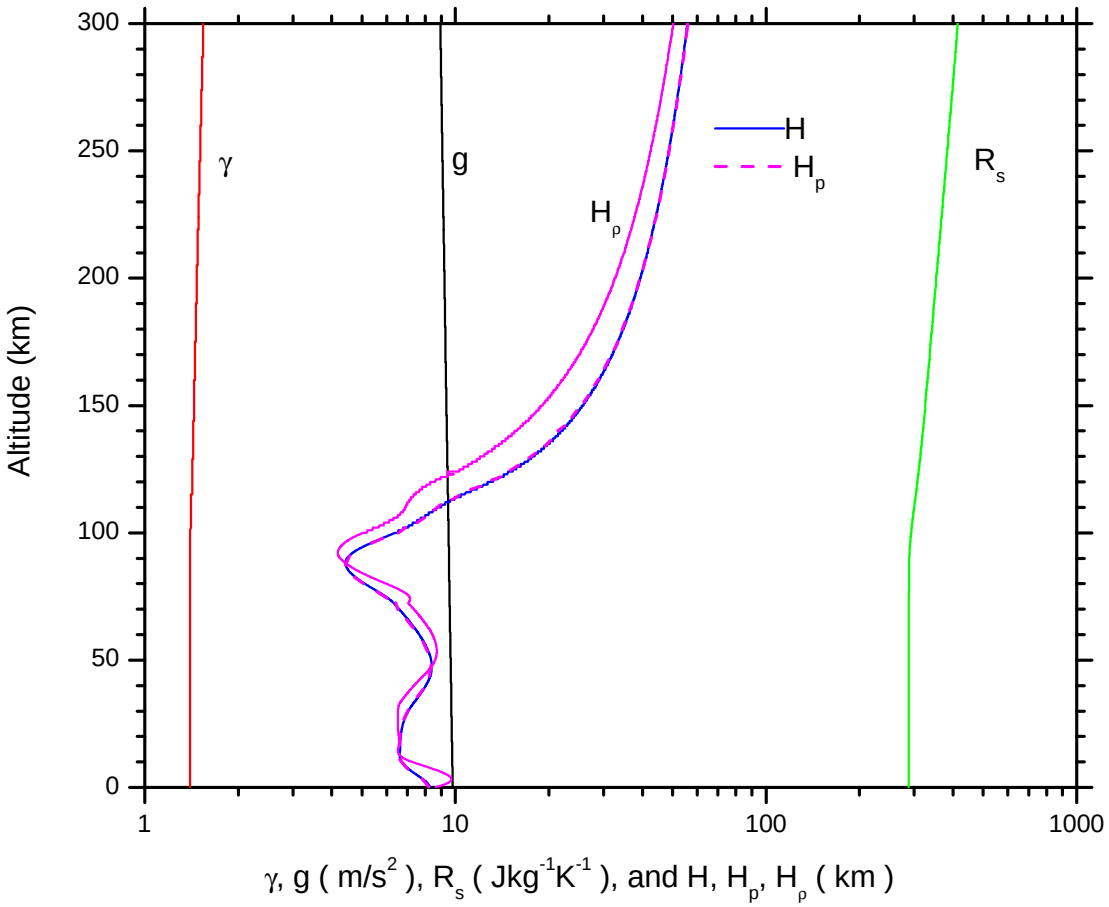

Figure 1 : Vertical pro˙les of input parameters in atmosphere: adiabatic index, γ (in red); gravitational acceleration, g (in black); specific gas constant, R_s (in green); and Hines' scale height, H (in blue), as well as the two scale heights in density, H_ρ (in solid pink), and in pressure, H_p (in dash pink), respectively. Note that $H = H_p \neq H_\rho$.

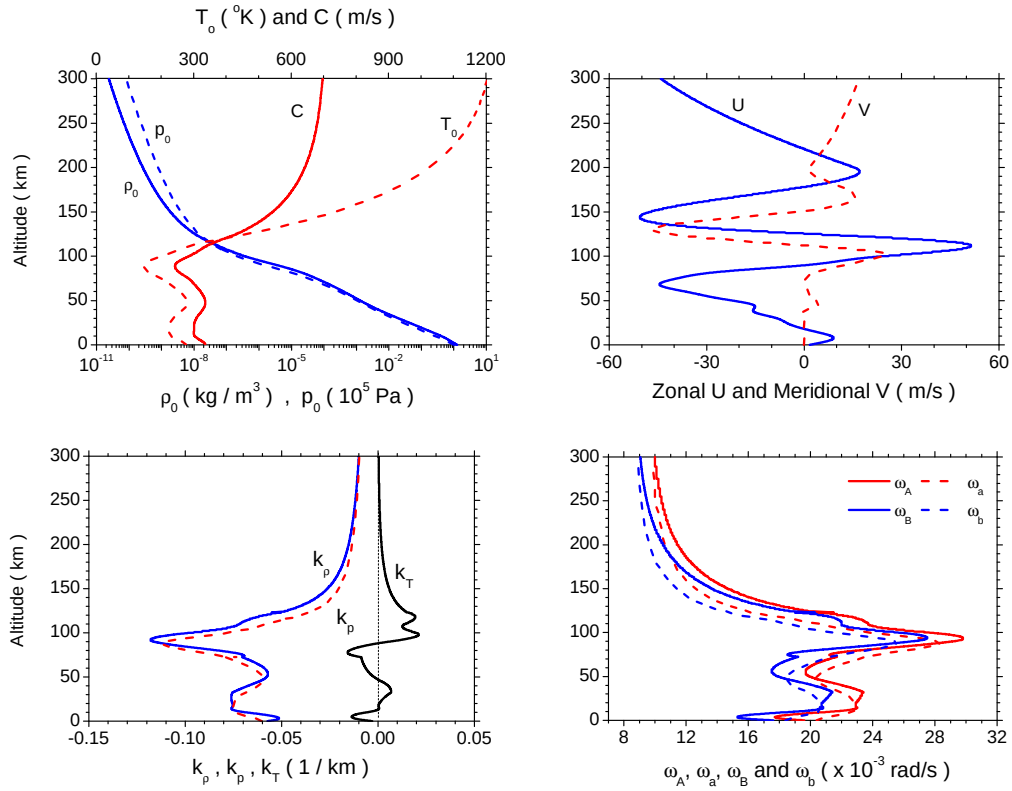

Figure 2 : Vertical profiles of atmospheric mean-field properties (upper two panels) from NRLMSISE-00 (*Picone et al.* 2002) and HWM93 (*Hedin et al.* 1996), and related gravity wave parameters (lower two panels). Upper left: mass density ρ_0 (solid blue), pressure p_0 (dash blue), sound speed C (solid red), and temperatur T_0 (dash red); upper right: zonal (eastward) wind U (solid blue) and meridional (northward) wind V (dash pink); lower left: density scale number k_ρ (solid blue), pressure scale number k_p (dash red), and temperature scale number k_T (solid black); lower right: cut-off frequencies ω_A (solid red) and ω_a (dash red), and buoyancy frequencies ω_B (solid blue) and ω_b (dash blue).

Notes

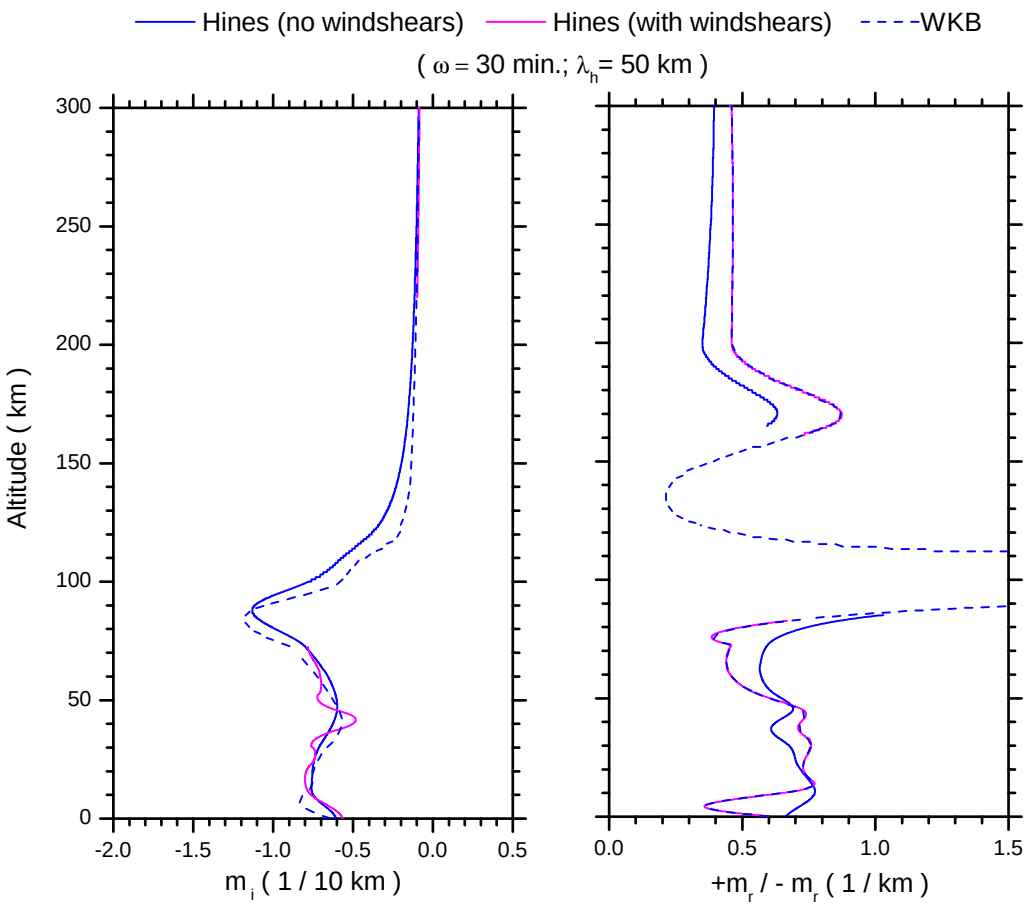

Figure 3 : Comparisons of growth rate m_i and vertical wavenumber m_r of gravity waves among three different dispersion relations: (1) *Hines* (1960)' non-windshear model (in solid blue), (2) Wind-shear model (Section 2; in red); and, (3) WKB model (Section 3; in dashed blue)

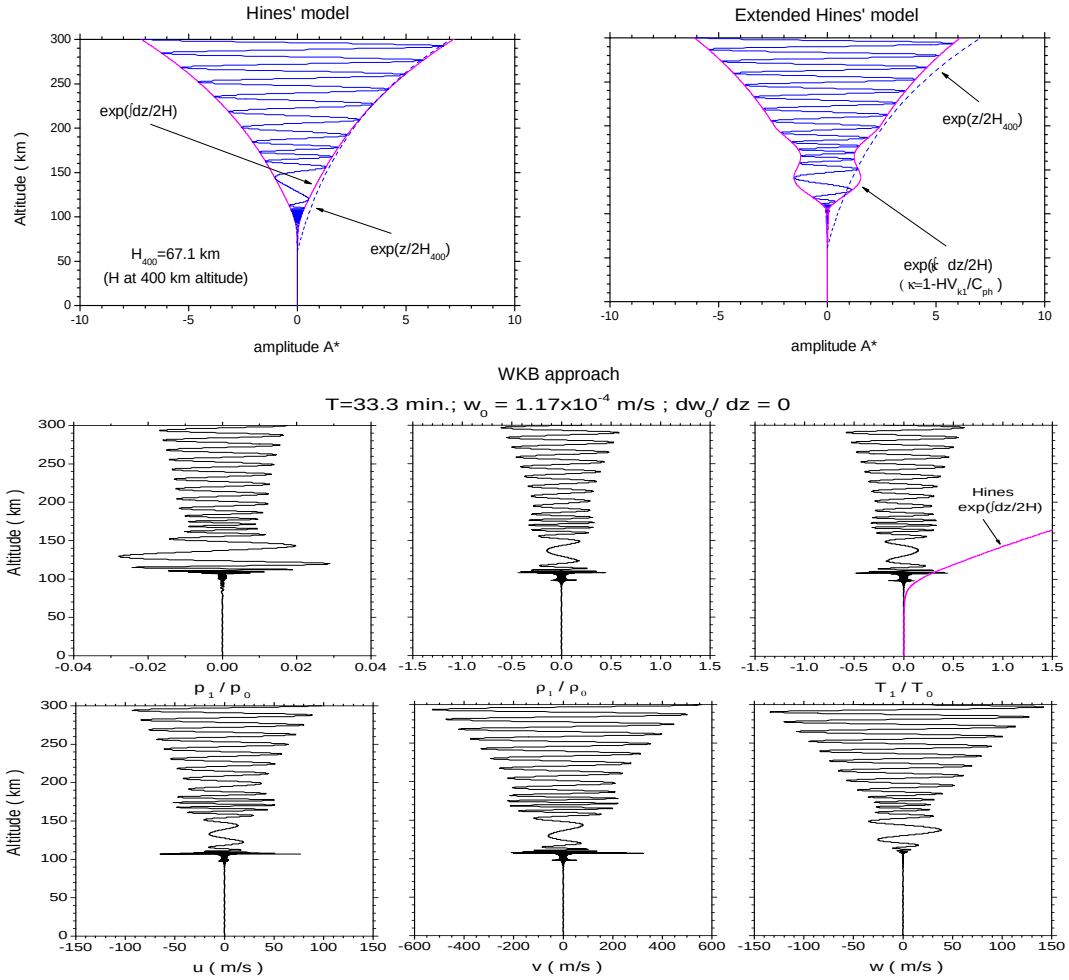

Figure 4 : Vertical growth of atmospheric perturbations from (1) Hines' model (top left panel); (2) extended Hines' model (top right panel); and (3) the WKB approach (lower six panels) under initial conditions of $w_0 = 1.17 \times 10^{-4}$ m/s and $\mathrm{d}w_0/\mathrm{d}z = 0$ for wave-period of $T = 33{:}3$ minutes. In the top two panels, $A^* = A(z)/A(0)$.

Notes

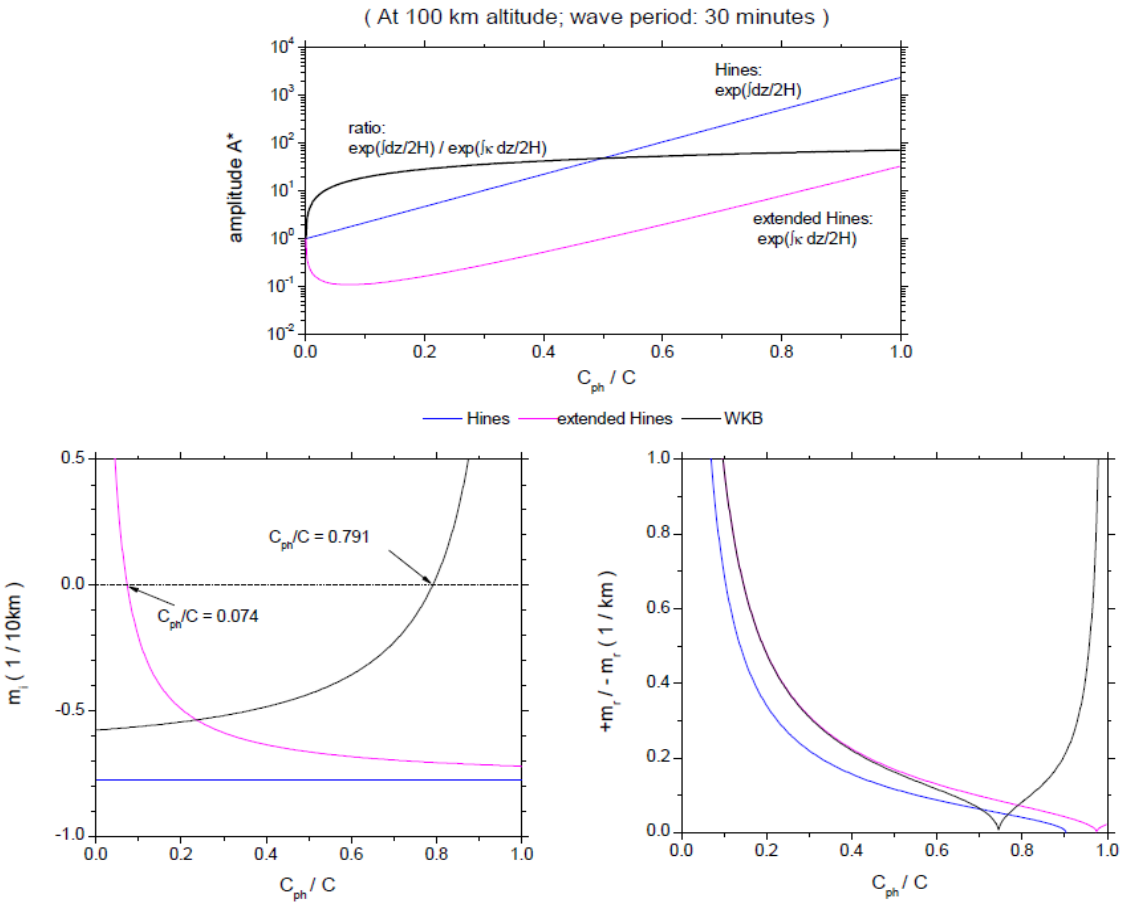

Figure 5 : Inuence of phase speed on the propagation of gravity waves in the three models

This page is intentionally left blank

Global Journal of Science Frontier Research: F
Mathematics and Decision Sciences
Volume 16 Issue 3 Version 1.0 Year 2016
Type : Double Blind Peer Reviewed International Research Journal
Publisher: Global Journals Inc. (USA)
Online ISSN: 2249-4626 & Print ISSN: 0975-5896

On Some Bicomplex Modules

By Mamta Amol Wagh
Deen Dayal Upadhyaya College, India

Abstract- A class of entire bicomplex sequences denoted by *B*, studied by Srivastava & Srivastava in 2007 is studied and is shown to be a bicomplex module. The subclasses of this class,studied by Wagh in 2008, are also shown to be bicomplex modules. Further they have been shown to form module structure over the class *B*.

GJSFR-F Classification : *MSC 2010: 46H25*

Strictly as per the compliance and regulations of :

5. Srivastava, Rajiv K. : "Certain topological aspects of Bicomplex space", Bull. Pure & Appl. Math. Dec., 2(2), 2008, 222-234.

On Some Bicomplex Modules

Mamta Amol Wagh

Abstract- A class of entire bicomplex sequences denoted by *B*, studied by Srivastava & Srivastava in 2007 is studied and is shown to be a bicomplex module. The subclasses of this class, studied by Wagh in 2008, are also shown to be bicomplex modules. Further they have been shown to form module structure over the class *B*.

I. Section: C

Bicomplex Numbers were introduced by Corrado Segre(1860–1924) in 1892. In[3], he defined an infinite set of algebras and gave the concept of multicomplex numbers. For the sake of brevity, we confine ourselves to the bicomplex version of his theory. The space of bicomplex numbers is the first in an infinite sequence of multicomplex spaces. The set of bicomplex numbers is denoted by C_2 and is defined as follows:

$$C_2 = \{x_1 + i_1 x_2 + i_2 x_3 + i_1 i_2 x_4 : x_1, x_2, x_3, x_4 \in C_0\}$$

Or equivalently

$$C_2 = \{z_1 + i_2 z_2 : z_1, z_2 \in C_1\}$$

where $i_1^2 = i_2^2 = -1$, $i_1 i_2 = i_2 i_1$ and C_0, C_1 denote the space of real and complex numbers respectively.

The binary compositions of addition and scalar multiplication on C_2 are defined coordinate wise and the multiplication in C_2 is defined term by term. With these binary compositions, C_2 becomes a commutative algebra with identity. Algebraic structure of C_2 differs from that of C_1 in many respects [2]. Few of them, which pertain to our work, are mentioned below:

a) Idempotent Elements

Besides 0 and 1, there are exactly two nontrivial idempotent elements in C_2 defined as $e_1 = (1 + i_1 i_2) / 2$, $e_2 = (1 - i_1 i_2) / 2$.
Note that $e_1 + e_2 = 1$ and $e_1.e_2 = e_2.e_1 = 0$.
A bicomplex number $\xi = z_1 + i_2 z_2$ has a unique idempotent representation, [5] as
$\xi = {}^1\xi\, e_1 + {}^2\xi\, e_2$ where ${}^1\xi = z_1 - i_1 z_2$, ${}^2\xi = z_1 + i_1 z_2$.

Author: *Assistant Professor, Deen Dayal Upadhyaya College, University of Delhi, Shivaji Marg, Karampura, New Delhi – 110015.*
e-mail: nigam.mamta@gmail.com

b) Two Principal Ideals

The Principal Ideals in C_2 generated by e_1 and e_2 are denoted by I_1 and I_2 respectively; thus

$$I_1 = \{\xi e_1 : \xi \in C_2\},$$

$$I_2 = \{\xi e_2 : \xi \in C_2\}.$$

Since $\xi = {}^1\xi e_1 + {}^2\xi e_2$, where ${}^1\xi$ and ${}^2\xi$ are the idempotent components of ξ, therefore these ideals can also be represented as

$$I_1 = \{(z_1 - i_1 z_2)e_1 : z_1, z_2 \in C_1\} = \{z e_1 : z \in C_1\}$$

$$I_2 = \{(z_1 + i_1 z_2)e_2 : z_1, z_2 \in C_1\} = \{z e_2 : z \in C_1\}$$

Note that $I_1 \cap I_2 = \{0\}$ and $I_1 \cup I_2 = O_2$, the set of all singular elements of C_2.

c) Zero Divisors

As we have seen, $e_1 . e_2 = e_2 . e_1 = 0$. Thus zero divisors exist in C_2. In fact, two Bicomplex numbers are divisors of zero if and only if one of them is a complex multiple of e_1 and the other is a complex multiple of e_2. In other words, two Bicomplex numbers are divisors of zero if and only if one of them is a member of $I_1 \sim \{0\}$ and the other is a member of $I_2 \sim \{0\}$.

d) Conjugates of a Bicomplex number

The i_2- conjugate of a bicomplex number is defined in [2] as follows:

$$\xi^{\#} = z_1 - i_2 z_2 = {}^2\xi e_1 + {}^1\xi e_2 \text{ where } \xi = z_1 + i_2 z_2$$

e) Norm of a Bicomplex number

The norm in C_2 is defined as

$$\|\xi\| = \left\{ |z_1|^2 + |z_2|^2 \right\}^{1/2} = \left[\frac{|{}^1\xi|^2 + |{}^2\xi|^2}{2} \right]^{1/2}$$

C_2 becomes a modified Banach algebra with respect to this norm in the sense that

$$\| \xi.\eta \| \leq \sqrt{2} \| \xi \| . \| \eta \|$$

f) Entire functions

A function f of a bicomplex variable is said to be an entire function if it is holomorphic in the entire bicomplex space C_2.

g) Entire Bicomplex Sequence

If $f(\xi) = \sum_{k \geq 1} \alpha_k (\xi - \eta)^k$ represents an entire function, the series $\sum \alpha_k$ is called entire bicomplex series and the sequence $\{\alpha_k\}$ is called entire bicomplex sequence.

Ref

2. Price, G. Baley : "An Introduction to Multicomplex spaces and functions", Marcel Dekker, Inc., 1991.

II. Class B and the Bicomplex Modules

Let's see at these classes for the ready reference.

The classes B, B', B'' of entire Bicomplex sequences:

Srivastava & Srivastava [4] defined the class B as

$$B = \left\{ f : f = \{ \xi_k \} = \left\{ {}^1\xi_k e_1 + {}^2\xi_k e_2 \right\} : \sup_{k\geq 1} k^k \left| {}^1\xi_k \right| < \infty, \sup_{k\geq 1} k^k \left| {}^2\xi_k \right| < \infty \right\} \quad (2.1.1)$$

Every element of class B is the sequence of coefficients of an entire function and is, therefore, an entire bicomplex sequence.

Algebraic structure of B, given by [4]

Binary compositions on B are defined as follows:

Let $f = \{ \xi_k \}$ and $g = \{ \eta_k \}$ be arbitrary members of B and $a \in C_0$

1. Addition : $f + g = \{ \alpha_k \}$ where $\alpha_k = \xi_k + \eta_k, \forall k \geq 1$.
2. Scalar multiplication : $a.f = \{\beta_k\}$ where $\beta_k = a.\xi_k$, $\forall k \geq 1$, $a \in C_0$.
3. Weighted Hadamard Multiplication : $f \times g = \{ \gamma_k \}$,

where $\gamma_k = k^k \ \xi_k \times \eta_k, \forall k \geq 1$

They have shown that B is a commutative algebra with identity, the element $u = \{k^{-k}\}$ being the identity element of B.

Two subclasses of the class B have been defined in [6] as follows:

$$B' = \left\{ f : f = \{ {}^1\xi_k e_1 \} : \sup_{k\geq 1} k^k \ \left| {}^1\xi_k \right| < \infty \right\} \quad (2.1.2)$$

$$B'' = \left\{ f : f = \{ {}^2\xi_k e_2 \} : \sup_{k\geq 1} k^k \left| {}^2\xi_k \right| < \infty \right\} \quad (2.1.3)$$

The elements of B' and B'' are the sequences with members in A_1 and A_2, respectively where A_1 and A_2 are the auxiliary space.

Note first that B' is closed with respect to the binary compositions induced on B' as a subset of B, owing to the consistency of idempotent representation and the algebraic structure of bicomplex numbers.

Norm in B' is defined as follows:

$$\| f \| = \sup_{k\geq 1} \left| {}^1\xi_k \right| , \ f = \{ {}^1\xi_k . e_1 \} \in B'.$$

B' is Gel'fand subalgebra of B [7]. B' is an algebra ideal of Bwhich is not a maximal ideal [7]. Zero divisors, Invertible and quasi invertible elements have also been characterised for this subclass [7].

Ref

4. Srivastava, Rajiv K. & Srivastava, Naveen K. : "On a class of Entire Bicomplex sequences", South East. Asian J. Math & Math. Sc. 5(3), 2007, pp. 47-68.

Definition 2.1.1: Bicomplex Modules (BC− module or T− module)

A $BC-$ module X over the ring BC of bicomplex numbers consists of an abelian group $(X, +)$ and an operation $BC\times X\to X$ such that for all $\xi,\eta\in BC$ and $x,y\in X$, we have

1. $\xi(x+y)=\xi x+\xi y$
2. $(\xi+\eta)x=\xi x+\eta x$
3. $(\xi\eta)x=\xi(\eta x)$
4. $1_{BC}\,x=x$, 1_{BC} is the multiplicative identity of BC.

The members of X are known as vectors and members of C_2 are known as scalar and in most of the books scalar are always in left and vector in right side, for example, $(x\,y)\xi=x(y\,\xi)$. As the ring of bicomplex numbers is commutative, we don't need to define left or right BC - modules.

If X is a BC - module, then some structural peculiarities of the set BC are immediately manifested in any bicomplex module, in contrast to the case of real, complex or even quaternionic linear spaces where the structure of linear space does not imply anything immediate about the space itself.
Consider the sets

$$X_{e_1}=e_1.X \text{ and } X_{e_2}=e_2.X\,.$$

Since, we know that

$$X_{e_1}\bigcap X_{e_2}=\{0\}$$

and
$$X=X_{e_1}+X_{e_2}\,, \qquad (2.1.4)$$

We can define two mappings:

$$P:X\to X\ ,\ Q:X\to X$$

by

$$P(x)=e_1\,x \qquad Q(x)=e_2\,x\,.$$

Since

$$P+Q=Id_X\,,P\circ Q=Q\circ P=0,P^2=P,Q^2=Q\ ,$$

the operators P and Q are mutually complementary projectors. (2.1.4) is called the idempotent decomposition of X, and it will play an important role in the development of the theory of bicomplex duals.
Consider the component – wise operations on X:
If $x=e_1\,x+e_2\,x\in X\,,y=e_1\,y+e_2\,y\in Y$ and if $\lambda=\lambda_1\,e_1+\lambda_2\,e_2$, then

$$x+y=e_1\,x+e_2\,x+e_1\,y+e_2\,y=(e_1\,x+e_1\,y)+(e_2\,x+e_2\,y)\,,$$

$$\lambda\,x=(\lambda_1\,e_1+\lambda_2\,e_2)(e_1\,x+e_2\,x)=\lambda_1\,x\,e_1+\lambda_2\,x\,e_2\,.$$

Since, X_{e_1} and X_{e_2} are $\mathrm{R}-, C_1(i_1)-$ and $C_1(i_2)-$ linear spaces as well as BC - modules , we have that

$$X = X_{e_1} \oplus X_{e_2} \ ,$$

where the direct sum $\oplus$ can be understood in the sense of $\mathrm{R}-, C_1(i_1)-$ and $C_1(i_2)-$ linear spaces, as well as BC - modules. By saying that X_{e_1} and X_{e_2} are $\mathrm{R}-, C_1(i_1)-$ and $C_1(i_2)-$ linear spaces as well as BC - modules, we mean that X_{e_1} and X_{e_2} are linear spaces over $\mathrm{R}, C_1(i_1), C_1(i_2)$ and are modules over the ring of bicomplex numbers.

If we consider X as a $C_1(i_1)-$ linear space, we denote it as $X_{C_1(i_1)}$ and if it is considered as $C_1(i_2)-$ linear space, then it is denoted as $X_{C_1(i_2)}$.

Theorem 2.1.1: Prove that the class B is a BC - module.

Proof: Let us take two bicomplex scalars $\alpha, \beta \in BC$ and $f=(\xi_k), g=(\eta_k) \in B$. *(B, +)* is an abelian group.

The operation $BC \times B \to B$ is well defined as

$\sup_k k^k \|\alpha f\| = \|\alpha\| \sup_k k^k \|f\| < \infty, \because f \in B$. This implies that $\alpha f \in B$

Now,

1. $\alpha(f+g) = \alpha(\xi_k + \eta_k) = \alpha\xi_k + \alpha\eta_k = \alpha f + \alpha g$,

   also $\sup_k k^k \|\alpha f + \beta g\| = \sup_k k^k \|\alpha\xi_k + \beta\eta_k\| \le \|\alpha\| \sup_k k^k \|\xi_k\| + \|\beta\| \sup_k k^k \|\eta_k\| < \infty$
2. $(\alpha+\beta) f = (\alpha+\beta)\xi_k = (\alpha\xi_k + \beta\xi_k) = \alpha f + \beta f$.
3. $(\alpha\beta) f = \alpha(\beta f)$
4. $1.f = f.$

Thus, we can say that B is a BC - module.

Theorem 2.1.2: Prove that the class B' is a BC - module.

Proof: Let $\alpha, \beta \in BC$ be two bicomplex scalars and let $f = ({}^1\xi_k\, e_1), g = ({}^1\eta_k\, e_1) \in B'$.
(B, +) is an abelian group.
The operation $BC \times B' \to B'$ is well defined as

$$\sup_k k^k \|\alpha f\| = \sup_k k^k \left\| ({}^1\alpha e_1 + {}^2\alpha e_2)({}^1 f\, e_1 + {}^2 f\, e_2) \right\|$$

$$= \sup_k k^k \left\| {}^1\alpha\, {}^1\xi_k\, e_1 + {}^2\alpha . 0\, e_2 \right\|, \because {}^2 f = 0$$

$$= \left| {}^1\alpha \right| \sup_k k^k \left| {}^1\xi_k \right| < \infty$$

This implies that $\alpha f \in B'$.
Now,

1. $\alpha(f+g) = \alpha({}^1\xi_k + {}^1\eta_k) e_1 + 0\, e_2$

$$={}^1\alpha\,{}^1\xi_k\,e_1+{}^1\alpha\,{}^1\eta_k\,e_1+{}^2\alpha\,0\,e_2+{}^2\alpha\,0\,e_2$$
$$=\left({}^1\alpha\,{}^1\xi_k\,e_1+{}^2\alpha\,0\,e_2\right)+\left({}^1\alpha\,{}^1\eta_k\,e_1+{}^2\alpha\,0\,e_2\right)$$
$$=\left({}^1\alpha\,e_1+{}^2\alpha\,e_2\right)\left({}^1\xi_k\,e_1+0\,e_2\right)+\left({}^1\alpha\,e_1+{}^2\alpha\,e_2\right)\left({}^1\eta_k\,e_1+0\,e_2\right)$$
$$=\alpha f+\alpha g$$

Also,

$$\sup_k k^k\left\|\alpha f+\alpha g\right\|=\sup_k k^k\left\|\alpha\,{}^1\xi_k\,e_1+\alpha\,{}^1\eta_k e_1\right\|\le\left|{}^1\alpha\right|\sup_k k^k\left|{}^1\xi_k\right|+\left|{}^1\alpha\right|\sup_k k^k\left|{}^1\eta_k\right|<\infty$$

2. $(\alpha+\beta)f=(\alpha+\beta)\,{}^1\xi_k\,e_1=({}^1\alpha\,{}^1\xi_k+{}^1\beta\,{}^1\xi_k)e_1+({}^2\alpha.0+{}^2\beta.0)e_2.$

$$=({}^1\alpha\,e_1+{}^2\alpha\,e_2)\,{}^1\xi_k\,e_1+({}^1\beta\,e_1+{}^2\beta\,e_2)\,{}^1\xi_k\,e_1$$
$$=\alpha f+\beta f$$

3. $(\alpha\beta)f=\left({}^1\alpha\,{}^1\beta\,e_1+{}^2\alpha\,{}^2\beta\,e_2\right){}^1\xi_k\,e_1=({}^1\alpha\,e_1+{}^2\alpha\,e_2).({}^1\beta\,e_1+{}^2\beta\,e_2)\,{}^1\xi_k\,e_1$

$=\alpha(\beta f).$

4. $1.f=f$, where 1 is the identity element of BC.

Thus, we can say that B' is a BC - module.

Theorem 2.1.3: Prove that the class B'' is a BC - module.

Proof: Let $\alpha,\beta\in BC$ be two bicomplex scalars and $f=({}^2\xi_k\,e_2),g=({}^2\eta_k\,e_2)\in B''$. $(B'',+)$ is an abelian group.

The operation $BC\times B''\to B''$ is well defined as

$$\sup_k k^k\left\|\alpha f\right\|=\sup_k k^k\left\|({}^1\alpha e_1+{}^2\alpha e_2)({}^1f\,e_1+{}^2f\,e_2)\right\|$$
$$=\sup_k k^k\left\|{}^1\alpha.0\,e_1+{}^2\alpha.{}^2\xi_k\,e_2\right\|,\because{}^1f=0$$
$$=\left|{}^2\alpha\right|\sup_k k^k\left|{}^2\xi_k\right|<\infty$$

This implies that $\alpha f\in B''$.

Now,

1. $\alpha(f+g)=({}^1\alpha\,e_1+{}^2\alpha\,e_2)\left[\left({}^1f+{}^1g\right)e_1+\left({}^2f+{}^2g\right)e_2\right]$

$$={}^1\alpha\left({}^1f+{}^1g\right)e_1+{}^2\alpha\left({}^2f+{}^2g\right)e_2$$
$$={}^1\alpha\left(0+0\right)e_1+{}^2\alpha\left({}^2\xi_k+{}^2\eta_k\right)e_2$$
$$=\left({}^1\alpha\,e_1+{}^2\alpha\,e_2\right)\left(0\,e_1+{}^2\xi_k\,e_2\right)+\left({}^1\alpha\,e_1+{}^2\alpha\,e_2\right)\left(0\,e_1+{}^2\eta_k\,e_2\right)$$
$$=\alpha f+\alpha g$$

Also

$$\sup_k k^k\left\|\alpha f+\alpha g\right\|=\sup_k k^k\left\|\alpha\,{}^2\xi_k\,e_2+\alpha\,{}^2\eta_k e_2\right\|$$

$$\leq \left|{}^2\alpha\right| \sup_k k^k \left|{}^2\xi_k\right| + \left|{}^2\alpha\right| \sup_k k^k \left|{}^2\eta_k\right| < \infty$$

2. $(\alpha+\beta) f = (\alpha+\beta)\,{}^2\xi_k e_2 = [({}^1\alpha + {}^1\beta)e_1 + ({}^2\alpha + {}^2\beta)e_2]\left({}^2\xi_k e_2\right).$

$$= ({}^1\alpha + {}^1\beta).0.e_1 + ({}^2\alpha + {}^2\beta)\,{}^2\xi_k e_2$$
$$= \left({}^1\alpha e_1 + {}^2\alpha e_2\right)\left(0e_1 + {}^2\xi_k e_2\right) + \left({}^1\beta e_1 + {}^2\beta e_2\right)\left(0e_1 + {}^2\xi_k e_2\right)$$
$$= \alpha f + \beta f$$

3. $(\alpha\beta) f = \left({}^1\alpha\,{}^1\beta e_1 + {}^2\alpha\,{}^2\beta e_2\right){}^2\xi_k e_2 = ({}^1\alpha e_1 + {}^2\alpha e_2).({}^1\beta e_1 + {}^2\beta e_2)\,{}^2\xi_k e_2$

$$= \alpha(\beta f).$$

4. *1. f = f*, where *1* is the identity element of BC.

Thus, we can say that B' is a BC - module.

Theorem 2.1.4: Prove that the subclasses B' and B'' are modules over the class B that is, they are bicomplex modules.

Proof: First of all observe that B given by (2.1.1) is a ring.
For all $f = (\xi_k), g = (\eta_k), h = (\zeta_k) \in B$

1. $f + g = (\xi_k + \eta_k) = (\eta_k + \xi_k) = g + f$
2. $(f+g)+h = (\xi_k + \eta_k) + \zeta_k = \xi_k + (\eta_k + \zeta_k) = f + (g+h)$
3. There exists $0 \in B$ such that $f + 0 = f$
4. There exists $-f = (-\xi_k) \in B$ such that $f + (-f) = 0$
5. $f(gh) = \xi_k\,(\eta_k\,\zeta_k) = (\xi_k\,\eta_k)\,\zeta_k = (fg)h$
6. $f(g+h) = \xi_k\,(\eta_k + \zeta_k) = \xi_k\,\eta_k + \xi_k\,\zeta_k = f\,g + f\,h$

$$(f+g)h = (\xi_k + \eta_k)\,\zeta_k = \xi_k\,\zeta_k + \eta_k\,\zeta_k = f\,h + g\,h$$

All the above properties can be easily verified with the help of idempotent representation.
Now the classes defined by Wagh [7], B' and B'' are shown to be modules over B.
First consider

$$B' = \left\{ f : f = \left\{{}^1\xi_k e_1\right\} : \sup_{k\geq 1} k^k \left|{}^1\xi_k\right| < \infty \right\}$$

In this direction, first it is needed to prove that B' is an additive abelian group;
For all $x = \left({}^1\xi_k e_1\right), y = \left({}^1\eta_k e_1\right), z = \left({}^1\zeta_k e_1\right) \in B'$

1. $x + y = \left({}^1\xi_k e_1\right) + \left({}^1\eta_k e_1\right) = \left({}^1\xi_k + {}^1\eta_k\right)e_1 = \left({}^1\eta_k + {}^1\xi_k\right)e_1 = y + x$, since ${}^1\xi_k, {}^1\eta_k$ are complex numbers and commutativity holds for them under addition.
2. By applying the same logic,

7. Wagh, Mamta A. : "On a Class of Bicomplex Sequences", Inter. J. Trends in Math. & Stats., 3(5), 2014, 158 – 171.

$$(x+y)+z=({}^1\xi_k\, e_1+{}^1\eta_k\, e_1)+\left({}^1\zeta_k\, e_1\right)=\{\left({}^1\xi_k+{}^1\eta_k\right)+\left({}^1\zeta_k\right)\}e_1$$

$$=\left\{\left({}^1\xi_k\right)+\left({}^1\eta_k+{}^1\zeta_k\right)\right\}e_1=x+(y+z)\,,$$

since associativity under addition holds for complex numbers.

3. Zero element, $0=0e_1$, exists in B' such that $x+0=x$.
4. Additive inverse of every element is present in B'.

Let $f=(\xi_k)\in B$ and $x=({}^1\zeta_k\, e_1)\in B'$

Now define an operation $B\times B'\to B'$. This map can be defined since

$$f\times x=x\times f=\left(k^k\,\xi_k\,{}^1\zeta_k\, e_1\right)=k^k\,({}^1\xi_k\, e_1+{}^2\xi_k\, e_2)\left({}^1\zeta_k\, e_1+0e_2\right)=k^k\,{}^1\xi_k\,{}^1\zeta_k\, e_1$$

and $$\sup_{k\geq 1} k^k\left|k^k\,{}^1\xi_k\,{}^1\zeta_k\right|\leq\sup_{k\geq 1} k^k\left|{}^1\xi_k\right|.\sup_{k\geq 1} k^k\left|{}^1\zeta_k\right|<\infty,\because\left({}^1\xi_k\, e_1\right),\left({}^1\zeta_k\, e_1\right)\in B'\ .$$

Therefore, $f\times x=x\times f\in B'$.

Thus, the above map is well defined such that for all

$$f=(\xi_k),g=(\eta_k)\in B\ \ \&\ x=\left({}^1\zeta_k\, e_1\right),y=\left({}^1\mu_k\, e_1\right)\in B'$$

1. $f(x+y)=\left\{\xi_k\left({}^1\eta_k\, e_1+{}^1\mu_k\, e_1\right)\right\}=\left(k^k\,{}^1\xi_k\,{}^1\eta_k\, e_1+k^k\,{}^1\xi_k\,{}^1\mu_k\, e_1\right)=f\,x+f\,y,$
   $\because e_1{}^2=e_1, e_2{}^2=e_2, e_1e_2=0$
2. $(f+g)x=(\xi_k+\eta_k)\left({}^1\zeta_k\, e_1\right)=k^k\left({}^1\xi_k\,{}^1\zeta_k\, e_1+{}^1\eta_k\,{}^1\zeta_k\, e_1\right)$
   $=k^k\,{}^1\xi_k\,{}^1\zeta_k\, e_1+k^k\,{}^1\eta_k\,{}^1\zeta_k\, e_1$
   $=f\,x+g\,x$
3. $(f\,g)x=\left(k^k\,\xi_k\,\eta_k\right)\left({}^1\zeta_k\, e_1\right)=k^k\left(k^k\,{}^1\xi_k\,{}^1\eta_k\,.\,{}^1\zeta_k\, e_1\right)=k^{2k}\,{}^1\xi_k\,{}^1\eta_k\,{}^1\zeta_k\, e_1$
   and $f(g\,x)=(\xi_k)\left(k^k\,{}^1\eta_k\,{}^1\zeta_k\, e_1\right)=k^k\,{}^1\xi_k\,.k^k\,{}^1\eta_k\,{}^1\zeta_k\, e_1=k^{2k}\,{}^1\xi_k\,{}^1\eta_k\,{}^1\zeta_k\, e_1$
   therefore, $(f\,g)x=f(g\,x)$.
4. $1_B=\left(k^{-k}\right)$ is the identity element of B, $(1_B)x=k^k\,.k^{-k}\,{}^1\zeta_k\, e_1=\left({}^1\zeta_k\, e_1\right)=x$

Hence, B' is a module over B.

Now consider other subclass:

$$B''=\left\{f: f=\left\{{}^2\xi_k e_2\right\}:\sup_{k\geq 1} k^k\ \ \left|{}^2\xi_k\right|<\infty\right\}$$

In this also, first we prove that B'' is an additive abelian group;

For all $x=\left({}^2\xi_k\, e_2\right),y=\left({}^2\eta_k\, e_2\right),z=\left({}^2\zeta_k\, e_2\right)\in B''$

1. $x+y=\left({}^2\xi_k\, e_2\right)+\left({}^2\eta_k\, e_2\right)=\left({}^2\xi_k+{}^2\eta_k\right)e_2=\left({}^2\eta_k+{}^2\xi_k\right)e_2=y+x\,,$

since ${}^2\xi_k, {}^2\eta_k$ are complex numbers and commutativity holds for them under addition.

2. By applying the same logic

$$(x+y)+z=({}^2\xi_k\, e_2+{}^2\eta_k\, e_2)+\left({}^2\zeta_k\, e_2\right)=\{\left({}^2\xi_k+{}^2\eta_k\right)+\left({}^2\zeta_k\right)\}e_2$$

$$=\left\{\left({}^2\xi_k\right)+\left({}^2\eta_k+{}^2\zeta_k\right)\right\}e_2=x+(y+z),$$

since associativity under addition holds for complex numbers.

3. Zero element, $0=0e_2$, exists in $B"$ such that $x+0=x$.
4. Additive inverse of every element is present in $B"$.

Let $$f=(\xi_k)\in B \;\&\; x=\left({}^2\zeta_k\, e_2\right)\in B"$$

Now we define an operation $B\times B"\to B"$.

$$f\times x=x\times f=\left(k^k\,\xi_k\,{}^2\zeta_k\, e_2\right)=k^k\,({}^1\xi_k\, e_1+{}^2\xi_k\, e_2)\left(0e_1+{}^2\zeta_k e_2\right)=k^k\,{}^2\xi_k\,{}^2\zeta_k\, e_2$$

and $$\sup_{k\geq 1} k^k\left|k^k\,{}^2\xi_k\,{}^2\zeta_k\right|\leq \sup_{k\geq 1} k^k\left|{}^2\xi_k\right|.\sup_{k\geq 1} k^k\left|{}^2\zeta_k\right|<\infty, \because \left({}^2\xi_k\, e_2\right),\left({}^2\zeta_k\, e_2\right)\in B" .$$

Therefore, $f\times x=x\times f\in B"$.
Thus, the above map is well defined such that for all

$$f=(\xi_k), g=(\eta_k)\in B \;\&\; x=\left({}^2\zeta_k\, e_2\right), y=\left({}^2\mu_k\, e_2\right)\in B"$$

1. $f(x+y)=\left\{\xi_k\left({}^2\eta_k\, e_2+{}^2\mu_k\, e_2\right)\right\}=\left(k^k\,{}^2\xi_k\,{}^2\eta_k\, e_2+k^k\,{}^2\xi_k\,{}^2\mu_k\, e_2\right)=f\,x+f\,y$

   Since, ${e_1}^2=e_1, {e_2}^2=e_2, e_1e_2=0$

2. $$(f+g)x=(\xi_k+\eta_k)({}^2\zeta_k\, e_2)=k^k\,({}^2\xi_k\,{}^2\zeta_k\, e_2+{}^2\eta_k\,{}^2\zeta_k\, e_2)$$
   $$=k^k\,{}^2\xi_k\,{}^2\zeta_k\, e_2+k^k\,{}^2\eta_k\,{}^2\zeta_k\, e_2$$
   $$=f\,x+g\,x$$

3. $(f\,g)x=\left(k^k\,\xi_k\,\eta_k\right)\left({}^2\zeta_k\, e_2\right)=k^k\left(k^k\,{}^2\xi_k\,{}^2\eta_k.{}^2\zeta_k\, e_2\right)=k^{2k}\,{}^2\xi_k\,{}^2\eta_k\,{}^2\zeta_k\, e_2$

   and $f(g\,x)=(\xi_k)\left(k^k\,{}^2\eta_k\,{}^2\zeta_k\, e_2\right)=k^k\,{}^2\xi_k.k^k\,{}^2\eta_k\,{}^2\zeta_k\, e_2=k^{2k}\,{}^2\xi_k\,{}^2\eta_k\,{}^2\zeta_k\, e_2$

   Therefore, $(f\,g)x=f(g\,x)$.

4. $1_B=\left(k^{-k}\right)$ is the identity element of B, $\left(1_B\right)x=k^k.k^{-k}\,{}^2\zeta_k\, e_2=\left({}^2\zeta_k\, e_2\right)=x$

Hence, $B"$ is also a module over B.

a) Construction of a BC - module, considering B and B' as complex linear spaces:

$$B'=\left\{f: f=\left\{{}^1\xi_k e_1\right\}: \sup_{k\geq 1} k^k\;\left|{}^1\xi_k\right|<\infty\right\}$$

Let α be a complex number and $f \in B'$, then

$$\alpha . f = (\alpha\, {}^{1}\xi_k) e_1 \in B'$$

Therefore, both B and B' are complex linear spaces.
We know that B is a ring and

$$B' = A_1 e_1 = (B)_{e_1}$$
$$B'' = A_2 e_2 = (B)_{e_2}$$

We have also shown that B and B' are ideals in the ring B and they have the properties

$$(B)_{e_1} \bigcap (B)_{e_2} = \{0\} \text{ and}$$

$B = B_{e_1} + B_{e_2}$, idempotent decomposition of B.

Both the ideals are uniquely determined but their elements admit different representations.
$(\xi_k) \in B$ can be written as

$$\xi_k = z_{1k} + i_2\, z_{2k} = \beta_{1k}\, e_1 + \beta_{2k}\, e_2 \qquad (3.1.1)$$

where,

$$\beta_{1k} = z_{1k} - i_1\, z_{2k}$$
$$\beta_{2k} = z_{1k} + i_1\, z_{2k}$$

(β_{1k}) and (β_{2k}) are complex sequences i.e., $\beta_{1k}, \beta_{2k} \in C_1(i_1)$.
(ξ_k) can also be written as

$$\xi_k = \eta_{1k} + i_1\, \eta_{2k} = \gamma_{1k}\, e_1 + \gamma_{2k}\, e_2 \qquad (3.1.2)$$

where,

$$\eta_{1k} = x_{1k} + i_2\, x_{2k},$$
$$\eta_{2k} = y_{1k} + i_2\, y_{2k},$$
$$\gamma_{1k} = \eta_{1k} - i_2\, \eta_{2k},$$
$$\gamma_{2k} = \eta_{1k} + i_2\, \eta_{2k}$$

All these sequences are complex sequences in $C_1(i_2)$.
(3.1.1) and (3.1.2) can be equally called the idempotent representations of a bicomplex sequence in B.

We can say that (3.1.1) is the idempotent representation for B when we consider elements are from

$$C^2(i_1) = C_1(i_1) \times C_1(i_1)$$

And (3.1.2) is the idempotent representation for B when we consider elements are from

$$C^2(i_1) = C_1(i_2) \times C_1(i_2).$$

We get similar results for both the representations. We can say that the consequences are similar but different.

Note 3.1.1: One point should be noted here that $(\beta_{1k})e_1=(\gamma_{1k})e_1$ and $(\beta_{1k})e_2=(\gamma_{1k})e_2$ although $\gamma_{1k},\gamma_{2k}\in C_1(i_2),\forall k\geq 1$ and $\beta_{1k},\beta_{2k}\in C_1(i_1),\forall k\geq 1$.
More specifically, given

$$\beta_{1k}=\mathrm{Re}(\beta_{1k})+i_1\,\mathrm{Im}(\beta_{1k})\ ,$$

the equality

$$\beta_{1k}\,e_1=\gamma_{1k}\,e_1$$

is true if and only if

$$\gamma_{1k}=\mathrm{Re}\ \beta_{1k}-i_2\,\mathrm{Im}\,\beta_{1k}\,.$$

Similarly, given

$$\beta_{2k}=\mathrm{Re}(\beta_{2k})+i_1\,\mathrm{Im}(\beta_{2k})$$

the equality

$$\beta_{1k}\,e_1=\gamma_{1k}\,e_1$$

is true if and only if

$$\gamma_{2k}=\mathrm{Re}\ \beta_{2k}-i_2\,\mathrm{Im}\,\beta_{2k}\,.\ [\text{c.f. } [1]]$$

Note 3.1.2: The decomposition $B=B_{e_1}+B_{e_1}$ can be written in any of the two equivalent forms

$$\mathrm{B}=\mathrm{A}_1\,\mathrm{e}_1+\mathrm{A}_2\,\mathrm{e}_2\,;B=(A_1)'\,e_1+(A_2)'\,e_2\,,$$

where $A_1,A_2\subseteq C_1(i_1)$ and $(A_1)',(A_2)'\subseteq C_1(i_2)$.
If B is seen as $C_1(i_1)$ - linear space, then the first decomposition becomes a direct sum.

And if seen as $C_1(i_2)$ - linear space, then the second decomposition becomes a direct sum.

Note 3.1.3: We know that idempotent representation is unique but (3.1.1) and (3.1.2) contradicts this fact. But each of them is unique in the following sense:
It is easy to show that

$$z=\beta_{1k}\,e_1+\beta_{2k}\,e_2=\eta_{1k}\,e_1+\eta_{2k}\,e_2\Rightarrow\beta_{1k}=\eta_{1k}\,,\beta_{2k}=\eta_{2k}\ ,$$

where $\beta_{1k},\beta_{2k},\eta_{1k},\eta_{2k}\in C_1(i_1)\,.$

Similarly $z=\gamma_{1k}\,e_1+\gamma_{2k}\,e_2=\xi_{1k}\,e_1+\xi_{2k}\,e_2\Rightarrow\gamma_{1k}=\xi_{1k}\,,\gamma_{2k}=\xi_{2k}\,,$

where $\gamma_{1k},\gamma_{2k},\xi_{1k},\xi_{2k}\in C_1(i_2)\,.$

Hence, idempotent representation for B is unique.

Ref

1. Alpay D., Luna – Elizarrarás M. E., Shapiro M., Struppa D.C. : "Basics of Functional Analysis" with Bicomplex Scalars, and Bicomplex Shur Analysis", arXiv 2013.

Note 3.1.4: The idempotent decomposition of B, $B=B_{e_1}+B_{e_1}$, plays an important role, as it allows to realize component wise the operations on B:

$$(\xi_k)=\left({}^1\xi_k\, e_1+{}^2\xi_k\, e_2\right)\ ,(\eta_k)=\left({}^1\eta_k\, e_1+{}^2\eta_k\, e_2\right)$$

$\lambda={}^1\lambda\, e_1+{}^2\lambda\, e_2$, then

$$\xi_k+\eta_k=\left({}^1\xi_k\, e_1+{}^2\xi_k\, e_2\right)+\left({}^1\eta_k\, e_1+{}^2\eta_k\, e_2\right)=\left({}^1\xi_k+{}^1\eta_k\right)e_1+\left({}^2\xi_k+{}^2\eta_k\right)e_2$$

$$\lambda(\xi_k)=\left({}^1\lambda\,{}^1\xi_k\right)e_1+\left({}^2\lambda\,{}^2\xi_k\right)e_2\,.$$

When B is considered as $C_1(i_1)$ - linear space we write $B_{C_1(i_1)}$ and when as $C_1(i_2)$ - linear space, it is written as $B_{C_1(i_2)}$.

B_{e_1} and B_{e_2} are R - linear, $C_1(i_1)$ - linear, $C_1(i_2)$ - linear and BC - modules.

We can write $B=B_{e_1}\oplus B_{e_2}$, where the direct sum $\oplus$ can be understood in the sense of R - , $C_1(i_1)$ - , $C_1(i_2)$ - linear spaces, as well as BC - modules.

References Références Referencias

1. Alpay D., Luna – Elizarrarás M. E., Shapiro M., Struppa D.C. : "Basics of Functional Analysis" with Bicomplex Scalars, and Bicomplex Shur Analysis", arXiv 2013.
2. Price, G. Baley : "An Introduction to Multicomplex spaces and functions",Marcel Dekker, Inc., 1991.
3. Segre C. : "Le Rappresentazioni Reali Delle Forme complesse e Gli Enti Iperalgebrici" Math. Ann., 40, 1892, 413-467.
4. Srivastava, Rajiv K. & Srivastava, Naveen K. : "On a class of Entire Bicomplex sequences", South East. Asian J. Math & Math. Sc. 5(3), 2007, pp. 47-68.
5. Srivastava, Rajiv K. : "Certain topological aspects of Bicomplex space", Bull. Pure & Appl. Math. Dec., 2(2), 2008, 222-234.
6. Wagh, Mamta A. : "On certain spaces of Bicomplex sequences ", Inter. J. Phy. Chem. and Math. fund.(IJPCMF), 7(1), 2014, 1 – 6.
7. Wagh, Mamta A. : "On a Class of Bicomplex Sequences", Inter. J. Trends in Math. & Stats., 3(5), 2014, 158 – 171.

Notes

Global Journal of Science Frontier Research: F
Mathematics and Decision Sciences
Volume 16 Issue 3 Version 1.0 Year 2016
Type : Double Blind Peer Reviewed International Research Journal
Publisher: Global Journals Inc. (USA)
Online ISSN: 2249-4626 & Print ISSN: 0975-5896

Effects of Nonisothermality and Wind-Shears on the Propagation of Gravity Waves (II): Ray-Tracing Images

By J. Z. G. Ma
California Institute of Integral Studies, United States

Abstract- We investigate the effects of the wind shears and nonisothermality on the ray propagation of acoustic-gravity waves in a nonhydrostatic atmosphere by generalizing *Marks & Eckermann's* WKB ray-tracing formalism (1995: J. Atmo. Sci., 52, 11, 1959-1984; cited as ME95). Five atmospheric conditions are considered, starting from the simplest isothermal and shearfree case. In every step case a set of ray equations is derived to numerically code into a global ray-tracing model and calculate the profiles of ray paths in space and time, wavelengths and intrinsic wave periods along the rays, meanfield temperature or horizontal zonal/meridional wind speeds, as well as their gradients, and the WKB criterion parameter, δ. Results include, but not limited to, the following: (1) Rays in shear-free and isothermal atmosphere follow straight lines in space; both forward and backward-mapping rays are superimposed upon each other; wavelengths ($\lambda_{x,y,z}$), as well as the intrinsic wave period (τ), keep constant versus altitude. (2) If Hines' locally isothermal condition is applied, i.e., including the effect of temperature variations in altitude, ray traces become non-straight; however, their projections in the horizontal plane keep straight; the forward and backward ray traces are no longer overlain; and, $\lambda_{x,y,z}$ show discernable changes but τ does not change. All the modulations happen at around 80-150 km altitudes.

GJSFR-F Classification : *MSC 2010: 76B15*

Strictly as per the compliance and regulations of :

Notes

Effects of Nonisothermality and Wind-Shears on the Propagation of Gravity Waves (II): Ray-Tracing Images

J. Z. G. Ma

Abstract- We investigate the effects of the wind shears and nonisothermality on the ray propagation of acoustic-gravity waves in a nonhydrostatic atmosphere by generalizing *Marks & Eckermann*'s WKB ray-tracing formalism (1995: J. Atmo. Sci., 52, 11, 1959-1984; cited as ME95). Five atmospheric conditions are considered, starting from the simplest isothermal and shearfree case. In every step case a set of ray equations is derived to numerically code into a global ray-tracing model and calculate the profiles of ray paths in space and time, wavelengths and intrinsic wave periods along the rays, meanfield temperature or horizontal zonal/meridional wind speeds, as well as their gradients, and the WKB criterion parameter, δ. Results include, but not limited to, the following: (1) Rays in shear-free and isothermal atmosphere follow straight lines in space; both forward and backward-mapping rays are superimposed upon each other; wavelengths ($\lambda_{x,y,z}$), as well as the intrinsic wave period (τ), keep constant versus altitude. (2) If Hines' locally isothermal condition is applied, i.e., including the effect of temperature variations in altitude, ray traces become non-straight; however, their projections in the horizontal plane keep straight; the forward and backward ray traces are no longer overlain; and, $\lambda_{x,y,z}$ show discernable changes but τ does not change. All the modulations happen at around 80-150 km altitudes. If the temperature constraint is relaxed to the nonisothermal condition by adding the effect of temperature gradients in x, y, z and t, the results do not exhibit perceptible differences. (3) If the atmosphere is only isothermal, rays are violently modulated by the zonal and meridional winds, and their shears in z, as well as gradients in x, y, t particularly during the 80-150 km altitudes where $\lambda_{x,y,z}$ and τ exhibit the most conspicuous modifications. More importantly, the forward and the backward rays never propagate along the same paths. If the isothermal condition is updated to the nonisothermal one by adding the effects of temperature gradients in x, y, z and t, modulations of the physical parameters in 0-80 km altitudes become significant. (4) While the WKB δ is below 0.4 in the Hines' model, it can be driven to close to 3 by the wind shears and nonisothermality in realistic atmosphere. In addition to the above, features of ray propagations under different initial wavelengths are also discussed.

I. Introduction

Gravity stratifies atmosphere and modifies the propagation of acoustic wave through a restoring force, namely, the buoyancy force, leading to the formation of acoustic-gravity wave, consisting of relatively higher-frequency acoustic and lower-frequency gravity branches (*Lamb* 1908; 1910). This force produces atmospheric oscillations featured by the buoyancy frequency, ω_b (isothermal condition) or ω_B (nonisothermal condition), also well-known as the Brunt-Väisälä frequency, satisfying (*Väisälä* 1925; *Brunt* 1927; *Eckart* 1960; *Hines* 1960; *Tolstoy* 1963)

$$\omega_b^2 = (\gamma - 1)\frac{g^2}{C^2}, \text{ or } \omega_B^2 = (\gamma - 1)\frac{g^2}{C^2} + \frac{g}{C^2}\frac{\mathrm{d}C^2}{\mathrm{d}z} \tag{1}$$

Author: *California Institute of Integral Studies, San Francisco, CA, USA. e-mail: zma@mymail.ciis.edu*

Global Journal of Science Frontier Research (F) Volume XVI Issue III Version I Year 2016
37

where γ is the adiabatic index; g is the gravitational constant; C is the speed of sound, and z is the vertical coordinate of the atmospheric frame of reference.

Acoustic-gravity waves were firstly found to be responsible for ionospheric ripples (*Hines* 1960), a traveling disturbance in space plasmas which causes the fading of radio signals (e.g., *Mimno* 1937; *Pierce & Mimno* 1940; *Munro* 1950, 1958; *Martyn* 1950; *Toman* 1955; *Heisler* 1958; *Hooke* 1968). In essence, the upward propagating waves are amplified by the exponential decrease in atmospheric density so as to trigger observable impulsive vertical undulations in Earth's atmosphere, transfer momentum and energy to plasma particles in ionosphere, and bring about detectable variations in parameters like, electron density (*Hines* 1972; *Peltier & Hines* 1976). This model was supported by a bulk of experiments (e.g., *Gershman & Grigor'ev* 1968; *Vasseur et al.* 1972; *Francis* 1974), e.g., the ionospheric observations following nuclear detonations in the atmosphere (*Hines* 1967; *Row* 1967). Tens of years of theoretical and experimental studies exposed that the possible origin of the waves also included other natural or artificial sources like, solar-wind irregularities, solar eclipses, meteors, polar and equatorial electrojets, rocket launches, thunderstorms, cold waves, tornadoes, tropical cyclones, vortexes, volcanic eruptions, tsunamis, earthquakes (e.g., *Bolt* 1964; *Harkrider* 1964; *Pierce & Coroniti* 1966; *Cole & Greifinger* 1969; *Tolstoy & Lau* 1971; *Francis* 1975; *Richmond* 1978; *Röttger*, 1981; *Huang et al.* 1985; *Fovell et al.* 1992; *Igarashi et al.* 1994; *Calais et al.* 1998; *Wan et al.* 1998; *Grigorev* 1999; *Šauli & Boška* 2001; *Fritts & Alexander* 2003, *Kanamori* 2004). Unexpectedly, space experiments confirmed that the excited waves were intrinsically linked to chemical processes in the airglow emissions in thermosphere, such as the hydroxyl (OH) nightglow fluctuations (e.g., *Krassovsky* 1972; *Peterson* 1979; *Walterscheid et al.* 1986), the 6300 Å redline (e.g., *Sobral et al.* 1978; *Hines & Tarasick* 1987; *Mendillo et al.* 1997; *Kubota et al.* 2001), and the far-ultraviolet 1356 Å emission (e.g., *Paxton et al.* 2003; *DeMajistre et al.* 2007).

The pioneer theoretical studies on acoustic-gravity waves happened during the 1950s and 1960s, when rudimentary theories and myriad effects of the waves had been investigated, as recorded by *Gossard & Munk* (1954); *Eckart* (1960); *Tolstoy* (1963); *Journal of Atmospheric and Terrestrial Physics* (1968); *Georges* (1968); *AGARD* (1972), and *Francis* (1975). Since then, particularly after the 1980s with the aid of ground-based and space-based measurements (e.g., radar, GPS), the understanding on the wave physics and its role played in the interactions between atmosphere and ionosphere have been made considerable progress (see details in, e.g., *Fritts* 1984,1989; *Hocke & Schlegel* 1996; *Fritts & Alexander* 2003; *Fritts & Lund* 2011). The advances rely dominantly on three kinds of approaches: (1) WKB (Wentzel-Kramers-Brillouin) approximation; (2) full-wave formulation; and (3) ray-tracing mapping. All of these methods intend to obtain solutions of respective set of perturbation equations originated from the same set of Navier-Stokes equations of the atmosphere under different conditions, based on the problems concerned.

Initiated by *Hines* (1960), WKB modeling draws the most attention due to its effectiveness to provide the vertical profiles of atmospheric perturbations by assuming the horizontal components of parameters, as well as the background atmosphere, change only slowly over the wave cycles of the vertical variations (*Pitteway & Hines* 1963; *Einaudi & Hines* 1970; *Hines* 1974; *Beer* 1974; *Gill* 1982; *Hickey & Cole* 1988; *Nappo* 2002; *Vadas* 2007), while the variation (k_m) of the vertical wavenumber (m) in altitude (z), $k_m = \partial(\ln m)/\partial z$,

Notes

is much smaller than m, i.e., $\delta = k_m/m \ll 1$; for large δ, this condition was assumed broken and waves were generally suggested reflected vertically (e.g., *Marks* & *Eckermann* 1995; cited as ME95 hereafter). The WKB approximation makes it valid to apply Taylor expansion to the set of Navier-Stokes equations of continuity, momentum, and energy, by assuming the solutions have the form of $\sim \exp[\pm i(kx + ly + mz - \omega t) + z/(2H)]$, where x and y are horizontal coordinates in the zonal and meridional directions, respectively, with corresponding wavenumbers k and l, H is the scale height, t is time, and ω is the ground-relative (Eulerian) wave angular frequency (e.g., *Hines* 1963; *Midgley* & *Liemohn* 1966; *Volland* 1969; *Francis* 1973; *Hickey* & *Cole* 1987; *Holton* 1992; *Fritts* & *Alexander* 2003). Neglecting ion-drag, viscosity and molecular diffusion below 200 km altitude, and using Hines' locally isothermal atmosphere which is horizontally uniform with background wind U along x and V along y, which are all shear-free in z, a classical dispersion equation can be obtained as follows (*Eckart* 1960; *Eckermann* 1997):

$$\Omega^2 \left(k_h^2 + k_z^2 - \frac{\Omega^2 - f^2}{C^2} \right) = \omega_b^2 k_h^2 + f^2 k_z^2 \tag{2}$$

where $\Omega = \omega - kU - lV$ is the intrinsic frequency, $f = 2\Omega_E \sin\phi$ is the Coriolis parameter (Ω_E is Earth's rotation rate and ϕ is latitude), $k_h^2 = k^2 + l^2$, $k_z^2 = m^2 + 1/(4H^2)$.

For the dissipative terms, *Pitteway* & *Hines* (1963) took advantage of a complex dispersion equation to confirm that they do contribute non-negligible effects at meteor heights. Besides, the shear-related Richardson number R_i was verified to provide a criterion, $R_i \sim 1/4$, which is a necessary but not sufficient condition for dynamic instability; however, this criterion might not rigorously apply to cases where the wind shear is tilted from zenith or when the molecular viscosity is important (*Hines* 1971; *Dutton* 1986; *Sonmor* & *Klaassen* 1997; *Liu* 2007). What is more, if more nonhydrodynamic terms (such as ion-drag) are included, the complexity of solving the perturbed equations made it hard to give as simple an expression of the dispersion relation as Eq.(2). Instead, *Francis* (1973); *Hickey* & *Cole* (1987) suggested a polynomial equation to demonstrate the dispersive properties of acoustic-gravity waves in the absence of wind shears, $\sum_j D_j R^j = 0$, where function R in the square of the complex vertical wave number, $\kappa = m + i/(2H)$, in which m becomes a complex; D_i is complex coefficient; and j is the number of the Navier-Stokes equations. Studies showed that the mean-field winds has a filter effect on waves (*Mayr et al.* 1984, 1990); and, waves of about 15-30 min periods and 200-400 km horizontal wavelengths are able to reach as high as 300 km altitude in the presence of dissipative terms (*Sun et al.* 2007). Note that the second point was in contrast with *Vadas* & *Fritts* (2004)'s earlier argument that the waves above ~200 km are often linked to auroral sources at high latitudes.

Unlike the WKB model, the full-wave formulation provides all the solutions of the perturbed equations, not only the WKB ones, but also those that rigorously accounts for the wave reflection. The formalism made use of the tridiagonal algorithm (*Bruce et al.* 1953; *Lindzen* & *Kuo* 1969) and assumed a single monochromatic wave of the form $f(z)e^{i(\omega t - kx - ly)}$ in an inhomogeneous atmosphere from the neutral troposphere upward to the mesosphere (50-85 km in altitude; i.e., ionospheric D region), and to a maximum altitude of 800 km in the F region, where $f(z)$ is a perturbation function as a function of z (e.g., *Yeh* & *Liu* 1974; *Lindzen* & *Tung* 1976; *Hickey et al.* 1997,2000; *Liang et*

al. 1998; *Schubert et al.* 2003). Note that there was no waveforms in z. In this case, all factors existing in realistic atmosphere can be considered, such as, height-dependent mean temperature, damping term associated with ion drag, molecular viscosity and thermal conduction, the filtering of background winds; the eddy and the molecular diffusion of heat and momentum, etc., subject to boundary conditions. The model provided the magnitude and phase of the perturbed z-dependent temperature, pressure, horizontal and vertical wind speeds (e.g., *Klostermeyer* 1972a,b,c; *Hickey et al.*, 1997, 1998, 2000, 2001; *Walterscheid* & *Hickey* 2001; *Schubert et al.* 2005). The model was not only applied to analyze Earth's acoustic waves (*Hickey et al.* 2001; *Schubert et al.* 2005; *Walterscheid* & *Hickey* 2005) and gravity waves (*Hickey et al.* 1997; *Walterscheid* & *Hickey* 2001), but also used for gravity-wave heating and cooling in Jupiters thermosphere (*Hickey et al.* 2000; *Schubert et al.* 2003).

By contrast, ray-tracing mapping is theoretically based on the WKB approximation. It comes from Fermat's principle in terms of Hamiltonian equations (*Landau* & *Lifshitz* 1959; *Whitham* 1961; *Yeh* & *Liu* 1972). In the application to acoustic-gravity waves, it formulates the spatial and temporal evolutions of a wave packet in a background wind with velocity $\mathbf{v}_0$, constrained by the WKB-approximated dispersion relation, $\omega = \omega(\mathbf{x}, \mathbf{k})$, where ω is the ground-based Eulerian or extrinsic wave frequency, $\mathbf{x}$ and $\mathbf{k}$ are the 3D position and wavenumber vectors, respectively (e.g., *Jones* 1969; *Lighthill* 1978; ME95; *Ding et al.* 2003). After *Hines* (1960) suggested that the upward propagating gravity waves can be reflected or refracted by mean-field winds, and, *Thome* (1968); *Francis* (1973) proposed that zero and higher order gravity wave modes under different isothermal conditions are able to travel horizontally as far as thousands of km, *Cowling et al.* (1971) discussed the background wind effects on the ray paths and proposed a directional filtering model. The authors argued that if gravity waves go along the winds, the intrinsic frequency is shifted downward; If the waves propagate against the winds, reflection may appear. *Yeh* & *Webb* (1972) and *Waldock* & *Jones* (1984) confirmed the filtering effect exerted by the winds on waves in a stratified atmosphere. The reflection was found to occur when wave propagate against wind; and, it is impossible for the waves to penetrate through either along or against high-speed winds. These studies were extended in a wider scope. For example, *Bertin et al.* (1975) adopted a reverse ray-tracing model to study the mechanism of wave excitation by wind perturbations in a jet stream bordering the polar front. *Waldock* & *Jones* (1984) considered the diurnal variation of the wind in the ray-tracing method. *Zhong et al.* (1995) examined the wind influence on the propagation of gravity waves in different seasons, and extended the ray-tracing simulations by including the tidal wind that has temporal and vertical variations in the study of the wave propagation through the middle atmosphere.

Particularly, ME95 set up a generalized, 3D WKB ray-tracing model to accommodate gravity waves of all frequencies in a rotating, stratified, compressible, but isothermal, nondissipative atmosphere. The nonhydrostatic model took advantage of three derived equations in dispersion, refraction, and amplitude, where excluded were wind shears, temperature gradients, and time-dependent components of the mean-field parameters. Based on Hines' locally isothermal dispersion relation, the authors exposed that the decrease in the horizontal wavenumber causes the reduction in the high-frequency cutoff; turbulent damping is more important than scale-related radiative damping; and climatological planetary waves heavily modulate ray paths of waves launched from different longitudes. After ME95's contribution, *Ding et al.* (2003) employed the same Hines' model and adopted the HWM93 wind & MSISE90 atmospheric models (*Hedin* 1991; *Hedin et al.* 1991) for

a detailed investigation on the relation between the waves and the winds. They obtained that, in response to the directions of the winds, waves are divided into three types: cut-off, reflected, and propagating; and, the ray paths of the waves can be horizontally prolonged, vertically steepened, reflected, or critically coupled. A more recent work was done by Wrasse et al. (2006) in the absence of dissipative terms. The authors followed ME95's study and derived reverse ray-tracing equations to estimate the sources of the gravity wave disturbances from wave signatures observed at 23°S (Brazil) and 7°S (Indonesia) by airglow imagers.

Notes

However, acoustic-gravity waves are so complicated in their propagation through the atmosphere that it is important to take into account convection, wind shear, dissipation, sources of transport in heat, momentum, and constituents (*Fritts & Alexaander* 2003). It is thus important to develop Hines' isothermal dispersion relation to a more general one which is able to expose the influences of factors like temperature gradient, Coriolis force, wind shear, molecular viscosity, thermal diffusivity, and ion-drag, in order to, on the one hand, understand the damping mechanism and physical effects of the waves in the coupling between atmosphere and ionosphere; on the other hand, validate and/or provide a reference to the numerical full-wave solutions. Toward this goal, an influential advance has been achieved in a series of contributions on isothermal and shear-free, but dynamically viscous and thermally diffusive atmosphere by *Vadas & Fritts* (2001, 2004, 2005, 2009). The work was recognized as the "*Vadas-Fritts* ray-tracing model" (cited as VF model hereafter), which consists of a near-field Fourier-Laplace integral representation for the around the convective source region, where rays are launched with initial conditions deduced there, and a far-field ray-tracing mapping for the propagation of the gravity waves binned in space-time grid cells, and the path of each ray is determined by its spectral amplitude and by the local density of rays within the grid cells (see details in Section 2 of *Broutman & Eckermann* 2012).

Said study improved over past efforts on WKB ray-tracing technique. Unlike using the traditional "complex-m approach" usually used in atmospheric physics by assuming a complex vertical wave number $(m_r + im_i)$ and a real wave frequency ω in, e.g., *Pitteway & Hines* (1963), the VF model adopted a "complex-ω approach" which is always employed in plasma physics by incorporating a complex wave frequency $(\omega_r + i\omega_i)$ but a real m into the dispersion relation. Otherwise, the authors claimed that the derived compressible, complex, dispersion equation, equipped with terms of molecular viscosity (ν) and thermal diffusivity (incorporated in the Prandtl number Pr), was unable to be solved. Though via a different approach, the model led to similar results as those obtained by *Pitteway & Hines* (1963), such as, wave damping by thermal conduction is the same order as viscous damping; amplitude of perturbations in an inviscid atmosphere always keeps constant, in addition to the factor of $1/(2H)$, regardless of any positions in space; in a viscid atmosphere, the wave growth depends entirely on ν. More significantly, the authors found that waves in high frequencies and large vertical wavelengths will propagate to high altitudes, and it is the integrated viscosity effect, rather than the local value of viscosity, that determines wave dissipation; molecular viscosity and thermal diffusivity act as filters on the wave spectrum, allowing only those high-frequency, large vertical wavelength waves to propagate up to high altitudes. The model was assumed not only to interpret measurements such as the airglow data near 85 km altitude (*Vadas et al.* 2009), but also to explain the ionospheric soundings near 250 km altitude (*Vadas & Crowley* 2010).

The achievements introduced above under isothermal and shear-free conditions are of great importance for us to gain fundamental understandings on the physics of generalized

acoustic-gravity waves, and then, based on this knowledge, to take incremental steps for suitable solutions of more realistic problems. Such a problem has arisen in last 15 years since lidar facilitates recorded both large wind shears (e.g., 100 m/s per km) and large temperature gradient (up to 100 °K per km) between ∼85 and 95 km altitudes (*Liu et al.* 2002; *Fritts et al.* 2004; *Franke et al.* 2005; *She et al.* 2006, 2009). Spaceborne data also confirmed that the criterion of wind-shear related Richardson number, $R_i \leq 1/4$, appeared to reach 1 at 90 km altitude over Svalbard (78°N, 16°E; *Hall et al.* 2007); and, measurements of airglow layer perturbations in O(^{1}S) (peak emission altitude ∼97 km) and OH (peak emission altitude ∼87 km) driven by propagating acoustic-gravity waves suggested that the factor of $1/(2H)$ should be modified by $(1-\beta)/(2H)$, where β is the so-called "damping factor" (*Liu & Swenson* 2003; *Vargas et al.* 2007). This parameter is positive, varying between 0.2 and 1.69 with a stronger positive correlation with the meridional wind shear than the zonal one, and a positive correlation for waves of shorter than 40 km vertical wavelengths, while a negative correlation for longer ones (*Ghodpage et al.* 2014). Considering the fact that both the ion drag and Coriolis force can be neglected below 600 km (*Volland* 1969), and viscosity can also be omitted as compared with heat conductivity within the same heights, while below about 200 km the later itself turns out to be evanescent (*Harris & Priester* 1962; *Pitteway & Hines* 1963; *Volland* 1969), influences by both wind shears and nonisothermality were consequently regarded as the candidates to exert impacts on the propagation of gravity waves through realistic mesosphere and lower thermosphere. The most recent study by *Ma et al.* (2014) exposed that (1) Wind shears and nonisothermality modulate Hines' model in both real and imaginary vertical wavenumbers. While negligible below 80 km altitude, the modulation is appreciable above 80 km altitude. It drives the atmosphere into a "sandwich" structure with three layers: 80-115 km, 115-150 km, and 150-200 km. (2) "Damping factor", β, keeps positive in the top and bottom layers where wave attenuations (damping effect) appear, while it is negative in the middle layer where wave intensification (amplifying effect) occurs. The sign of β is determined by $\cos\theta$, where θ is the angle between the mean-field wind velocity and horizontal wave vector. (3) The strongest intensification happens at 125 km altitude at which the imaginary vertical wave-number, m_i, is - 0.25 km^{-1}; the three strongest attenuations happen at 90, 100, 180 km altitudes with m_i =+0.01, +0.03, +0.05 km^{-1}, respectively. (4) Within the acoustic and gravity wave-periods, usually no more than tens of minutes, the Coriolis effect plays an unrecognized role, whileas it affects the inertial waves, the waveperiod of which is in the order of hours.

Therefore, the isothermal and shear-free assumptions may be inadequate to be applied for a quantitative explanation of the observations in much more complicated situations in atmosphere, especially in the modeling and analyses of spaceborne data from, e.g., RADAR, GPS. Nevertheless, we argue that the formalism under previous assumptions is help ful, at least qualitatively speaking, as a good reference for us to treat realistic atmospheric situations (e.g., *Wrassea et al.* 2006) where both the temperature and wind gradients in the vertical direction are unable to be neglected, as demonstrated by the airglow measurements below 200 km altitude. It is thus necessary to take into account these important factors in ray-tracing imaging so as to have a better understanding on the propagation of acoustic-gravity waves in the presence of nonisothermality and wind shears. This paper will extend the VF model by incorporating the vertical temperature inhomogeneity and wind shear into a perturbed set of mass, momentum, and energy equations, but adopting ME95's simplification of ignoring the dissipation terms (i.e., molecular viscosity, heat source, ion drag). The negligence of these terms had already been validated by classical work of, e.g., *Harris & Priester* (1962); *Pitteway & Hines* (1963); *Volland* (1969). We follow ME95's algebra and nomenclature by taking the traditional complex-k_z approach

to manipulate dispersion equation for ray-tracing equations, rather than the complex-ω algebra used in the VF model. In order to clearly illustrate the propagating paths of 3D rays driven by diverse, localized, and intermittent sources (such as, tsunami, volcano) in realistic atmosphere, we intentionally expand the inviscid heights from 0∼200 km to 0∼300 km in ray-tracing simulations.

The structure of the paper is as follows. Section 2 develops ME95's locally isothermal ray-tracing model to a generalized set of ray-tracing equations of acoustic-gravity waves under wind-shearing and nonisothermal conditions. Section 3 presents numerical results of ray-tracing images in five different atmospheric situations, starting from the simplest isothermal and shear-free model to the most complicated nonisothermal and wind-shearing model, to expose the effects of the nonisothermality and wind shears. The vertical profile of the WKB δ parameter is also exhibited under some typical situations. Section 4 offers a quick summary and discussion. SI units are used throughout the paper, with exceptions noted wherever necessary.

Notes

II. Ray-Tracing Equations

a) Formulation

The classical formulation of ray-tracing theory is briefly described as follows. Let ω be the ground-based (Eulerian, or, extrinsic) wave frequency, $\mathbf{r} = \{x, y, z\}$ and $\mathbf{k} = \{k, l, m_r\}$ are the position vector, and wavenumber vector, respectively, where subscript "$_r$" attached to m denotes the "real" part of the vertical wavenumber m. It will be omitted for simplification throughout the rest of the text. Based on Fermat's principle in terms of Hamiltonian equations (e.g., *Landau* & *Lifshitz* 1959; *Whitham* 1961; *Yeh* & *Liu* 1972), the ray-path, Γ, of internal gravity waves are determined both spatially and temporally by the dispersion relationship, $\omega = \omega(\mathbf{r}, \mathbf{k})$ (e.g., *Jones* 1969; *Lighthill* 1978):

$$\Gamma = \Gamma(\mathbf{r}, t; \mathbf{k}, \omega) \tag{3}$$

and m is constrained by the WKB dispersion equation along the rays:

$$m = m(\mathbf{r}, t; k_h, \omega) \tag{4}$$

For any rays with a generalized phase Φ,

$$\Phi = \int_{\Gamma(t)} (\omega \mathrm{d}t - \mathbf{k} \cdot \mathrm{d}\mathbf{r}) \tag{5}$$

only those with steady phase values are able to be observed and measured. Mathematically, this requires that the variation of Φ is zero, namely,

$$\delta\Phi = \delta \int_{\Gamma(t)} G \mathrm{d}t = \delta \int_{\Gamma(t)} \left(\omega - \mathbf{k} \cdot \frac{\mathrm{d}\mathbf{r}}{\mathrm{d}t} \right) \mathrm{d}t = 0 \tag{6}$$

in which

$$G = \omega - \mathbf{k} \cdot \frac{\mathrm{d}\mathbf{r}}{\mathrm{d}t} \tag{7}$$

is a functional to be integrated. The calculus of variations provides the following set of differential equations:

$$\frac{\partial G}{\partial \omega}=0\ ,\ \frac{\partial G}{\partial \mathbf{k}}=0\ ,\ \frac{\partial G}{\partial \mathbf{r}}-\frac{\mathrm{d}}{\mathrm{d}t}\frac{\partial G}{\partial \dot{r}_t}=0 \tag{8}$$

where $\dot{r}_t=\mathrm{d}\mathbf{r}/\mathrm{d}t$. Specifically, the set of vector equations is as follows:

$$\frac{\mathrm{d}\mathbf{x}}{\mathrm{d}t}=\frac{\partial \omega}{\partial \mathbf{k}}=\frac{\partial(\Omega+\mathbf{k}\cdot\mathbf{v}_0)}{\partial \mathbf{k}},\ \text{or},\ \mathbf{c}_g=\mathbf{v}_0+\mathbf{c}_{g*} \tag{9}$$

and

$$\frac{\mathrm{d}\mathbf{k}}{\mathrm{d}t}=-\frac{\partial \omega}{\partial \mathbf{x}}=-\frac{\partial(\Omega+\mathbf{k}\cdot\mathbf{v}_0)}{\partial \mathbf{x}}=-\frac{\partial(\mathbf{k}\cdot\mathbf{v}_0)}{\partial \mathbf{x}}-\frac{\partial \Omega}{\partial \mathbf{x}} \tag{10}$$

where

$$\Omega=\omega-\mathbf{k}\cdot\mathbf{v}_0=\omega-\mathbf{k}_h\cdot\mathbf{v}_0,\quad \mathbf{c}_g=\frac{\partial \omega}{\partial \mathbf{k}},\quad \mathbf{c}_{g*}=\frac{\partial \Omega}{\partial \mathbf{k}} \tag{11}$$

are the Doppler-shifted (Lagrangian, or, intrinsic) wave frequency, the extrinsic and intrinsic group velocities, respectively, in which $\mathbf{k}_h=\{k,l\}$ and $\mathbf{v}_0=\{U,V,0\}$.

b) ME95's model and its generalization

Based on Hines (1960)'s locally isothermal and shear-free dispersion relation, ME95 developed a global WKB ray-tracing model of a set of six equations to accommodate gravity waves of all frequencies in a nonhydrostatic, rotating, stratified, and compressible atmosphere characterized by nonuniformities which are supposed to change slowly in real space (x,y,z), but keep constant in time (t), that is, wave period ($2\pi/\omega$; tens of minutes) $\ll$ Earth's daily rotation period ($1/f$ ~12 hours). As a result, the mean-field horizontal wind of velocity $\mathbf{v}_0=\{U(x,y,z),V(x,y,z),0\}$ holds $\partial U/\partial t=\partial V/\partial t=0$. The model assumed that each ray starts from an initial spatial position of specific longitude, latitude, and altitude, and both k_h and ω were supposed constant in time along ray paths due to the condition of $\partial/\partial t=0$. A set of six ray equations was obtained, as given in Eq.(A3) of ME95.

We extend ME95's model by incorporating three additional effects: (1) nonisothermal effect, i.e., $k_T\neq 0$; and (2) wind-shear effects, i.e., $\partial U/\partial z\neq 0$ and $\partial V/\partial z\neq 0$; and, (3) time-dependent effect, i.e., $\partial/\partial t\neq 0$. Consequently, not only do additional terms appear in ME95's six equations, which are related to temperature gradient and wind shears, but also a new equation to demonstrate the temporal dependence of wave frequency Ω comes into being. The set of ray equations from Eqs.(9,10) are thus expressed as follows, which generalizes ME95's Eq.(A3):

$$\left.\begin{aligned}
&\frac{\mathrm{d}x}{\mathrm{d}t}=U+c_{g*x}=U+\frac{\partial\Omega}{\partial m}\frac{\partial m}{\partial k},\ \frac{\mathrm{d}y}{\mathrm{d}t}=V+c_{g*y}=V+\frac{\partial\Omega}{\partial m}\frac{\partial m}{\partial l},\ \frac{\mathrm{d}z}{\mathrm{d}t}=c_{g*z}=\frac{\partial\Omega}{\partial m}\\
&\frac{\mathrm{d}k}{\mathrm{d}t}=-\left(k\frac{\partial U}{\partial x}+l\frac{\partial V}{\partial x}\right)-\frac{\partial\Omega}{\partial m}\frac{\partial m}{\partial x},\ \frac{\mathrm{d}l}{\mathrm{d}t}=-\left(k\frac{\partial U}{\partial y}+l\frac{\partial V}{\partial y}\right)-\frac{\partial\Omega}{\partial m}\frac{\partial m}{\partial y},\\
&\frac{\mathrm{d}m}{\mathrm{d}t}=-\left(k\frac{\partial U}{\partial z}+l\frac{\partial V}{\partial z}\right)-\frac{\partial\Omega}{\partial m}\frac{\partial m}{\partial z},\ \frac{\mathrm{d}\Omega}{\mathrm{d}t}=\frac{\partial\Omega}{\partial m}\frac{\partial m}{\partial t}
\end{aligned}\right\} \tag{12}$$

Notes

c) Ray equations under nonisothermal and wind-sheared conditions

Instead of Eq.(1b) in ME95, which was rewritten from Eq.(2) in the Introduction of this paper, the dispersion relation used in Eq.(12) is updated to the generalized expression as given by Eq.(12) of *Ma et al.* (2014):

$$m^2 = \frac{\Omega^2 - \omega_A^2}{C^2} + k_h^2 \left[\frac{\omega_B^2 - \Omega^2}{\Omega^2} - \frac{1}{2}\frac{\omega_{\mathrm{v}}^2}{\Omega^2} \left(\frac{2-\gamma}{\gamma} \frac{\Omega^2}{k_h^2 V_p V_{ph}} + \frac{1}{2}\cos\theta \right) \cos\theta \right] \tag{13}$$

in which

$$\left.\begin{aligned} &\omega_A^2 = \omega_a^2 + g k_T,\ C^2 = \gamma \tfrac{k_B T_0}{M},\ \omega_{\mathrm{v}} = \sqrt{\left(\tfrac{\mathrm{d}U}{\mathrm{d}z}\right)^2 + \left(\tfrac{\mathrm{d}V}{\mathrm{d}z}\right)^2},\ \cos\theta = \tfrac{\mathbf{k}_h \cdot \mathbf{v}_0}{k_h \sqrt{U^2+V^2}} \\ &V_p = \tfrac{\omega_{\mathbf{v}}}{k_p},\ V_{ph} = \tfrac{\Omega}{k_h};\ \text{and},\ \omega_a^2 = \tfrac{\gamma^2}{4(\gamma-1)}\omega_b^2,\ k_T = \tfrac{\mathrm{d}(\ln T_0)}{\mathrm{d}z},\ k_p = \tfrac{\mathrm{d}(\ln p_0)}{\mathrm{d}z} \end{aligned}\right\} \tag{14}$$

where ω_A and ω_a are the nonisothermal and isothermal cut-off frequencies, respectively; k_T and k_p are the scale numbers in temperature and pressure, respectively; k_B is Boltzmann's constant; T_0 is the mean-field temperature; M is the mean molecular mass of atmosphere; ω_{v} is the synthesized wind shear; θ is the angle between $\mathbf{k}_h$ and $\mathbf{v}_0$; V_p is a quasi-phase speed related to ω_{v} and k_p, and V_{ph} is the horizontal quasi-phase speed. Note that the f-terms are omitted due to their negligible roles played in the band of gravity waves. Applying Eq.(13) to Eq.(12) produces a set of generalized, nontrivial ray-tracing equations as follows, where the algebra involved is notoriously tedious but straightforward:

$$\left.\begin{aligned} &\tfrac{\mathrm{d}x}{\mathrm{d}t} = U - A_{11}k + A_{12}\tfrac{\partial U}{\partial z},\ \tfrac{\mathrm{d}y}{\mathrm{d}t} = V - A_{11}l + A_{12}\tfrac{\partial V}{\partial z},\ \tfrac{\mathrm{d}z}{\mathrm{d}t} = \tfrac{\Omega^2}{\Omega^2-\omega_B^2}A_{11}m \\ &\tfrac{\mathrm{d}k}{\mathrm{d}t} = -\left(k\tfrac{\partial U}{\partial x} + l\tfrac{\partial V}{\partial x}\right) - A_{22}k_c,\ \tfrac{\mathrm{d}l}{\mathrm{d}t} = -\left(k\tfrac{\partial U}{\partial y} + l\tfrac{\partial V}{\partial y}\right) - A_{22}l_c \\ &\tfrac{\mathrm{d}m}{\mathrm{d}t} = -\left(k\tfrac{\partial U}{\partial z} + l\tfrac{\partial V}{\partial z}\right) - A_{22}m_c,\ \tfrac{\mathrm{d}\Omega}{\mathrm{d}t} = -A_{21}\left(k\tfrac{\partial U}{\partial t} + l\tfrac{\partial V}{\partial t}\right) + A_{22}c_t \end{aligned}\right\} \tag{15}$$

in which

$$\left.\begin{aligned} &A_{11} = (\Omega^2 - \omega_B^2)\,\Omega C^2/A_0,\ A_{12} = -\Omega^3 C^2/(A_0 V_*) \\ &A_{21} = (\Omega^4 - C^2 k_h^2 \omega_B^2)/A_0,\ A_{22} = A_{12}V_*\left(K_*^2 - k_g^2 + \tfrac{\omega_{\mathrm{v}}^2}{4V_{ph}^2}\cos^2\theta\right) \\ &k_c = \tfrac{\partial(\ln C)}{\partial x},\ l_c = \tfrac{\partial(\ln C)}{\partial y},\ m_c = \tfrac{\partial(\ln C)}{\partial z},\ c_t = \tfrac{\partial(\ln C)}{\partial t} \end{aligned}\right\} \tag{16}$$

where

$$\left.\begin{aligned} &A_0 = \Omega^4 - C^2(k_h^2\omega_B^2 + K_*^2\Omega^2),\ V_* = 4V_{ph}\tfrac{k_h/k_p}{\frac{2-\gamma}{\gamma} + \frac{V_p}{V_{ph}}\cos\theta} \\ &K_*^2 = -\tfrac{1}{4}k_p\tfrac{\omega_{\mathrm{v}}}{V_{ph}}\left(\tfrac{2-\gamma}{\gamma} + \tfrac{V_p}{V_{ph}}\cos\theta\right)\cos\theta \end{aligned}\right\} \tag{17}$$

Because sound speed C is determined by temperature T, we see that the nonisothermal T-effect is converted to C-effect. Clearly, Eq.(15) demonstrates that the gradients of $\{U, V, C\}$ in the 4D spacetime (3D space + 1D time) play a leading role in the development of the ray path $\{x, y, z\}$. Note that this development is also coupled with wave vector $\{k, l, m\}$. It also deserves to stress here that the above ray equations are derived under the WKB assumption. As pointed out by *Einaudi* & *Hines* (1970); *Gossard* & *Hooke* (1975); and ME95, the validity of this condition can be exhibited by a criterion parameter, δ, expressed as (e.g., ME95)

$$\delta = \frac{1}{m}\left|\frac{\partial(\ln m)}{\partial z}\right| \tag{18}$$

Under isothermal and shear-free conditions, ME95 showed that for large δ (or, equivalently, $m \to 0$) when wave approaches a caustic, the WKB approximation breaks and ray integration terminates in simulations (see ME95 for details). The feature of this parameter will also be discussed based on our calculations.

III. Numerical Results

We expose by steps the numerical calculations of ray images about the effects of wind shears and nonisothermality on the propagation of acoustic-gravity waves, starting from the simplest case and ending at the most complicated one. We consider following five atmospheric models with six simulation steps to describe the atmosphere where ray-tracing imaging calculations are performed: (1) fully isothermal, and shear-free; (2) Hines' locally isothermal and shear-free; (3) nonisothermal and shear-free; (4) fully isothermal and wind-shearing; (5) nonisothermal and wind-shearing (generalized formulation); and, (6) nonisothermal and wind-shearing (influence of initial wavelengths). Both hydrostatic and quasi-hydrostatic cases are considered in the first two situations.

a) Fully isothermal, and shear-free atmosphere

i. *Hydrostatic*

This is the simplest case: $U = V = 0$ and T (or C) is uniform in space and constant in time. Naturally, $\nabla U = \nabla V = 0$ and $\partial U/\partial t = \partial V/\partial t = 0$. Eqs.(15-17) reduce to the following:

$$\frac{\mathrm{d}x}{\mathrm{d}t} = -A_{11}k,\ \frac{\mathrm{d}y}{\mathrm{d}t} = -A_{11}l,\ \frac{\mathrm{d}z}{\mathrm{d}t} = \frac{1}{A_0^*};\ \ \frac{\mathrm{d}k}{\mathrm{d}t} = \frac{\mathrm{d}l}{\mathrm{d}t} = \frac{\mathrm{d}m}{\mathrm{d}t} = \frac{\mathrm{d}\Omega}{\mathrm{d}t} = 0 \tag{19}$$

where

$$A_0^* = \frac{A_0}{mC^2\Omega^3},\ A_{11} = \frac{\Omega C^2}{A_0}\left(\Omega^2 - \omega_b^2\right),\ A_0 = \Omega^4 - C^2\omega_b^2 k_h^2 \tag{20}$$

Eqs.(19,20) provide following equation of 3D straight rays due to the invariant nature of all the input parameters:

$$\frac{x}{k} = \frac{y}{l} = \frac{z}{m}\left(\frac{\omega_b^2}{\Omega^2} - 1\right), \quad \text{along with } \Omega = \omega \tag{21}$$

where parameters k, l, m, ω, Ω, and ω_b are all constant in time. We arbitrarily choose horizontal wavelengths of $\lambda_x = 350$ km and $\lambda_y = 50$ km and illustrate the features of ray images in Fig.1. The top panel depicts the ray path propagating in 3D space (thick line), and its three projections (thin lines) in XY/YZ/XZ planes. The two arrows indicate both forward and backward traces, respectively, which are superimposed upon each other. The bottom four smaller panels in the figure present the propagating length and altitude of the ray versus time (upper left), the vertical profiles of sound speed C (upper right), the three wavelengths λ_x, λ_y, and λ_z (lower left), and, wave period $\tau = 2\pi/\Omega$, cut-off period $\tau_a = 2\pi/\omega_a$, and buoyancy period $\tau_b = 2\pi/\omega_b$ (lower right).

As displayed in the top panel, either the forward or the backward ray is a straight line. Relative to one end, the other end is 262.89 km away along x and 1840.2 km away along y. Clearly, $x/y = k/l$, following Eq.(21). The lapse of time that the ray travels between the two ends is given in the upper left panel of the bottom 4 small ones. It is 185 minutes, a little more than 3 hours, propagating a distance of vertically 300 km, but 1840.2 km long in space. In addition, the sound speed C is given in the upper right panel, calculated by assuming $T_0 = 288$ °K. It keeps constant at different altitudes due to the isothermal condition. Furthermore, the lower left panel exposes the vertical profiles of the three wavelengths λ_x, λ_y, and λ_z. All of them do not change versus height. Lastly, the lower right panel exposes the three periods which also keep the same in altitudes.

ii. *Quasi-hydrostatic*

If the hydrostatic condition is relaxed to quasi-hydrostatic, that is, the wind components are nonzero ($U \neq 0$ and/or $V \neq 0$) but uniform in space, while keeping other constraints unchanged, Eqs.(15-17) provide

$$\frac{\mathrm{d}x}{\mathrm{d}t} = U - A_{11}k, \ \frac{\mathrm{d}y}{\mathrm{d}t} = V - A_{11}l, \ \frac{\mathrm{d}z}{\mathrm{d}t} = \frac{1}{A_0^*} \tag{22}$$

along with the same coefficients as defined by Eq.(20). Eq.(21) is thus updated as follows:

$$\frac{x}{k - k_s} = \frac{y}{l - l_s} = \frac{z}{m}\left(\frac{\omega_b^2}{\Omega^2} - 1\right), \quad \text{along with } \Omega = \omega - \omega_s \tag{23}$$

Obviously, Eq.(23) is a generalized expression of Eq.(21) to describe straight rays in space but with shifts k_s, l_s, and ω_s in k, l, and ω, respectively:

$$k_s = \frac{U}{A_{11}} = \frac{\Omega^4 - C^2\omega_b^2 k_h^2}{\Omega C^2\left(\Omega^2 - \omega_b^2\right)}U \approx \frac{k_h^2}{\Omega}U, \ l_s = \frac{V}{A_{11}} \approx \frac{k_h^2}{\Omega}V, \ \omega_s = kU + lV \tag{24}$$

Accordingly, regardless of the shifts, rays are still straight lines propagating in space, similar to Fig.1.

b) Hines' locally isothermal and shear-free atmosphere

i. *Hydrostatic*

If the atmosphere is hydrostatic ($U = V = 0$), and T (or C) is constant in time and uniform locally (i.e., $k_T = 0$), the set of ray equations of Hines' model assumes can be obtained from Eqs.(15-17) as follows:

$$\left.\begin{array}{l} \frac{\mathrm{d}x}{\mathrm{d}t} = -A_{11}k,\ \frac{\mathrm{d}y}{\mathrm{d}t} = -A_{11}l,\ \frac{\mathrm{d}z}{\mathrm{d}t} = \frac{1}{A_0^*} \\ \frac{\mathrm{d}k}{\mathrm{d}t} = -A_{22}k_c,\ \frac{\mathrm{d}l}{\mathrm{d}t} = -A_{22}l_c,\ \frac{\mathrm{d}m}{\mathrm{d}t} = -A_{22}m_c \end{array}\right\} \tag{25}$$

where

$$\left.\begin{array}{l} A_0^* = \frac{A_0}{mC^2\Omega^3},\ A_{11} = \frac{\Omega C^2}{A_0}\left(\Omega^2 - \omega_b^2\right),\ A_{22} = \frac{\Omega^3 C^2}{A_0}k_g^2,\ A_0 = \Omega^4 - C^2k_h^2\omega_b^2 \\ k_c = \frac{\partial(\ln C)}{\partial x},\ l_c = \frac{\partial(\ln C)}{\partial y},\ m_c = \frac{\partial(\ln C)}{\partial z} \end{array}\right\} \tag{26}$$

Eq.(**??**) produces a set of ray equations:

$$\frac{\mathrm{d}x}{k} = \frac{\mathrm{d}y}{l} = \left(\frac{\omega_b^2}{\Omega^2} - 1\right)\frac{\mathrm{d}z}{m};\quad \frac{\mathrm{d}k}{k_c} = \frac{\mathrm{d}l}{l_c} = \frac{\mathrm{d}m}{m_c},\quad \text{along with } \Omega = \omega \tag{27}$$

from which we see that in the horizontal x-y plane the projection of the ray trace should be close to a straight line due to the fact that $k_c \sim l_c \ll m_c$, leading to small changes in both k and l, if there are, compared to m.

Fig.2 illustrates the ray features in Hines' locally isothermal and shear-free atmosphere in both forward (in blue) and backward (in red) propagations. The upper left panel displays the 3D traces. Clearly, the rays are no longer straight anymore, in contrast with Fig.1. Impressively, there appear dramatic changes in the range of 85-120 km in altitude. However, as predicted in the above, the projections of the rays in the x-y plane appear straight. The upper right panel shows a distinct difference between the forward and backward rays in the length and time of propagation with the same 300 km height travelled: the forward ray flies away as long as a distance of 700 km in ∼380 min (about 6.5 hours); while the backward one has a journey of 1100 km long in ∼600 min (about 10 hours). The lower two panels expose the vertical profiles of the three wavelengths λ_x, λ_y, & λ_z (left) and the three periods $\tau_a = 2\pi/\omega_a$, $\tau_b = 2\pi/\omega_b$, & $\tau = 2\pi/\Omega$ (right), respectively. Obviously, λ_x and λ_y vary little compared to λ_z; in addition, λ_z is modulated the most between 85 and 120 km altitudes; what is more, τ_a and τ_b have peaks between 85 and 100 km.

To understand the mechanism of these ray features, we plot the mean-field parameters along ray paths in both Fig.3 and Fig.4. The former presents T_0 and C (upper left panel), $\mathrm{d}T_0/\mathrm{d}x$ (upper right panel), $\mathrm{d}T_0/\mathrm{d}y$ (lower left panel), and $\mathrm{d}T_0/\mathrm{d}z$ (lower right panel); and the latter depicts ρ_0 and p_0 (upper left panel), $\mathrm{d}\rho_0/\mathrm{d}x$ (upper right panel), $\mathrm{d}\rho_0/\mathrm{d}y$ (lower left panel), and $\mathrm{d}\rho_0/\mathrm{d}z$ (lower right panel). It is seen that T_0 (or C), rather than ρ_0

(or p_0), is responsible for the profile of wave periods. More importantly, it is the gradients of T_0, rather than those of ρ_0, that are correlated evidentally with the abnormal features of the ray propagations. Note that the gradients in the horizontal plane ($\mathrm{d}T_0/\mathrm{d}x$ and $\mathrm{d}T_0/\mathrm{d}y$) is 2 or 3 orders smaller than that in the vertical direction ($\mathrm{d}T_0/\mathrm{d}z$). Thus, the vertical gradient in temperature dominates the modulation.

Notes

Fig.5 draws the altitude profiles of the WKB δ parameter in the forward and backward propagations. The parameter is lower on average in the former case than in the latter case. In either case, it is smaller than 1. Interestingly, in the 85-120 km altitudes, The magnitude becomes apparently higher than that in other altitudes.

ii. *Quasi-hydrostatic*

If the hydrostatic condition is relaxed to quasi-hydrostatic, that is, the wind components are nonzero ($U \neq 0$ and/or $V \neq 0$) but uniform in space, while keeping other constraints unchanged, Eqs.(15-17) provide

$$\left.\begin{array}{l} \frac{\mathrm{d}x}{\mathrm{d}t} = U - A_{11}k,\ \frac{\mathrm{d}y}{\mathrm{d}t} = V - A_{11}l,\ \frac{\mathrm{d}z}{\mathrm{d}t} = \frac{1}{A_0^*} \\ \frac{\mathrm{d}k}{\mathrm{d}t} = -A_{22}k_c,\ \frac{\mathrm{d}l}{\mathrm{d}t} = -A_{22}l_c,\ \frac{\mathrm{d}m}{\mathrm{d}t} = -A_{22}m_c \end{array}\right\} \tag{28}$$

where the coefficients are those expressed in Eq.(**??**). This set of equations updates Eq.(**??**) as follows:

$$\frac{\mathrm{d}x}{k-k_s} = \frac{\mathrm{d}y}{l-l_s} = \left(\frac{\omega_b^2}{\Omega^2} - 1\right)\frac{\mathrm{d}z}{m};\quad \frac{\mathrm{d}k}{k_c} = \frac{\mathrm{d}l}{l_c} = \frac{\mathrm{d}m}{m_c},\quad \text{along with } \Omega = \omega - \omega_s \tag{29}$$

in which shifts k_s, l_s, and ω_s in k, l, and ω, respectively, are already given in Eq.(24). Accordingly, regardless of the shifts, the profiles of rays are similar to Figs.2∼4 in this quasi-static case.

c) Nonisothermal and shear-free atmosphere

Realistic atmosphere is nonisothermal, i.e., $k_T \neq 0$. We therefore extend Hines' locally isothermal model for more generalized situation where ω_a and ω_b are substituted by ω_A and ω_B, respectively. To save space, we just take the hydrostatic case ($U = V = 0$) as an example. In this case, Eqs.(15-17) provide

$$\left.\begin{array}{l} \frac{\mathrm{d}x}{\mathrm{d}t} = -A_{11}k,\ \frac{\mathrm{d}y}{\mathrm{d}t} = -A_{11}l,\ \frac{\mathrm{d}z}{\mathrm{d}t} = \frac{1}{A_0^*} \\ \frac{\mathrm{d}k}{\mathrm{d}t} = -A_{22}k_c,\ \frac{\mathrm{d}l}{\mathrm{d}t} = -A_{22}l_c,\ \frac{\mathrm{d}m}{\mathrm{d}t} = -A_{22}m_c \end{array}\right\} \tag{30}$$

where

$$\left.\begin{array}{l} A_0^* = \frac{A_0}{mC^2\Omega^3},\ A_{11} = \frac{\Omega C^2}{A_0}\left(\Omega^2 - \omega_B^2\right),\ A_{22} = \frac{\Omega^3 C^2}{A_0}k_g^2,\ A_0 = \Omega^4 - C^2k_h^2\omega_B^2 \\ k_c = \frac{\partial(\ln C)}{\partial x},\ l_c = \frac{\partial(\ln C)}{\partial y},\ m_c = \frac{\partial(\ln C)}{\partial z} \end{array}\right\} \tag{31}$$

Eq.(30) produces a set of ray equations:

$$\frac{\mathrm{d}x}{k}=\frac{\mathrm{d}y}{l}=\left(\frac{\omega_B^2}{\Omega^2}-1\right)\frac{\mathrm{d}z}{m};\quad \frac{\mathrm{d}k}{k_c}=\frac{\mathrm{d}l}{l_c}=\frac{\mathrm{d}m}{m_c},\quad \text{along with } \Omega=\omega \tag{32}$$

Eqs.(30∼32) are similar to Eqs.(25∼27), respectively. Thus, the ray features in the present nonisothermal case are basically the same as Hines' locally isothermal case. For example, in the horizontal x-y plane the projection of the ray trace is straight approximately due to the fact that $k_c \sim l_c \ll m_c$ and thus k and l are nearly constant compared to m. As introduced in the last subsection, ray features are dominantly influenced by the mean-field temperature and its spatial gradients. Fig.6 presents the characteristics of ray propagation: the 3D ray traces in the upper left panel; the ray distances versus time in the upper right panel; the three wavelengths λ_x, λ_y, & λ_z in the lower left panel, and the three periods $\tau_A = 2\pi/\omega_A$, $\tau_B = 2\pi/\omega_B$, and $\tau = 2\pi/\Omega$ in the lower right panel. Fig.7 displays the altitude profiles of mean-field T_0 and C (upper left), $\mathrm{d}T_0/\mathrm{d}x$ (upper right), $\mathrm{d}T_0/\mathrm{d}y$ (lower left), and $\mathrm{d}T_0/\mathrm{d}z$ (lower right), respectively.

Comparing Hines' model (Figs.2 & 3) with the nonisothermal model (Figs.6 & 7) reveals that the introduction of the new ingredient, k_T, in the cut-off and buoyancy periods results in (1) mitigated bulges of the two ray traces in the 85-120 km altitude; (2) lower speeds of ray propagation in space, e.g., Hines' model gives an average of 1.8 km/min (about 1100 km in 600 minutes), while the nonisothermal model shows 1.3 km/min (1050 km in 800 minutes) in the backward case. However, it is subtle to discern its effects on the profiles of wavelengths, periods, temperature (or, equivalently, sound speed), as well as the temperature gradients.

d) Fully isothermal and wind-shearing atmosphere

In this case, $k_T = 0$, but $\mathbf{v}_0 \neq 0$, $\partial\mathbf{v}_0/\partial t \neq 0$, and $\partial\mathbf{v}_0/\partial\mathbf{r} \neq 0$. Eqs.(15-17) yield

$$\left.\begin{aligned}&\tfrac{\mathrm{d}t}{\mathrm{d}z}=A_0,\ \tfrac{\mathrm{d}x}{\mathrm{d}z}=A_0\left(U-A_{11}k+A_{12}\tfrac{\partial U}{\partial z}\right),\ \tfrac{\mathrm{d}y}{\mathrm{d}z}=A_0\left(V-A_{11}l+A_{12}\tfrac{\partial V}{\partial z}\right)\\&\tfrac{\mathrm{d}k}{\mathrm{d}z}=-A_0\Delta_x,\ \tfrac{\mathrm{d}l}{\mathrm{d}z}=-A_0\Delta_y,\ \tfrac{\mathrm{d}m}{\mathrm{d}z}=-A_0\Delta_z,\ \tfrac{\mathrm{d}\Omega}{\mathrm{d}z}=-A_0A_{21}\Delta_t\end{aligned}\right\} \tag{33}$$

where

$$\left.\begin{aligned}&\Delta_x=k\tfrac{\partial U}{\partial x}+l\tfrac{\partial V}{\partial x},\ \Delta_y=k\tfrac{\partial U}{\partial y}+l\tfrac{\partial V}{\partial y},\ \Delta_z=k\tfrac{\partial U}{\partial z}+l\tfrac{\partial V}{\partial z},\ \Delta_t=k\tfrac{\partial U}{\partial t}+l\tfrac{\partial V}{\partial t}\\&A_0=\tfrac{A_{00}}{mC^2\Omega^3},\ A_{11}=\tfrac{\Omega C^2\left(\Omega^2-\omega_b^2\right)}{A_{00}},\ A_{12}=\tfrac{\eta\Omega^3C^2/\Delta_z}{A_{00}},\ A_{21}=\tfrac{\Omega^4-C^2k_h^2\omega_b^2}{A_{00}}\end{aligned}\right\} \tag{34}$$

in which $A_{00}=\Omega^4-C^2(\omega_b^2k_h^2+\eta\Omega^2)$ and $\eta=(1-\gamma/2)\,g\Delta_z/(2\Omega C^2)-\Delta_z^2/(4\Omega^2)$.

Under the isothermal condition, Figs.8∼11 display the heavy impacts of wind shears on the characteristics of ray propagation. In Fig.8, the upper left panel is the 3D ray traces. Both the forward and backward rays are wriggling through the 3D space by following two different paths. The difference is obviously shown in the upper right panel: the forward ray (in blue) travels ∼530 km in about 380 minutes between the sea level and the 300 km altitude, while the backward ray (in red) hikes around 750 km in about 320 minutes. The

Notes

lower two panels of the figure present the wave lengths and intrinsic wave periods of the propagation, respectively. In the LHS panel, λ_y appears constant in altitude, relatively speaking, and does λ_z except the heights of 100-150 km. The altitude dependance of λ_x in the LHS panel is similar to that of τ in the RHS panel: (1) below 80 km altitude they keep roughly unchanged. (2) λ_x and τ stabilize with their respective minimum values in 120-135 km altitude in the forward propagation, while with maximum values in 130-145 km altitude in the backward propagation. The two arrow lines label these values. (3) above 200 km altitude, the forward parameters increase monotonously and the backward ones do not change anymore.

Along ray paths the altitude profiles of the mean-field zonal wind U and meridional wind V are described in the upper left and upper right panels in Fig.9, respectively. The WKB δ parameter is given in the lower panel. Below 80 km altitude and above 200 km altitude both U and V are either unchanging or vary quasi-linearly. On the contrary, between the two altitudes, they exhibit oscillatory features with both positive and negative speeds. As far as δ, most of its amplitudes are smaller than 1, while in 100-150 km altitudes there are a couple of peaks for both forward and backward situations, respectively. Between the peaks of each pair, there exists zero-δ heights of 120-135 km in the forward case and of 130-145 km in the backward case. The two zero-δ slots correspond to the two zones of the minimum λ_x and τ values, respectively, in the lower two panels of Fig.8. Note that δ can be as high as 8, which is larger than 1, for regular ray propagation as exposed in the upper left panel of Fig.8.

The altitude profiles of the mean-field wind gradients in temporal coordinate t and spatial ones (x, y, z) are illustrated in Figs.10 and Fig.11. The gradients in U and V have following characteristics: (1) The magnitude of all the U-gradients is larger than that of the V-gradients, particularly below 50 km altitude where the V-gradients are nearly zero. (2) While $\mathrm{d}(U,V)/\mathrm{d}t \sim$ several m/s per hour in magnitude, $\mathrm{d}(U,V)/\mathrm{d}x \sim \mathrm{d}(U,V)/\mathrm{d}y \ll \mathrm{d}(U,V)/\mathrm{d}z \sim$ several m/s per km in magnitude. This indicates that it is the wind shears (horizontal wind velocity gradients in altitude), rather than its gradients in the horizontal plane, that play the dominant role to influence wave propagation in atmosphere. (3) Below 80 km and above 200 km altitudes, all the wind gradients are smaller than that between the two altitudes. This reminds us that the effects of the wind gradients on wave propagation cannot not be omitted, especially in the middle atmosphere.

e) Nonisothermal and wind-shearing atmosphere: Generalized formulation

To adopt $k_T \neq 0$ by relaxing the constraint of $k_T = 0$ in the above Subsection, Eqs.(15-17) gives rise to the most generalized set of ray-tracing equations as follows:

$$\left.\begin{array}{l} \frac{\mathrm{d}t}{\mathrm{d}z} = A_0,\ \frac{\mathrm{d}x}{\mathrm{d}z} = A_0\left(U - A_{11}k + A_{12}\frac{\partial U}{\partial z}\right),\ \frac{\mathrm{d}y}{\mathrm{d}z} = A_0\left(V - A_{11}l + A_{12}\frac{\partial V}{\partial z}\right) \\ \frac{\mathrm{d}k}{\mathrm{d}z} = -A_0\left(\Delta_x + A_{22}C_x\right),\ \frac{\mathrm{d}l}{\mathrm{d}z} = -A_0\left(\Delta_y + A_{22}C_y\right),\ \frac{\mathrm{d}m}{\mathrm{d}z} = -A_0\left(\Delta_z + A_{22}C_z\right) \\ \frac{\mathrm{d}\Omega}{\mathrm{d}z} = -A_0\left(A_{21}\Delta_t - A_{22}C_t\right) \end{array}\right\} \quad (35)$$

where $\Delta_{x,y,z,t}$ are expressed in Eq.(34), and,

$$\left.\begin{array}{l} C_x = \frac{1}{C}\frac{\partial C}{\partial x},\ C_y = \frac{1}{C}\frac{\partial C}{\partial y},\ C_z = \frac{1}{C}\frac{\partial C}{\partial z},\ C_t = \frac{1}{C}\frac{\partial C}{\partial t}; \\ A_0 = \frac{A_{00}}{mC^2\Omega^3},\ A_{11} = \frac{\Omega C^2\left(\Omega^2-\omega_B^2\right)}{A_{00}},\ A_{12} = \frac{\eta\Omega^3C^2/\Delta_z}{A_{00}}, \\ A_{21} = \frac{\Omega^4-C^2k_h^2\omega_B^2}{A_{00}},\ A_{22} = \frac{\Omega^3(\omega_A^2-C^2K^2-\frac{\Delta_z^2C^2}{4\Omega^2})}{A_{00}} \end{array}\right\} \quad (36)$$

in which $A_{00} = \Omega^4 - C^2(\omega_B^2 k_h^2 + \eta\Omega^2)$ and η keeps the same as that attached to Eq.(34).

In addition to the effects of the mean-field wind, this generalized case takes into consideration the influences of altitude-dependent temperature, as well as the density (and thus the pressure), and their gradients in time and space on the ray propagation. Figs.12∼17 illustrate the results. In comparison with that of Fig.8, the upper left panel of Fig.12 exhibits a less wriggling feature in both forward and backward propagations. The upper right panel shows that, while the forward ray (in blue) passes ∼400 km in about 250 minutes between the sea level and the 300 km altitude, the backward one (in red) spends about 380 minutes to fly back to the sea level after a ∼800 km journey. The speed of the former (400/250≈1.6 km/min) is higher than that in Fig.8 (530/380≈1.4 km/min), while the speed of the latter (800/380≈2.1 km/min) is approximately the same as that in Fig.8 (750/320≈2.3 km/min). In addition, the altitude profiles of both the three wavelengths (lower left panel) and the intrinsic wave period (lower right panel) demonstrate that below 150 km nonisothermality results in stronger fluctuations in comparison with Fig.8, especially lower than 100 km altitude. Interestingly, the forward wave period is shorter than the backward one in Fig.12 at most altitudes, in contrast to the fact that it is always longer than that in Fig.8.

In Fig.13, the upper panel portrays the altitude profiles along ray paths of WKB δ. The parameter is smaller than 0.2 above 160 km altitude. Below the altitude, the forward δ is larger than the backward one between 130 km and 160 km; but it always is smaller below 130 km. This is different from the results given in Fig.9, where the the forward δ is usually larger than the backward one, particularly in the 100-150 km altitude. With respect to the mean-field zonal wind (lower left panel) and the meridional wind (lower right panel), the profiles in Fig.13 are similar to those in Fig.9.

Figs.14 & 15 draw the altitude profiles of density gradients (LHS panels) and temperature gradients (RHS panels) in t, x, y, and z. Except the t-related ones, these structures reproduce those presented in Figs.3 & 4, respectively, with the same order of magnitudes. For $\mathrm{d}\rho_0/\mathrm{d}t$ and $\mathrm{d}T_0/\mathrm{d}t$, their appearances follow the patterns of their respective families, but with different units of each. In addition, Figs.16 & 17 delineate the altitude profiles of zonal wind gradients (LHS panels) and meridional ones (RHS panels) in t, x, y, and z. The figures do not disclose discernable changes from those given in 10 & 11, respectively.

f) Nonisothermal and wind-shearing atmosphere: Influence of initial wavelengths

In the above Subsections, we arbitrarily selected the same group of initial horizontal wavelengths, $\lambda_{x0} = 350$ km and $\lambda_{y0} = 50$ km, to exhibit the features of the ray propagation under different acoustic-gravity wave modes. In this Subsection, we choose several groups of initial horizontal wavelengths to exhibit the influence of the parameter on the ray propagation (taking the forward situation as an example) in the generalized nonisothermal and shearing mode. The considered wavelengths include following two groups of pairs: (1) $\{\lambda_{x0}, \lambda_{y0}\} = \{2\pi\times 350, 2\pi\times 50\}$, $\{2\pi\times 350, -2\pi\times 50\}$, $\{-2\pi\times 350, 2\pi\times 50\}$,

$\{-2\pi \times 350, -2\pi \times 50\}$; and (2) $\{\lambda_{x0}, \lambda_{y0}\} = \{2\pi \times 50, 2\pi \times 350\}$, $\{2\pi \times 50, -2\pi \times 350\}$, $\{-2\pi \times 50, 2\pi \times 350\}$, $\{-2\pi \times 50, -2\pi \times 350\}$, where the unit of all the parameters are in km, and the negative values represent the propagating direction of the related wave components is in the reverse direction of the coordinate in the frame of reference. In the simulation, the initial extrinsic wave period ω keeps unchanged at 30 minutes.

Notes

Fig.18 demonstrates the ray paths in space with these two groups of initial wavelengths. In each group, the four cases are discriminated by four different colors (black, blue, red, and green), respectively. Several distinct features of the ray propagation are exposed by both the upper and lower panels of the figure: (1) All the rays propagate in space along non-straight paths in a quadrant determined by, and opposite to, the initial wave vectors, respectively, in the horizontal plane, $\{k_0 = 2\pi/\lambda_{x0}, l_0 = 2\pi/\lambda_{x0}\}$. For example, in the two panels, the ray in black ($\lambda_{x0} > 0$ and $\lambda_{y0} > 0$) is oriented to evolve in the third quadrant ($x < 0$ and $y < 0$); similarly, the ray in blue ($\lambda_{x0} > 0$ and $\lambda_{y0} < 0$) is in the second quadrant ($x < 0$ and $y > 0$). (2) In the horizontal plane, the ratio between the x-displacement, Δx, and the y-displacement, Δy, of any projected ray paths is in the same order of that of the corresponding wavenumbers. For instance, the ray in red in the upper panel has a ratio of $\Delta x/\Delta y \approx 45/270 = 0.16$ while the wavenumber ratio is $k_0/l_0 = 0.14$; also, the ray in black in the lower panel has a ratio of $\Delta x/\Delta y \approx 320/40 = 8$ while the wavenumber ratio is $k_0/l_0 = 7$. (3) Between 80 km and 150 km altitude all rays experience the most serious modulations. According to the analysis in the previous Subsections, these influences are exerted dominantly by the mean-field wind components and their shears. (4) By comparison with the upper left panel of Fig.12, these modulations caused by the wind components and their shears become mitigated if the horizontal wavelengths are longer, as shown in the upper panel of Fig.18.

Fig.19 portrays the temporal features of both the ray length (thick lines) and the vertical increments (thin lines) in the above two groups of the wave propagations. All the ray paths are approximately proportional to time, with a propagation speed of 15∼18 km/min in space: the upper panel gives 400/23≈17 km/min (black), 400/26≈15 km/min (blue), 400/27≈15 km/min (red), and 400/25=16 km/min (green); and the lower panel presents 450/32≈14 (black), 400/22≈18 km/min (blue), 360/20=18 km/min (red), and 400/25=16 km/min (green). Relatively, the vertical propagation speed is lower, around 9∼15 km/min, if assuming a linear relation between the height and time. These speeds are much higher than those obtained from the upper right panel of Fig.12: it is merely no more than 2 km/min for the four traces. Thus, rays with longer initial horizontal wavelengths travel faster. In fact, all the rays in Fig.19 reach heights of 300-400 km in only no more than 30 minutes; by contrast, those in Fig.12 arrive 300-800 km altitudes after more than 260 minutes.

Fig.20 displays the development of the wavelengths λ_x (upper left panel), λ_y (upper right panel), λ_z (lower left panel), and the intrinsic wave period τ (lower right panel) along the ray paths in the two groups of wave propagations. The most conspicuous feature stays in the modulations of the four parameters below 200 km altitude, particularly at the height of 100-150 km. By checking Fig.19 we know this corresponds to 80-120 km altitude, the most extreme changing region of both the mean-field temperature (Fig.7,14,15) and zonal & meridional winds (Fig.13,16,17). Besides, for the horizontal wavelength (λ_x or λ_y; the upper two panels in the two groups), its magnitude becomes higher than the initial value

(λ_{x0} or λ_{y0}) if the value is positive, i.e., the initial wave vector component is in the x (or y) direction. For example, in the upper right panel in the first group, the red curve denotes the case of $\lambda_{y0} = 2\pi \times 50 > 0$ km. Along the ray, λ_y increases and peaks at 150 km distance along the ray with 51.2 km. By contrast, if λ_{x0} (or λ_{y0}) is negative, i.e., the initial wave vector component is opposite to the x (or y) direction, the magnitude of λ_x (or λ_y) decreases. See the green curve in the upper right panel in the second group. In this case, $\lambda_{y0} = -2\pi \times 350 < 0$ km. Along the ray, $\mid \lambda_y \mid$ decreases to 300 km at about 100 km distance along the ray.

However, the vertical wavelength, λ_z, behaves differently as exhibited by the two lower left panels in the two groups. Irrelevant to the directions of initial horizontal wavevectors, the upward propagating waves have negative λ_z. Its magnitude starts at $\lambda_{z0} = 2\pi \times 12$ km. After a surprising drop of $\lambda_z/(2\pi)$ to below 8 km in within 20 km ray path, it undergoes a large swing between 3 and 8 km in the first group, and between 3 and 11 km in the second group, before stabilizing at 3-5 km and 3-9.5 km, respectively, after a journey of 300 km long in the ray propagation. These final values correspond to $\lambda_z \sim$ 20-60 km. Impressively, the wave period τ has a similar trend as shown in the two lower right panels of the two groups: it decreases sharply at first, then goes up and down, and recovers finally to stabilize at a period which diverge only within 1 minute (the first group) and 2 minutes (the second group) from the initial values, respectively. Because the initial perod is 30 minutes, we may neglect this divergence in dealing with measurements, that is, the wave period can be assumed constant in wave propagations.

IV. Summary and Discussion

Since the 1960s, the influence of mean-field properties (such as zonal and meridional winds, background temperature) on the propagation of atmospheric acoustic-gravity waves has become one of the important topics in space physics. The related ray-tracing technique has also been developed to investigate gravity wave propagation under the effects of background wind and temperature variations. Due to the importance of an accurate description of mean-field properties and their effects in the clarification of the observed wave-driven phenomena in atmosphere (e.g., *Hickey et al.* 1998), we first of all took into account the wind-shearing and nonisothermal effects, as well as the Coriolis effect, to extend Hines' locally isothermal and shear-free model to describe the modes of generalized inertio-acoustic-gravity waves under different situations below 200 km altitude, where all dissipative terms (such as viscosity and heat conductivity) were neglected (*Ma et al.* 2014). The obtained dispersion relation recovers all the known atmospheric wave modes.

In this paper, we used the generalized dispersion relation to investigate the effects of the wind shears and nonisothermality on the ray propagation of acoustic-gravity waves. The derived general set of ray equations not only reproduces ME95's derivations under Hines' locally isothermal and shear-free conditions, but also provides the equation to describe the time-dependent variation of the intrinsic wave frequency. Our ray-tracing simulations accommodate five different types of atmospheric models, starting from the simplest situation to the most complicated one: (1) fully isothermal, and shear-free atmosphere under both hydrostatic and quasi-hydrostatic conditions; (2) Hines' locally isothermal and shear-free atmosphere under both hydrostatic and quasi-hydrostatic conditions; (3) nonisothermal and shear-free atmosphere under hydrostatic conditions; (4) fully isothermal and wind-shearing atmosphere; (5) nonisothermal and wind-shearing atmosphere (generalized formulation; influence of initial wavelengths). In every step, a set of ray equations was derived to numerically code into a global ray-tracing model and calculate the profiles of ray traces in space and time; that of the wavelengths and intrinsic wave periods along

Notes

the ray paths; that of the mean-field density, pressure, or temperature and the horizontal winds, as well as their gradients if available; and that of the WKB criterion parameter, δ in a few typical cases.

Our studies demonstrated the influences of wind shears and atmospheric nonisothermality on the ray propagation. In an isothermal and shear-free atmosphere, ray paths follow straight lines in space and time; both forward and backward-mapping traces are superimposed upon each other; wavelengths ($\lambda_{x,y,z}$), as well as the intrinsic wave period (τ), keep constant versus altitude. If Hines' locally isothermal condition is applied, i.e., including the effect of the altitude-dependent temperature, rays become non-straight spatially, but their projections in the horizontal plane keep straight. In this case, the forward and backward rays are no longer overlain, and $\lambda_{x,y,z}$ give discernable changes but τ does not change. All the obvious variations happen in 80-150 km altitude. If the temperature constraint is relaxed to the nonisothermal condition by adding the effect of temperature gradients in x, y, z and t, the results do not exhibit perceptible difference. In the presence of wind shears, as well as zonal and meridional wind gradients in space and time, but the atmosphere keeps isothermal, ray paths are violently modulated, particularly at 80-150 km altitude where $\lambda_{x,y,z}$ and τ exhibit striking variations. More importantly, the forward rays and the backward ones never propagate along the same paths. If the nonisothermal condition is employed by considering the effects of temperature variations in x, y, z and t, the modulations at 0-80 km altitude also become obvious. As far as the WKB δ parameter, though it is smaller than 0.4 in Hines' locally isothermal model, in agreement with ME95's estimation, it can be driven to close to 3 by the wind shears and nonisothermality. Lastly, we found that longer initial horizontal wavelengths bring about mitigated modulations to ray paths and faster speeds in ray propagation.

We stress that ME95's ray-tracing model is based on the dispersion relation derived from Hines locally isothermal and shear- free model. By contrast, our study expends ME95's formulation to obtain a generalized set of ray-tracing equations by taking into account the effects of wind shears and atmospheric nonisothermality on the ray propagation. The focus of this paper is to illustrate the influences of the effects on acoustic-gravity waves travelling from sea level to 200 km altitude within which the dissipation terms can be reasonably neglected. We therefore pay attention dominantly to the waves which are able to penetrate atmosphere and reach the ionospheric height above 80 km altitude, with little energy attenuation, and ignore those waves which are either reflected or in the cut-off region (for details of the wave features in these two cases see, e.g., *Ding et al.* 2003). Naturally, we avoid to consider such terms related to, e.g., WKB violation, wave saturation or damping, energy attenuation or intensification, dynamical and convective instabilities, which are of little relevance to our study. Instead, we concentrate on the waves which are capable of survival from every damping process during their propagations upward from the sea level to some observational heights. Thus, the result shown in this paper are suitable to provide a reference for data-fit modeling studies with measurements in space, e.g., mesosphere and/or troposphere, where information of the background wind and temperature profiles are available, owing to the fact that the close relationship between the ray paths and the mean-field atmospheric properties can be demonstrated more evidently than before via the approach provided in the text.

V. Acknowledgments

The Fortran code and simulation data in this paper are available on request to John.

References Références Referencias

1. AGARD (1972), Effects of Atmospheric Acoustic Gravity Waves on Electromagnetic Wave Propagation, *Conf. Proc., 115*, Harford House, London.
2. Beer, T. (1974), Atmospheric Waves, John Wiley, New York.
3. Bertin, F., J. Testud, and L. Kersley (1975), Medium scale gravity waves in the ionospheric F-region and their possible origin in weather disturbances, *Planet. Space Sci.*, 23, 493-507.
4. Bolt, B. A. (1964), Seismic air waves from the great 1964 Alaska earthquake, *Nature, 202*, 1095-1096.
5. Broutman, D., and S. D. Eckermann (2012), Analysis of a ray-tracing model for gravity waves generated by tropospheric convection, *J. Geophys. Res., 117*, D05132, doi:10.1029/2011 JD016975.
6. Bruce, C. H., D. W. Peaceman, H. H. Rachford, and J. P. Rice (1953), Calculations of unsteady-state gas flow through porous media, *J. Petrol. Tech.*, 5, 79-92.
7. Brunt, D. (1927), The period of simple vertical oscillations in the atmosphere, *Quart. J. Royal Meteor. Soc.*, 53, 30-32.
8. Calais, E., J. B. Minster, M. A. Hofton, and M. A. H. Gedlin (1998), Ionospheric signature of surface mine blasts from global positioning system measurements, *Geophys. J. Int., 132*, 191-202.
9. Cole, J. D., and C. Greifinger (1969), Acoustic-gravity waves from an energy source at the ground in an isothermal atmosphere, *J. Geophys. Res., 74*, 3693-3703.
10. Cowling, D. H., H. D. Webb, and K. C. Yeh (1971), Group rays of internal gravity waves in a wind-stratified atmosphere, *J. Geophys. Res., 76*, 213-220.
11. DeMajistre, R., L. J. Paxton, and D. Bilitza (2007), Comparison of ionospheric measurements made by digisondes with those inferred from ultraviolet airglow, *Adv. Space Res., 39,* 918-925.
12. Ding, F., W. X. Wan, and H. Yuan (2003), The influence of background winds and attenuation on the propagation of atmospheric gravity waves, *J. Atmos. and Solar-Terr. Phys., 65*, 857-869.
13. Dutton, J. A. (1986), The Ceaseless Wind, Dover, New York.
14. Eckart, C. (1960), Hydrodynamics of oceans and atmospheres, Pergamon, New York.
15. Eckermann, S. D. (1997), Influence of wave propagation on the Doppler spreading of atmospheric gravity waves, *J. Atmos. Sci., 54*, 2554-2573.
16. Einaudi, F. and Hines, C. O. (1970), WKB approximation in application to acousticgravity waves, *Can. J. Phys., 48*, 14581471.
17. Fovell, R., D. Durran, J. R. Holton (1992), Numerical simulations of convectively generated stratospheric gravity waves. *J. Atmos. Sci., 49*, 1427-.
18. Francis, S. H. (1973), Acoustic-gravity modes and large-scale traveling ionospheric disturbances of a realistic, dissipative atmosphere, *J. Geophys. Res., 78*, 2278-2301.
19. Francis, S. H. (1974), A theory of medium-scale traveling ionospheric disturbances, *J. Geophys. Res., 79*, 5245-5260.
20. Francis, S. H. (1975), Global propagation of atmospheric gravity waves: a review. *J. Atmos. Terr. Phys., 37*, 10111030, IN9, 10311054.
21. Franke, S. J., X. Chu, A. Z. Liu, and W. K. Hocking (2005), Comparison of meteor radar and Na Doppler lidar measurements of winds in the mesopause region above Maui, HI, *J. Geophys. Res., 110*, D09S02, doi:10.1029/2003JD004486.
22. Fritts, D. C. (1984), Gravity wave saturation in the middle atmosphere: A review of theory and observations, *Rev. Geophys. Space Phys., 22*, 275-308.

Notes

Notes

23. Fritts, D. C. (1989), A review of gravity wave saturation processes, effects, and variability in the middle atmosphere, *Pure Appl. Geophys., 130*, 343-371.
24. Fritts, D. C., and M. J. Alexander (2003), Gravity wave dynamics and effects in the middle atmosphere, *Rev. Geophys., 41*, 1003, doi:10.1029/2001RG000106.
25. Fritts, D. C., and T. S. Lund (2011), Gravity wave influences in the thermosphere and ionosphere: Observations and recent modeling, in: *Aeronomy of the Earths Atmosphere and Ionosphere*, ed.: Abdu, M. A., Pancheva, D., and Bhattacharyya, A., Springer, 109-130.
26. Fritts, D. C., B. P. Williams, C. Y. She, J. D. Vance, M. Rapp, F.-J. LΥubken, A. Mullemann, F. J. Schmidlin, and R. A. Goldberg (2004), Observations of extreme temperature and wind gradients near the summer mesopause during the MaCWAVE/MIDAS rocket campaign, *Geophys. Res. Lett., 31*, L24S06, doi:10.1029/2003GL019389.
27. Georges, T. M. (1968), Acoustic-gravity waves in the atmosphere, Symposium Proceedings, U .S. Government Printing Office, Washinton, D. C.
28. Gershman, B. N., and G. I. Grigor'ev (1968), Traveling ionospheric disturbances–A review, *Izv. Vyssh. Ucheb. Zaved. Radiofizika* (Engl. Transl.), 11, 5-27.
29. Ghodpage, R. N., A. Taori, P. T. Patil, S. Gurubaran, A. K. Sharma, S. Nikte, and D. Nade (2014), Airglow measurements of gravity wave propagation and damping over Kolhapur (16.5◦N, 74.2◦E), Intern. *J. Geophys., 2014*, ID514937, 1-9.
30. Gill, A. E. (1982), Atmosphere-ocean dynamics. Academic Press, Orlando, FL, International Geophysics Series.
31. Gossard, E. E., and W. H. Munk (1954), On gravity waves in the atmosphere, *J. Meteorol., 11*, 259-269.
32. Grigorev, G. I. (1999), Acoustic-gravity waves in the Earth's atmosphere (review). *Radio- phys. Quant. Electron., 42*, 3-25.
33. Hall, C. M., T. Aso, and M. Tsutsumi (2007), Atmospheric stability at 90 km, 78°N, 16°E, *Earth Planets Space, 59*, 157-164.
34. Harkrider, D. G. (1964), Theoretical and observed acoustic-gravity waves from explosive sources in the atmosphere, *J. Geophys. Res.*, 69, 5295-5321.
35. Harris, I. and W. Priester (1962), Time dependent structure of the upper atmosphere, *J. Atmos. Sci.*, 19, 286-301.
36. Hedin, A. E. (1991), Extension of the MSIS thermosphere model into the middle and lower atmosphere, *J. Geophys. Res., 96*, 11591172.
37. Hedin, A. E., M. A. Biondi, R. G. Burnside, G. Hernandez, R. M. Johnson, T. L. Killeen, C. Mazaudier, J. W. Meriwether, J. E. Salah, R. J. Sica, R. W. Smith, N. W. Spencer, V. B. Wickwar, T. S. Virdi (1991). Revised global model of thermosphere winds using satellite and ground-based observations. *J. Geophys. Res., 96*, 7657-7688.
38. Hedin, A. E., E. L. Fleming, A. H. Manson, F. J. Schmidlin, S. K. Avery, R. R. Clark, S. J. Franke, G. J. Fraser, T. Tsuda, F. Vial, and R. A. Vincent (1996), Empirical wind model for the upper, middle and lower atmosphere, *J. Atmos. Terr. Phys*. 58, 1421-1447.
39. Heisler, L. H. (1958), Anomalies in ionosonde records due to travelling ionospheric disturbances, *Aust. J. Phys., 11*, 79-90.
40. Hickey M. P., and K. D. Cole (1987), A quantic dispersion equation for internal gravity waves in the thermosphere, *J. Atmos. Terr. Phys., 49*, 889-899.

41. Hickey M. P., and K. D. Cole (1988), A numerical model for gravity wave dissipation in the thermosphere, *J. Atmos. Terr. Phys., 50*, 689-697.
42. Hickey, M. P., Richard L. Walterscheid, Michael J. Taylor, William Ward, Gerald Schubert, Qihou Zhou, Francisco Garcia, Michael C. Kelly, and G. G. Shepherd (1997), Numerical simulations of gravity waves imaged over Arecibo during the 10-day January 1993 campaign, *J. Geophys. Res., 102*, 11,475-11,489.
43. Hickey, M. P., M. J. Taylor, C. S. Gardner, and C. R. Gibbons (1998). Full-wave modeling of small-scale gravity waves using Airborne Lidar and Observations of the Hawaiian Airglow (ALOHA-93) O(^{1}S) images and coincident Na wind/temperature lidar measurements. *J. Geophys. Res., 103*, 6439-6453.
44. Hickey, M. P., R. L. Walterscheid, and G. Schubert (2000), Gravity wave heating and cooling in Jupiters thermosphere, *Icarus, 148*, 266–281.
45. Hickey, M. P., G. Schubert, and R. L. Walterscheid (2001), Acoustic wave heating of the thermosphere, *J. Geophys. Res., 106*, 21,543-21,548.
46. Hickey, M. P., G. Schubert, and R. L. Walterscheid (2009), Propagation of tsunami-driven gravity waves into the thermosphere and ionosphere, *J. Geophys. Res., 114*, A08304, doi:10.1029/2009JA014105
47. Hines, C. O. (1960), Internal atmospheric gravity waves at ionospheric heights, *Can. J. Phys., 38*, 1441-1481.
48. Hines, C. O. (1963), The upper atmosphere in motion. *Q.J.R. Meteorol. Soc.*, 89, 1-42.
49. Hines, C. O. (1967), On the nature of traveling ionospheric disturbances launched by the low-altitude nuclear explosions, *J. Geophys. Res., 72*, 1877-1882.
50. Hines, C. O. (1971), Generalization of the Richardson criterion for the onset of atmospheric turbulence, *Q. J. R. Met Soc., 97*, 429-439.
51. Hines, C. O. (1972), Gravity waves in the atmosphere, *Nature, 239*, 73-78.
52. Hines, C. O. (1974) WKB Approximation in Application to Acoustic-Gravity Waves, in: *The Upper Atmosphere in Motion*, American Geophysical Union, Washington, D. C., 508-530.
53. Hines, C. O., and D.W. Tarasick (1987), On the detection and utilization of gravity waves in airglow studies, *Planet. Space Sci.*, 35, 851-866.
54. Hocke, K., and K. Schlegel (1996), A review of atmospheric gravity waves and travelling ionospheric disturbances: 1982-1995, *Ann. Geophys.*, 14, 917-940.
55. Holton, J. R. (1992), An Introduction to Dynamic Meteorology. Academic Press, San Diego.
56. Hooke, W. H. (1968), Ionospheric irregularities produced by internal atmospheric gravity waves, *J. Atmosph. Sol.-Terr. Phys., 30*, 795-823.
57. Huang, Y. N., K. Cheng, and S. W. Chen (1985), On the detection of acoustic-gravity waves generated by typhoon by use of real time HF Doppler frequency shift sounding system, *Radio Sci., 20*, 897-906.
58. Igarashi, K., S. Kainuma, I. Nishmuta, S. Okamoto, H. Kuroiwa, T. Tanaka, T. Ogawa (1994), Ionospheric and atmospheric disturbances around Japan caused by the eruption of Mount Pinatubo on June 15, 1991. *J. Atmos. Terr. Phys., 56*, 1227-1234.
59. Jones, W. L. (1969), Ray tracing for internal gravity waves. *J. Geophys. Res., 74*, 2028- 2033.
60. Journal of Atmospheric and Terrestrial Physics (1968), Symposium on upper atmospheric winds, waves and ionospheric drift, *J. Atmos. Terr. Phys.* (Spec. Issue), 30 (5).

Notes

Notes

61. Kaladze, T. D., O. A. Pokhotelov, L. Stenflo, H. A. Shah, G. V. Jandieri (2007), Electromagnetic inertio-gravity waves in the ionospheric E-layer, *Phys. Scr., 76*, 343-.
62. Kanamori, H. (2004), Some fluid-mechanical problems in geophysicswaves in the atmosphere and fault lubrication. *Fluid Dyn. Res., 34*, 1-19.
63. Klostermeyer, J. (1972a), Numerical calculation of gravity wave propagation in a realistic thermosphere, *J. Atmos. Terr. Phys., 34*, 765-774.
64. Klostermeyer, J. (1972b), Comparison between observed and numerically calculated atmospheric gravity waves in the F-region, *J. Atmos. Terr. Phys., 34*, 1393-1401.
65. Klostermeyer, J. (1972c), Influence of viscosity, thermal conduction, and ion drag on the propagation of atmospheric gravity waves in the thermosphere, *Z. Geophys., 38*, 881-890.
66. Krassovsky, V. I. (1972), Infrasonic variations of OH emission in the upper atmosphere, *Ann. Geophys., 28*, 739-746.
67. Kubota, M., H. Kukunishi, and S. Okano (2001), Characteristics of medium- and largescale TIDs over Japan derived from OI 630-nm nightglow observations, *Earth Planets. Space, 53*, 741-751.
68. Kundu, P. K. (1990), Fluid Mechanics, Academic Press, San Diego.
69. Lamb, H. (1908), On the theory of waves propagated vertically in the upper atmosphere, *Proc. London Math. Soc., 7*, 122-141.
70. Lamb, H. (1910), On the atmospheric oscillations, Proc. Roy. Soc. (Ser. A), 84, 551-572.
71. Landau, L. D., and E. M. Lifshitz (1959), Fluid mechanics, Pergamon, New York.
72. Liang, J., W. Wan, and H. Yuan (1998), Ducting of acoustic-gravity waves in a nonisothermal atmosphere around a spherical globe, *J. Geophys. Res., 103*, 11,22911,234.
73. Lighthill, M. J. (1978), Waves in fluids, Cambridge University Press, Cambridge.
74. Lindzen, R. S., and H. L. Kuo (1969), A reliable method for the numerical integration of a large class of ordinary and partial differential equations, *Mon. Weather Rev., 97*, 732-734.
75. Lindzen, R. S., and K.-K. Tung (1976), Banded convective activity and ducted gravity waves, *Mon. Wea. Rev., 104*, 1602-1617.
76. Liu, H.-L. (2007), On the large wind shear and fast meridional transport above the mesopause, *Geophys. Res. Lett., 34*, L08815, doi:10.1029/2006GL028789.
77. Liu, A. Z., and G. R. Swenson (2003), A modeling study of O2 and OH airglow perturbations induced by atmospheric gravity waves, *J. Geophys. Res., 108*, 4151, doi:10.1029/2002JD002474, D4.
78. Liu, A. Z., W. K. Hocking, S. J. Franke, and T. Thayaparan (2002), Comparison of Na lidar and meteor radar wind measurements at Starfire Optical Range, NM, USA, *J. Atmos. Terr. Phys., 64*, 3140.
79. Liu, X., J. Xu, J. Yue, and S. L. Vadas (2013), Numerical modeling study of the momentum deposition of small amplitude gravity waves in the thermosphere, *Ann. Geophys., 31*, 114.
80. Ma, J. Z. G., M. P. Hickey, (2014), Effects of wind shears and nonisothermality on the propagation of acoustic-gravity waves: Attenuation or intensification? *JMSE,* 51 pages, to be submitted.
81. Marks, C. J., and S. D. Eckermann (1995), A three-dimensional nonhydrostatic raytracing model for gravity waves: Formulation and preliminary results for the middle atmosphere, *J. Atmos. Sci.*, 52, 1959-1984 (cited also as ME95 in the text).

82. Martyn, D. F. (1950), Cellular atmospheric waves in the ionosphere and troposphere, *Proc. Roy. Soc.* (Ser. A), 201, 216-234.
83. Mayr, H. G., I. Harris, F. Varosi, and F. A. Herrero (1984), Global excitation of wave phenomena in a dissipative multiconstituent medium, *J. Geophys. Res.*, 89, 10,929-10,959.
84. Mayr, H. G., I. Harris, F. A. Herrero, N. W. Spencer, F. Varosi, and W. D. Pesnell (1990), Thermospheric gravity waves: observations and interpretation using the transfer function model (TFM), *Space Sci. Rev., 54*, 297-375.
85. Mendillo, M., J. Baumgardner, D. Nottingham, J. Aarons, B. Reinisch, J. Scali, and M.C. Kelley (1997), Investigations of thermospheric-ionospheric dynamics with 6300-Å images from the Arecibo Observatory, *J. Geophys. Res., 102*, 7331-7343.
86. Midgley, J. E., and H. B. Liemohn (1966), Gravity waves in a realistic atmosphere, *J. Geophys. Res., 71*, 3729-3748.
87. Mimno, H. R. (1937), The physics of the ionosphere, *Rev. Mod. Phys.*, 9, 1-43.
88. Nappo, C. J. (2002), An Introduction to Atmospheric Gravity Waves, Academic, San Diego, California.
89. Munro, G. H. (1950), Traveling disturbances in the ionosphere, *Proc. Roy. Soc.* (Ser. A), 202, 208-223.
90. Munro, G. H. (1958), Travelling ionospheric disturbances in the F region, *Aust. J. Phys.*, 11, 91-112.
91. Paxton, L. J., D. Morrison, D. J. Strickland, M. J. McHarg, Y. Zhang, B. Wolven, H. Kil, G. Crowley, A. B. Christensen, and C.-I. Meng (2003), The use of far ultraviolet remote sensing to monitor space weather, *Adv. Space Res., 31,* 813-818.
92. Peltier, W. R., and C. O. Hines (1976), On the possible detection of tsunamis by a monitoring of the ionosphere, *J. Geophys. Res., 81*, 1995-2000.
93. Peterson, A.W. (1979), Airglow events visible to the naked eye, *Appl. Opt., 18,* 3390-3393.
94. Picone, J. M., A. E. Hedin, D. P. Drob, and A. C. Aikin (2002), NRLMSISE-00 empirical model of the atmosphere: Statistical comparisons and scientific issues, *J. Geophys. Res.*, 107(A12), 1468, doi:10.1029/2002JA009430.
95. Pierce, J. A., and H. R. Mimno (1940), The reception of radio echoes from distant ionospheric irregularities, *Phys. Rev., 57*, 95-105.
96. Pierce, A. D., and S. C. Coroniti (1966), A mechanism for the generation of acousticgravity waves during thunderstorm formation, *Nature, 210*, 1209-1210.
97. Pitteway, M. L. V., and C. O. Hines (1963), The viscous damping of atmospheric gravity waves, *Can. J. Phys., 41*, 1935-1948.
98. Richmond, A. D. (1978), Gravity-wave generation, propagation, and dissipation in thermosphere, *J. Geophys. Res., 83*, 4131-4145.
99. Roper, R. G. and J. W. Brosnahan (1997), Imaging Doppler interferometry and the measurement of atmospheric turbulence, *Radio Sci., 32*, 11371148.
100. Röttger, J. (1981), Equatorial spread-F by electric fields and atmospheric gravity waves generated by thunderstorms. *J. Atmos. Terr. Phys., 43*, 453-462.
101. Row, R. V. (1967), Acoustic-gravity waves in the upper atmosphere due to a nuclear detonation and an earthquake, *J. Geophys. Res., 72*, 1599-1610.
102. Šauli, P., and J. Boška (2001), Tropospheric events and possible related gravity wave activity effects on the ionosphere, *J. Atmos. Solar-Terr. Phys., 63*, 945-950.
103. Schubert, G., M. P. Hickey, and R. L. Walterscheid (2003), Heating of Jupiters thermosphere by the dissipation of upward propagating acoustic waves, *ICARUS, 163,* 398-413.

Notes

Notes

104. Schubert, G., M. P. Hickey, and R. L. Walterscheid (2005), Physical processes in acoustic wave heating of the thermosphere, *J. Geophys. Res., 110*, DOI:10.1029/2004JD005488.
105. She, C. Y., B. P. Williams, P. Hoffmann, R. Latteck, G. Baumgarten, J. D. Vance, J. Fiedler, P. Acott, D. C. Fritts, and F.-J. Luebken (2006), Observation of anti-correlation between sodium atoms and PMSE/NLC in summer mesopause at ALOMAR, Norway (69N, 12E), *J. Atmos. Sol. Terr. Phys., 68*, 93-101.
106. She, C. Y., D. A. Krueger, R. Akmaev, H. Schmidt, E. Talaat, and S. Yee (2009), Longterm variability in mesopause region temperatures over Fort Collins, Colorado (41N, 105W) based on lidar observations from 1990 through 2007, *J. Terr. Sol. Atmos. Phys., 71*, 1558-1564.
107. Sobral, J. H. A., H. C. Carlson, D. T. Farley, and W. E. Swartz (1978), Nighttime dynamics of the F region near Arecibo as mapped by airglow features, *J. Geophys. Res., 83*, 2561-2566.
108. Sonmor, L. J., and G. P. Klaassen (1997), Toward a unified theory of gravity wave breaking, *J. Atmos. Sci., 54*, 2655-2680.
109. Sun, L., W. Wan, F. Ding, and T. Mao (2007), Gravity wave propagation in the realistic atmosphere based on a three-dimensional transfer function model, *Ann. Geophys., 25*, 1979-1986.
110. Thome, G. D. (1968), Long-period waves generated in the polar ionosphere during the onset of magnetic stroms, *J. Geophys. Res., 73*, 6319-6336.
111. Tolstoy, I. (1963), The theory of waves in stratified fluids including the effects of gravity and rotation, *Rev. Mod. Phys., 35*, 207-230.
112. Tolstoy, I., J. Lau (1971), Generation of long internal gravity waves in waveguides by rising buoyant air masses and other sources. *Geophys. J. Royal Astron. Soc., 26*, 295-.
113. Toman, K. (1955), Movement of the F region, *J. Geophys. Res., 60*, 57-70.
114. Turner, J. S. (1973), Buoyancy Effects in Fluids, Cambridge University Press.
115. Vadas, S. L. (2007), Horizontal and vertical propagation and dissipation of gravity waves in the thermosphere from lower atmospheric and thermospheric sources, *J. Geophys. Res., 112*, A06305, doi:10.1029/2006JA011845.
116. Vadas, S. L., and G. Crowley (2010), Sources of the traveling ionospheric disturbances observed by the ionospheric TIDDBIT sounder near Wallops Island on 30 October 2007, *J. Geophys. Res.*, 115, A07324, doi:10.1029/2009JA015053.
117. Vadas, S. L., and D. C. Fritts (2001), Gravity wave radiation and mean responses to local body forces in the atmosphere, *J. Atmos. Sci., 58*, 2249-2279.
118. Vadas, S. L., and D. C. Fritts (2004), Thermospheric responses to gravity waves arising from mesoscale convective complexes, *J. Atmos. Sol. Terr. Phys., 66*, 781-804.
119. Vadas, S. L., and D. C. Fritts (2005), Thermospheric responses to gravity waves: Influences of increasing viscosity and thermal diffusivity, *J. Geophys. Res., 110*, D15103, doi:10.1029/2004JD005574.
120. Vadas, S. L., and D. C. Fritts (2009), Reconstruction of the gravity wave field from convective plumes via ray tracing, *Ann. Geophys., 27*, 147-177.
121. Vadas, S. L., J. Yue, C.-Y. She, P. A. Stamus, and A. L. Liu (2009), A model study of the effects of winds on concentric rings of gravity waves from a convective plume near Fort Collins on 11 May 2004, *J. Geophys. Res., 114*, D06103, doi:10.1029/2008JD010753.
122. Väisälä, V. (1925), Über die wirkung der windschwankungen auf die pilotbeobachtungen, *Soc. Sci. Fenn. Comment. Phys. Math. II*, 19, 1-46.

123. Vargas, F., G. Swenson, A. Liu, and D. Gobbi (2007), O(^{1}S), OH, and O_2 airglow layer perturbations due to AGWs and their implied effects on the atmosphere, *J. Geophys. Res., 112*, D14102, doi:10.1029/2006JD007642.
124. Vasseur, G., C. A. Reddy, and J. Testud (1972), Observations of waves and travelling disturbances, *Space Res., 12*, 1109-1131.
125. Volland, H. (1969), The upper atmosphere as a multiple refractive medium for neutral air motions, *J. Atmos. Terr. Phys., 31*, 491-514.
126. Waldock, J. A., T. B. Jones (1984), The effects of neutral winds on the propagation of medium scale atmospheric gravity waves at mid-latitudes, *J. Atmos. Terr. Phys., 46*, 217-231.
127. Walterscheid, R. L., and M. P. Hickey (2001), One-gas models with height-dependent mean molecular weight: Effects on gravity wave propagation, *J. Geophys. Res., 106*, 28,831-28,839.
128. Walterscheid, R. L., and M. P. Hickey (2005), Acoustic waves generated by gusty flow over hilly terrain, *J. Geophys. Res., 110*, DOI: 10.1029/2005JA011166.
129. Walterscheid, R. L., G. G. Sivjee, G. Schubert, and R. M. Hamwey (1986), Largeamplitude semidiurnal temperature variations in the polar mesopause: evidence of a pseudotide, *Nature, 324*, 347-349.
130. Wan, W. X., H. Yuan, B. Q. Ning, J. Liang, and F. Ding (1998), Traveling ionospheric disturbances associated with the tropospheric vortexes around Qinghai-Tibet Platcau, *Geophys. Res. Lett., 25*, 3775-3778.
131. Weinstock, J. (1978), Vertical turbulent diffusion in a stably stratified fluid, *J. Atmos. Sci., 35*, 10221027.
132. Whitham, G. B. (1961), Group velocity and energy propagation for three dimensional waves, *Commun. Pure Appl. Math., 14*, 675-691.
133. Wrassea, C. M., T. Nakamura, T. Tsuda, H. Takahashi, A. F. Medeiros, M. J. Taylor, D. Gobbi, A. Salatun, Suratno, E. Achmad, and A. G. Admiranto (2006), Reverse ray tracing of the mesospheric gravity waves observed at 23°S (Brazil) and 7°S (Indonesia) in airglow imagers, *J. Atmos. Solar-Terr. Phys., 68*, 163181.
134. Yeh, K. C., and C. H. Liu (1972), Theory of Ionospheric Waves, Academic, New York.
135. Yeh, K. C., and C. H. Liu (1974), Acoustic-gravity waves in the upper atmosphere, *Rev. Geophys. Space Sci., 12*, 193-216.
136. Yeh, K. C., H. D. Webb (1972), Evidence of directional fltering of travelling ionospheric disturbance. *Nature, 235*, 131-133.
137. Zhong, L., L. J. Sonmor, A. H. Manson, and C. E. Meek (1995), The influence of timedependent wind on gravity-wave propagation in the middle atmosphere. *Ann. Geophys., 13*, 375-394.

Notes

Notes

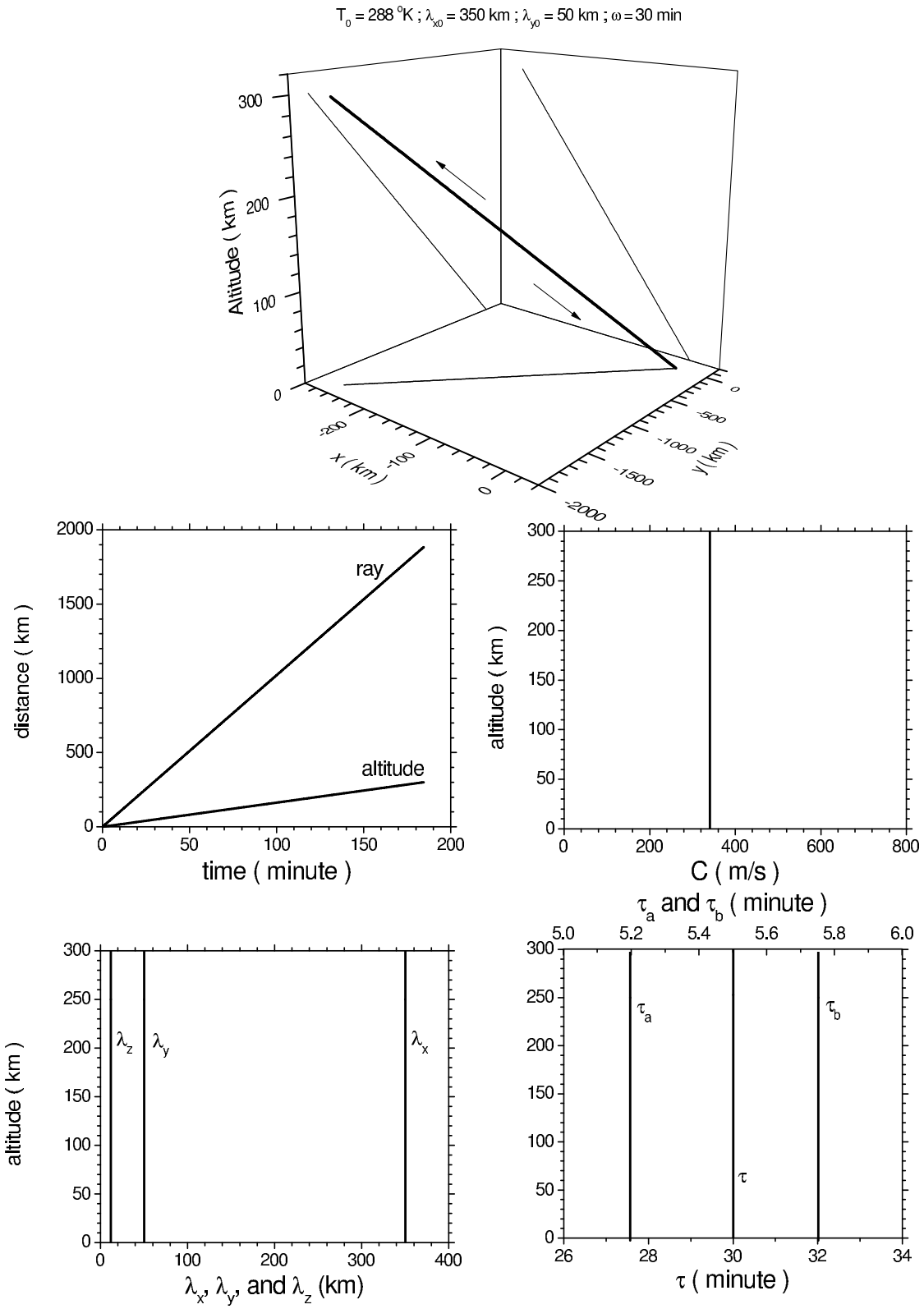

Figure 1 : Case 1: Ray features in hydrostatic, fully isothermal and shear-free atmosphere

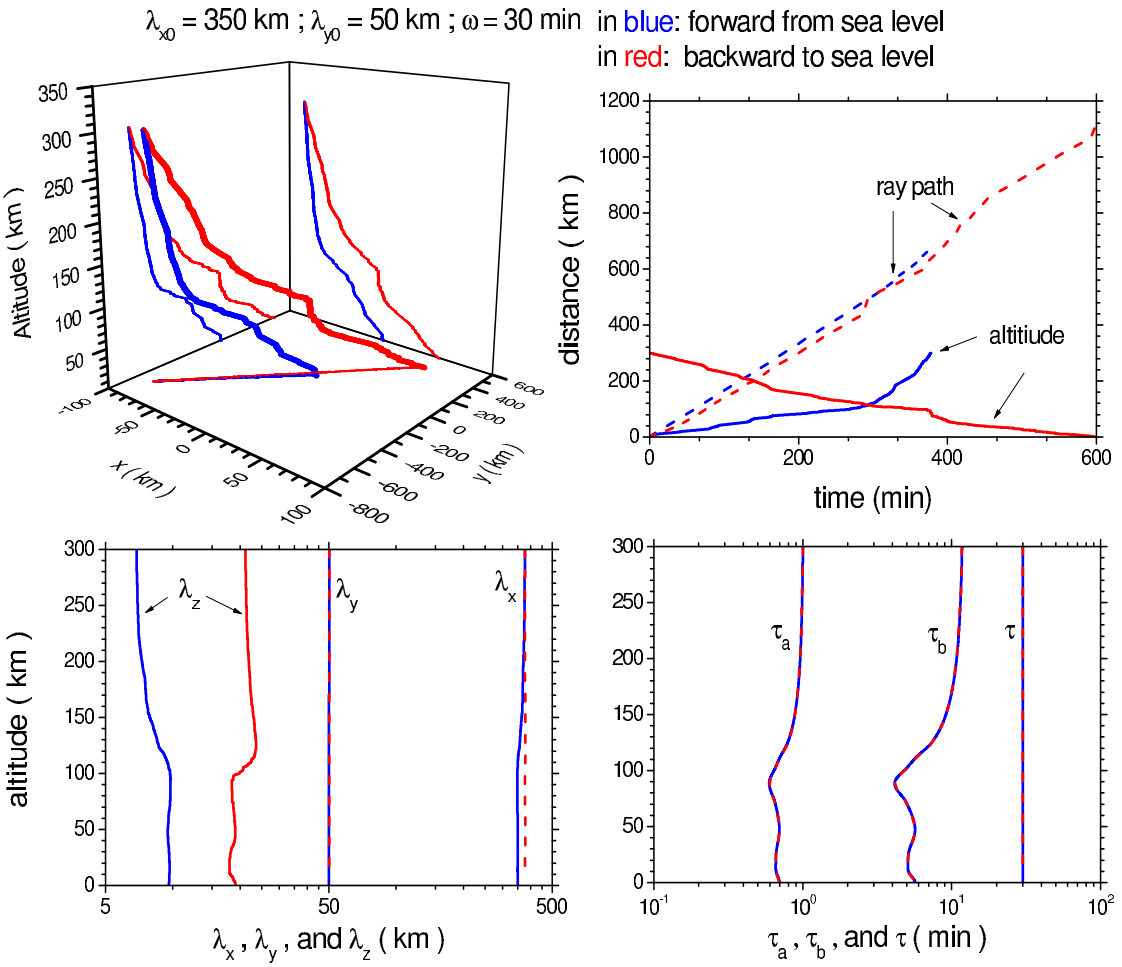

Figure 2 : Case 2-1: Ray propagation in hydrostatic, Hines' locally isothermal and shear-free atmosphere

Notes

Notes

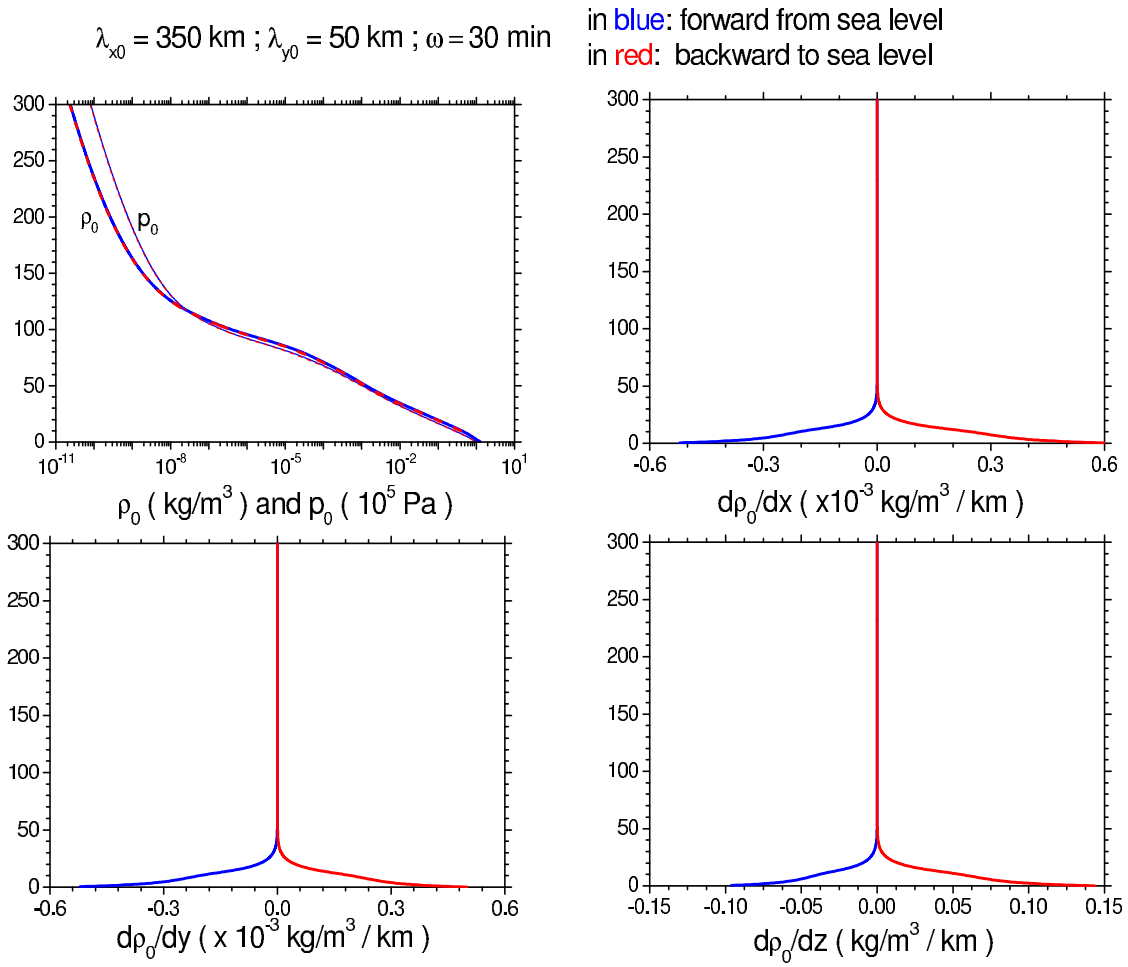

Figure 3 : Case 2-2: Altitude profiles of ˙0 and its gradients, as well as p0, in hydrostatic, Hines' locally isothermal and shear-free atmosphere

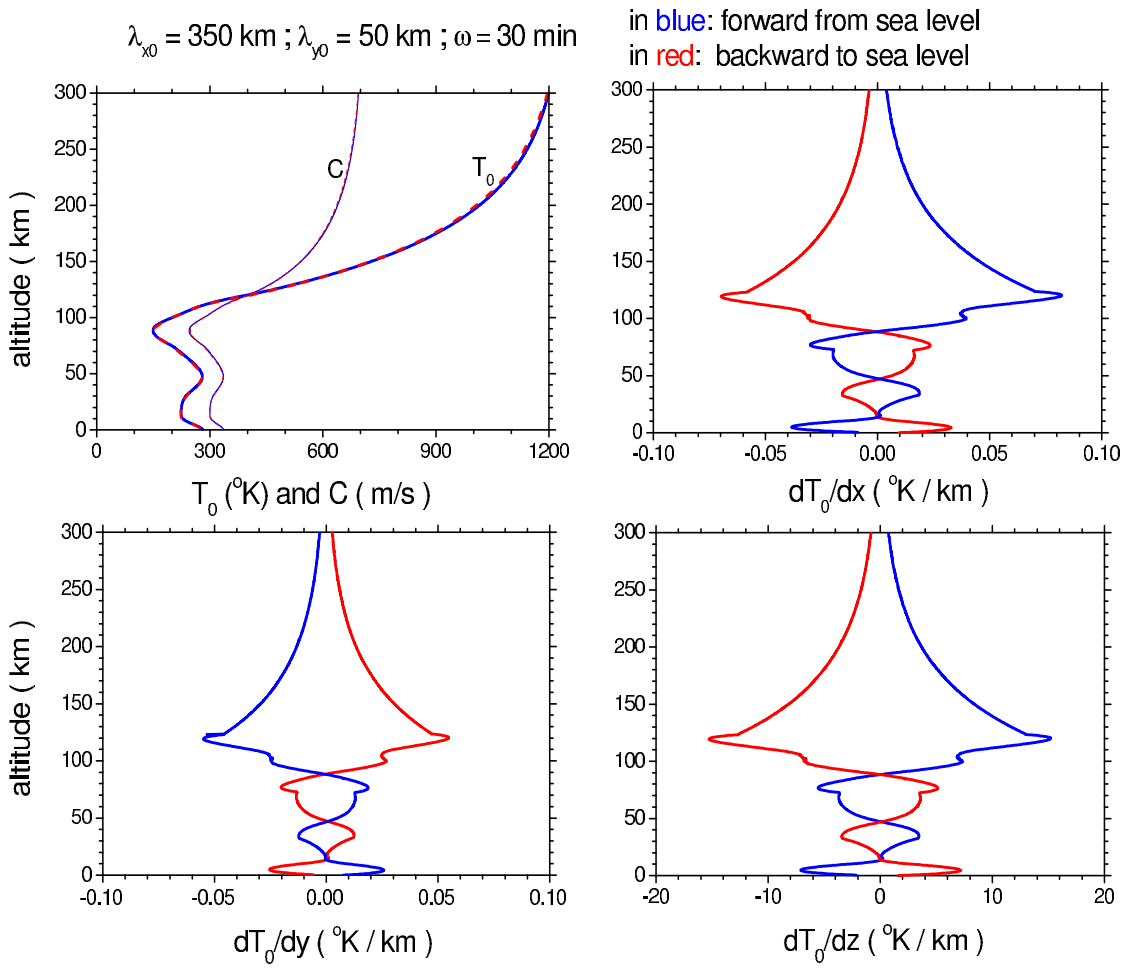

Figure 4 : Case 2-3: Altitude profiles of T_0 and its gradients, as well as C, in hydrostatic, Hines' locally isothermal and shear-free atmosphere

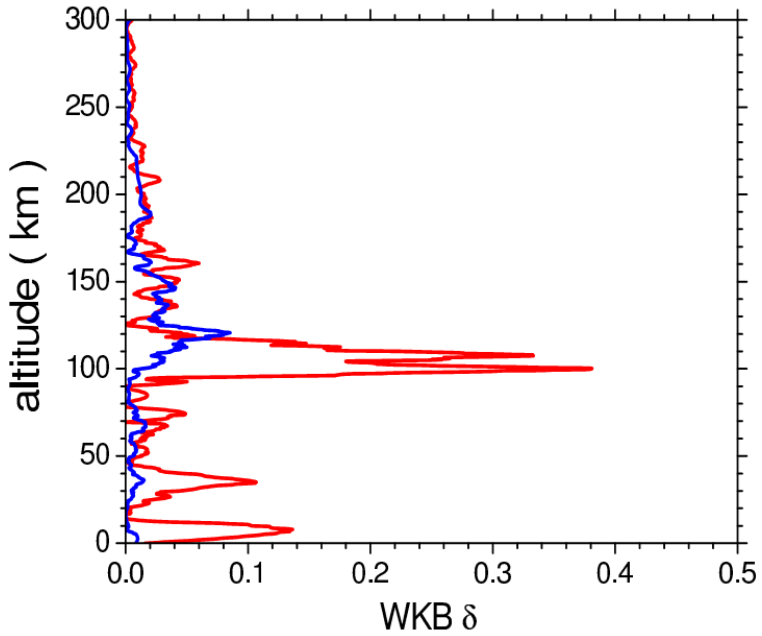

Figure 5 : Case 2-4: Altitude profiles of WKB ˙ in hydrostatic, Hines' locally isothermal and shear-free atmosphere

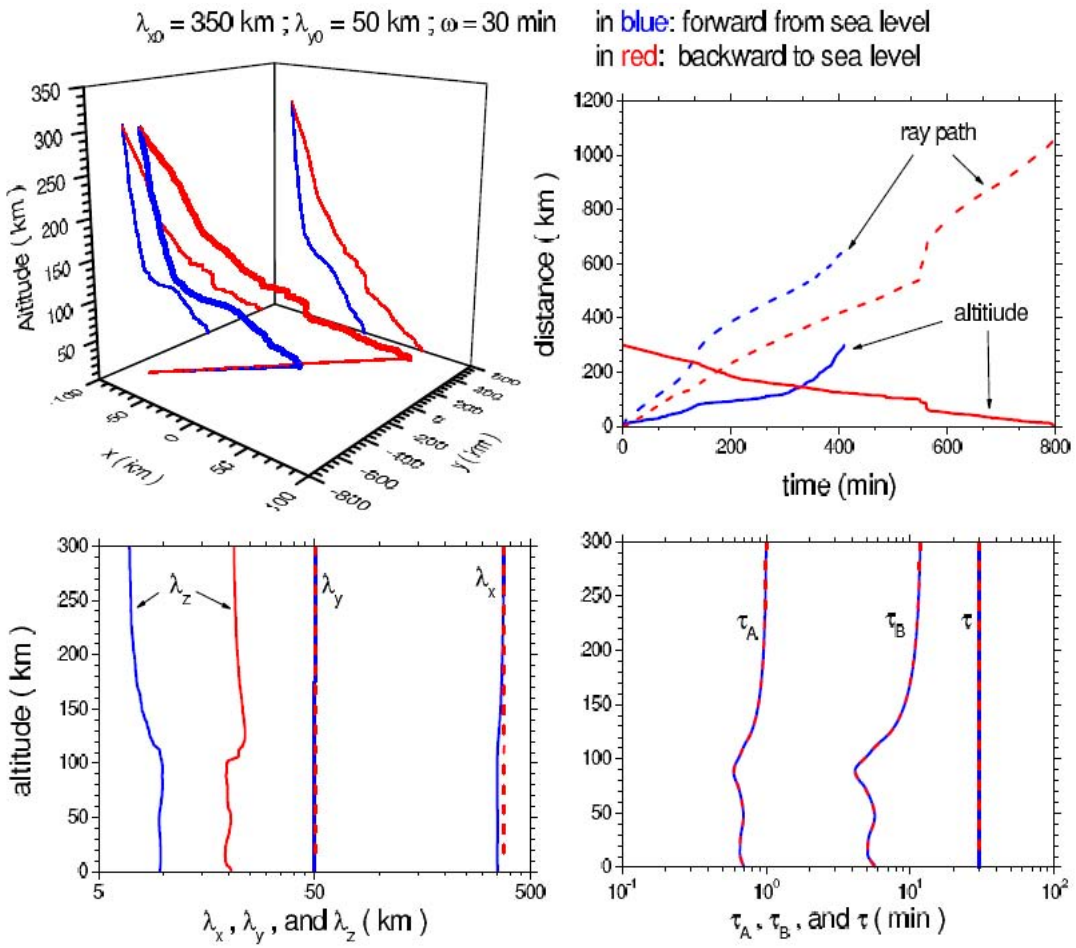

Figure 6 : Case 3-1: Ray propagation in both space (upper left panel) and time (upper right panel), and altitude profiles of wavelengths (lower left panel) and intrinsic wave periods (lower right panel) in hydrostatic, nonisothermal and shear-free atmosphere.

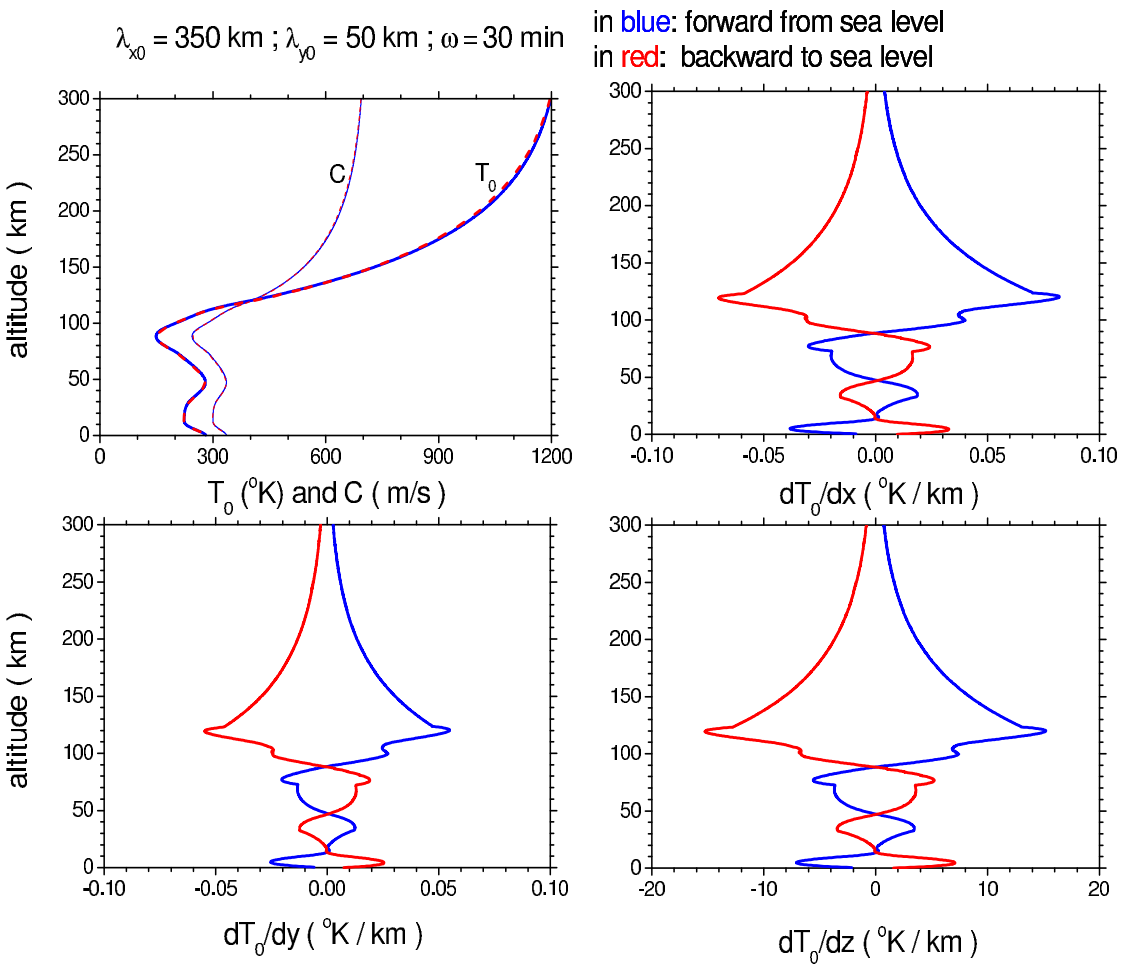

Figure 7 : Case 3-2: Altitude profiles of mean-field temperature (upper left panel) and its gradients in x (upper right panel), y (lower left panel), and z (lower right panel) in hydrostatic, nonisothermal and shear-free atmosphere

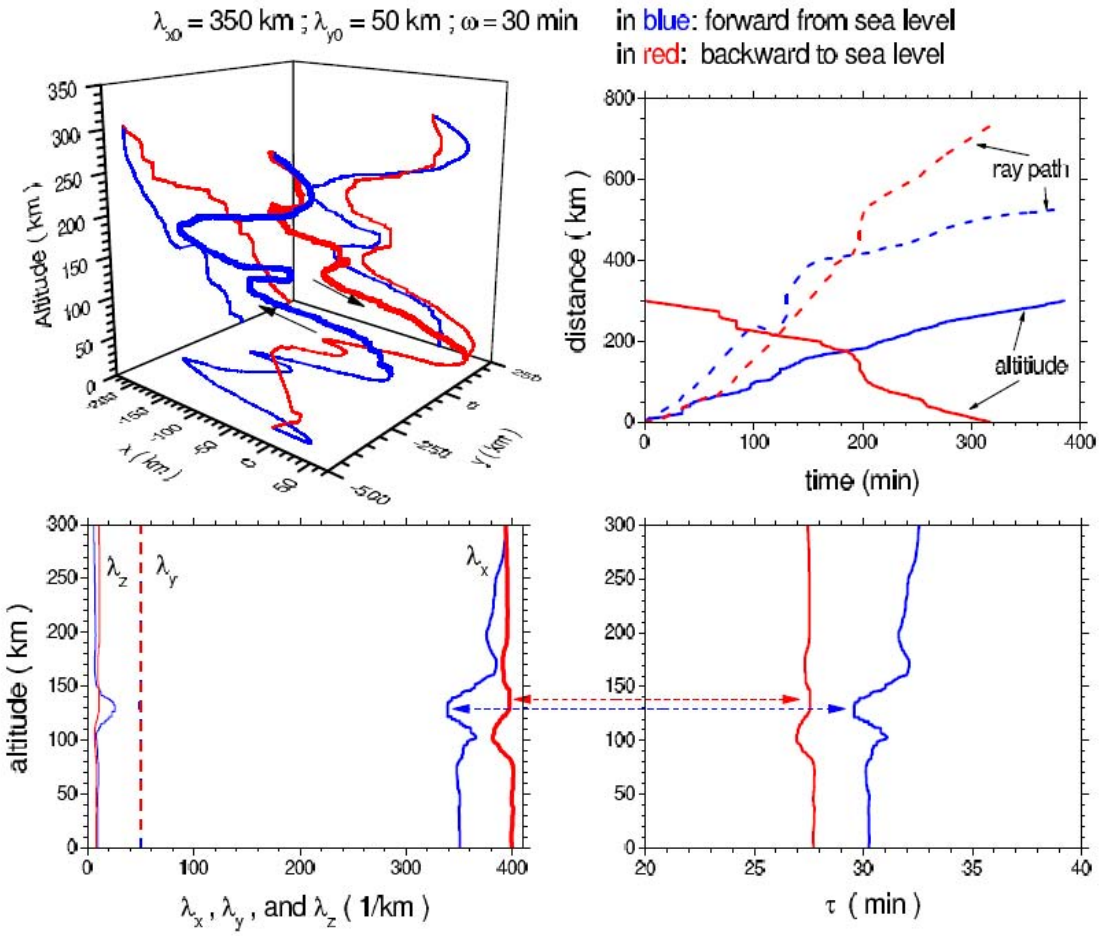

Figure 8 : Case 4-1: Ray propagation in both space (upper left panel) and time (upper right panel), and altitude profiles of wavelengths (lower left panel) and intrinsic wave periods (lower right panel) in isothermal and wind-shearing atmosphere

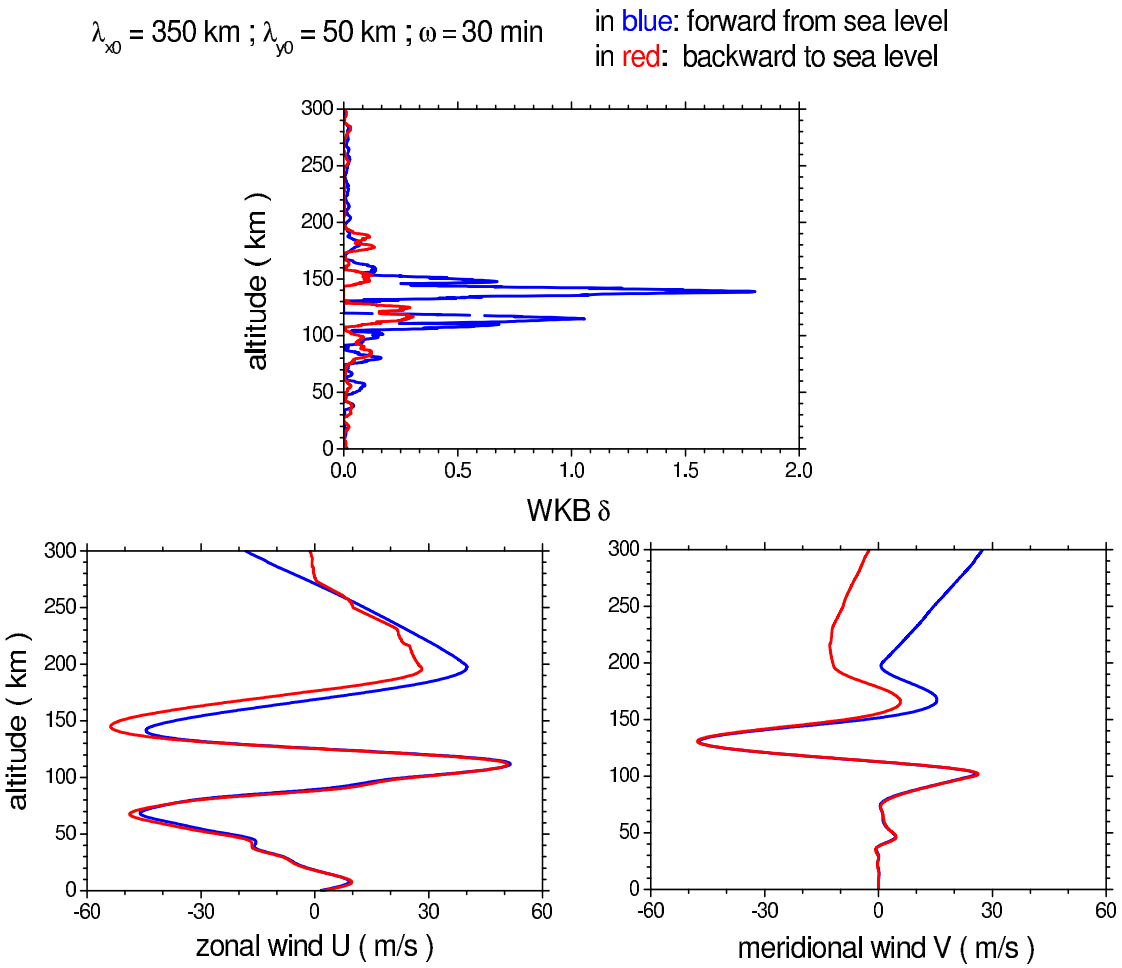

Figure 9 : Case 4-2: Altitude profiles along ray paths of WKB ˙ (upper panel), and mean-field wind (lower left panel: zonal direction; lower right panel: meridional direction) in isothermal and wind-shearing atmosphere

Notes

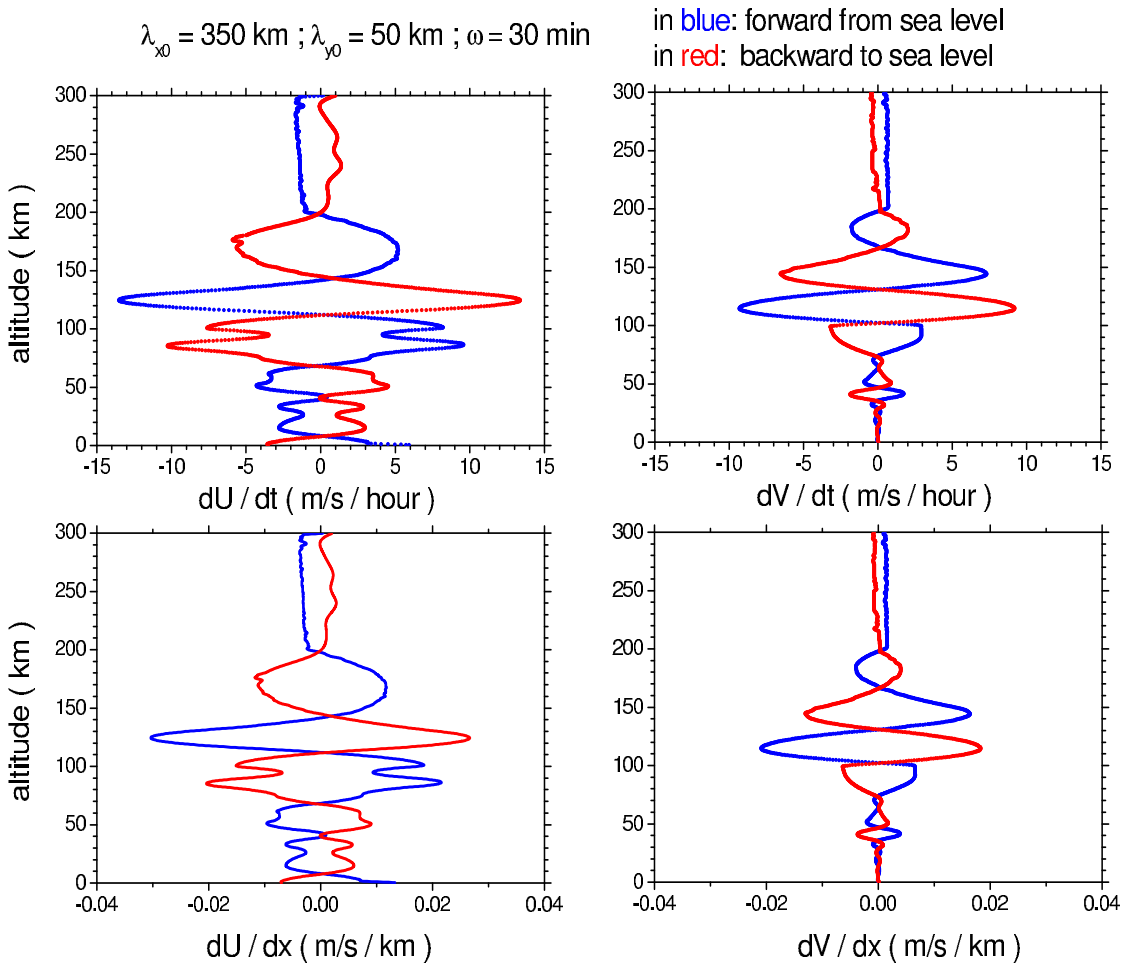

Figure 10 : Case 4-3: Altitude profiles of zonal wind gradients (LHS two panels) and meridional wind gradients (RHS two panels) in t (upper two panels) and x (lower two panels) in isothermal and sheared atmosphere

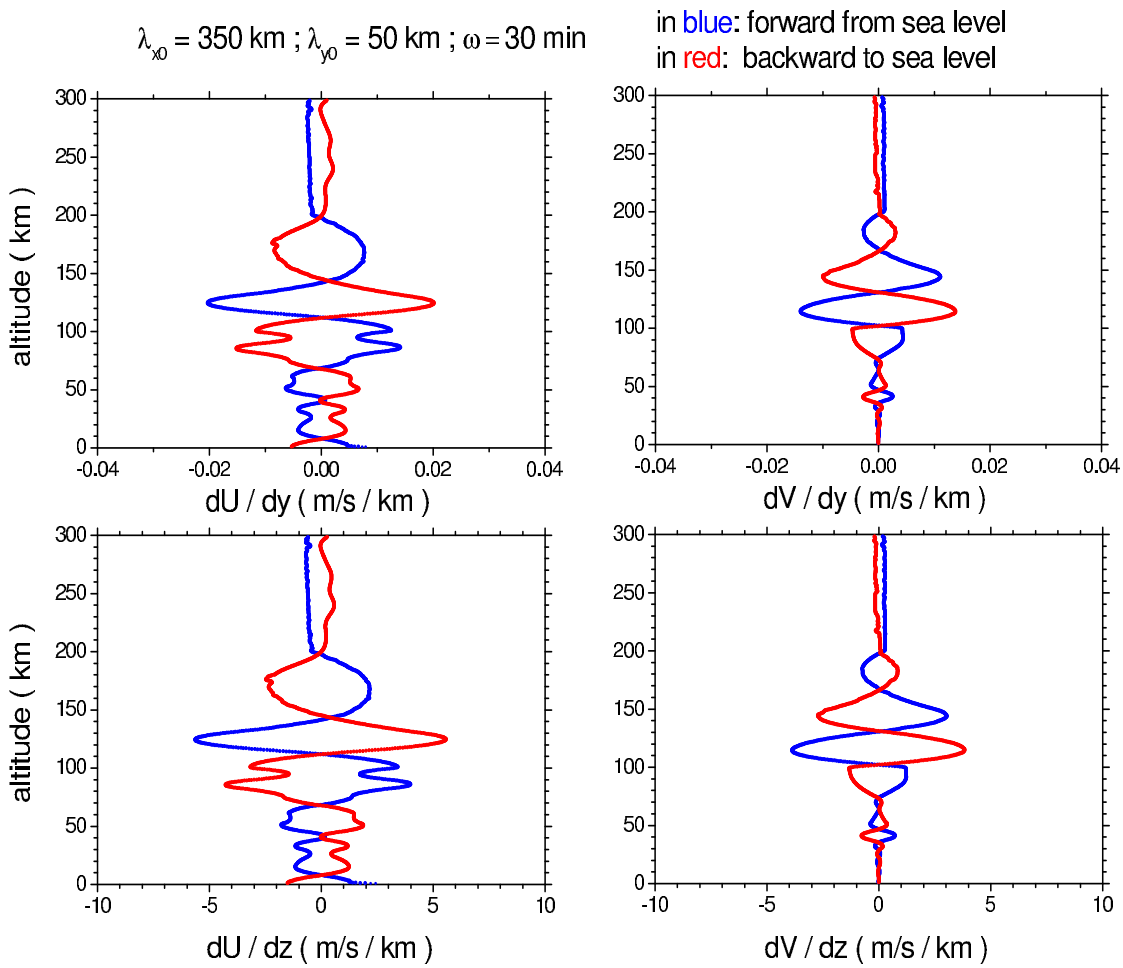

Figure 11 : Case 4-4: Altitude profiles of zonal wind gradients (LHS two panels) and meridional wind gradients (RHS two panels) in y (upper two panels) and z (lower two panels) in isothermal and sheared atmosphere

Notes

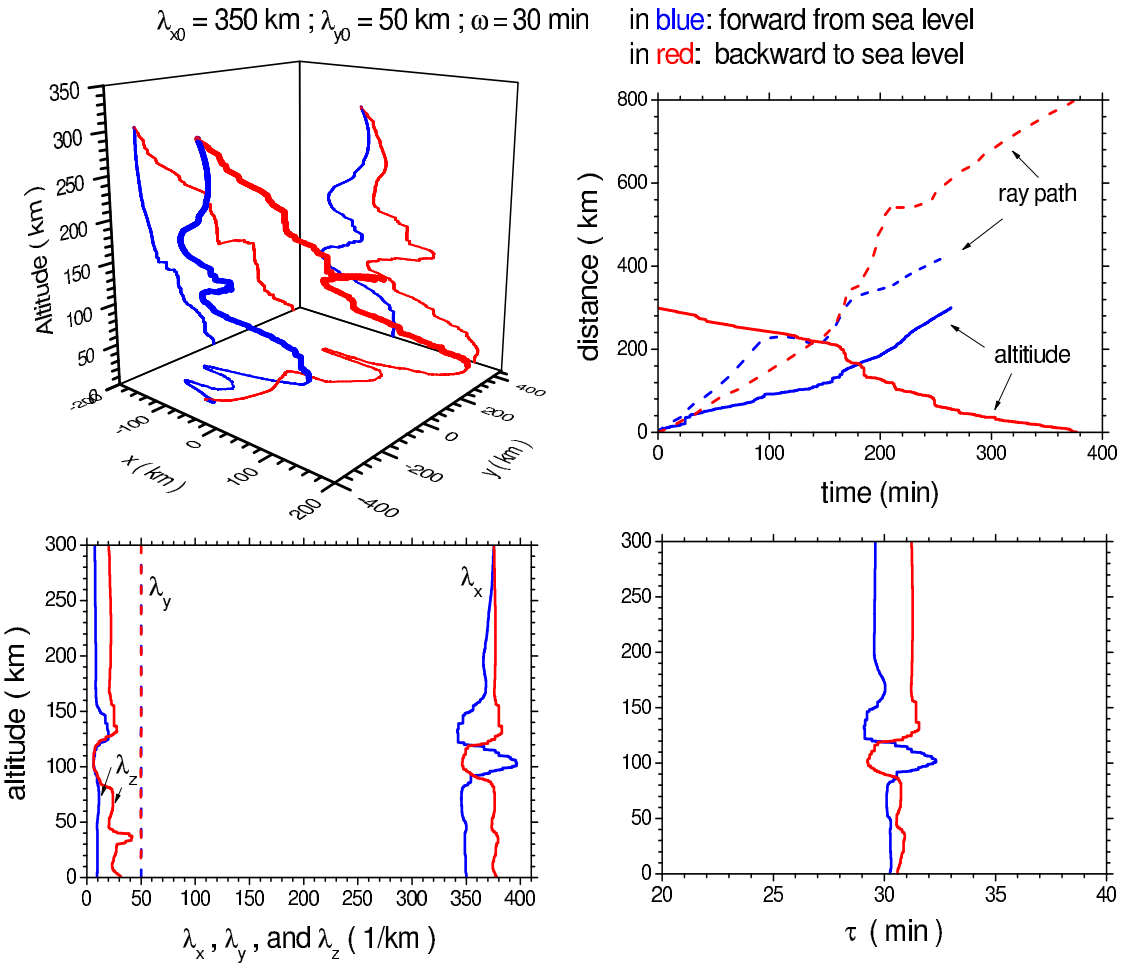

Figure 12 : Case 5-1: Ray propagation in both space (upper left panel) and time (upper right panel), and altitude profiles of wavelengths (lower left panel) and intrinsic wave periods (lower right panel) in nonisothermal and wind-shearing atmosphere

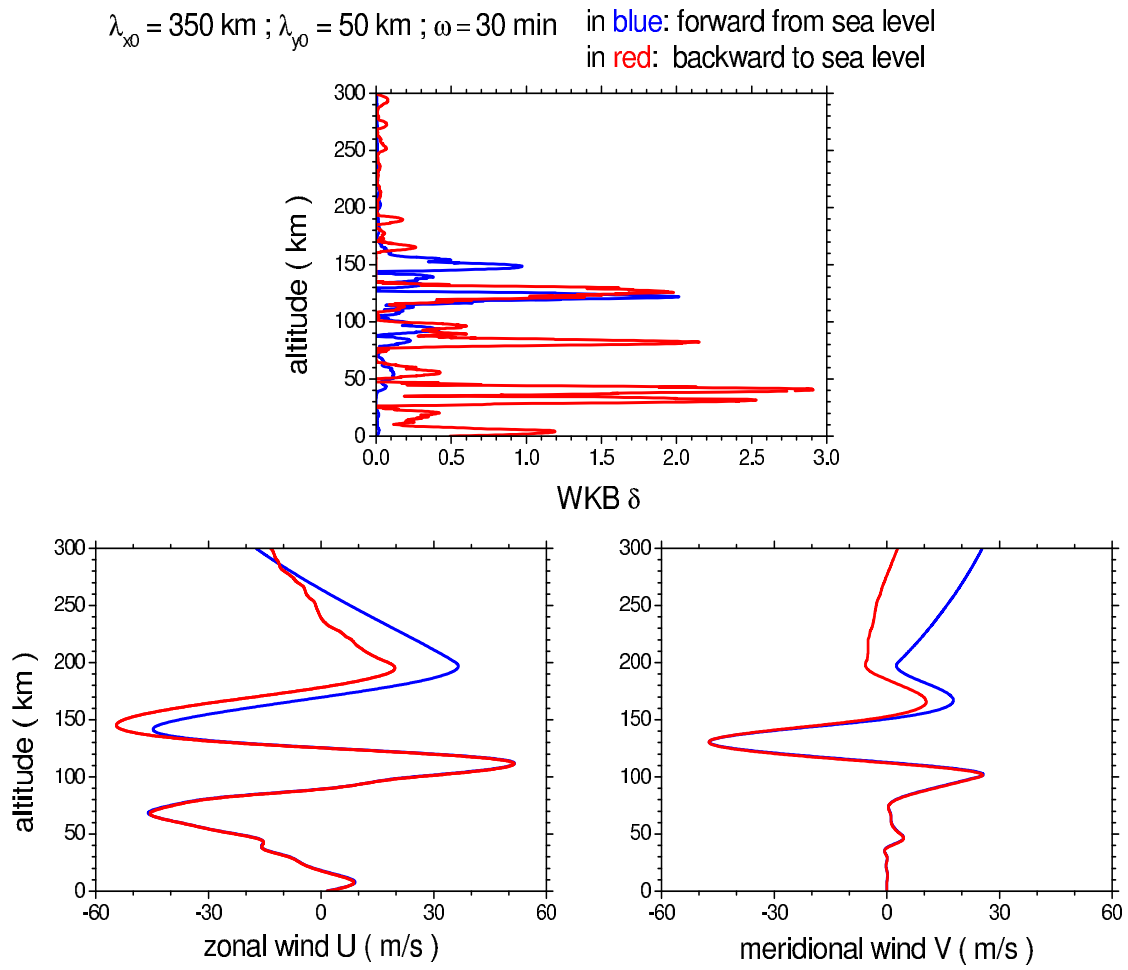

Figure 13 : Case 5-2: Altitude profiles along ray paths of WKB δ (upper panel), and mean-field wind (lower left panel: zonal direction; lower right panel: meridional direction) in nonisothermal and wind-shearing atmosphere

Notes

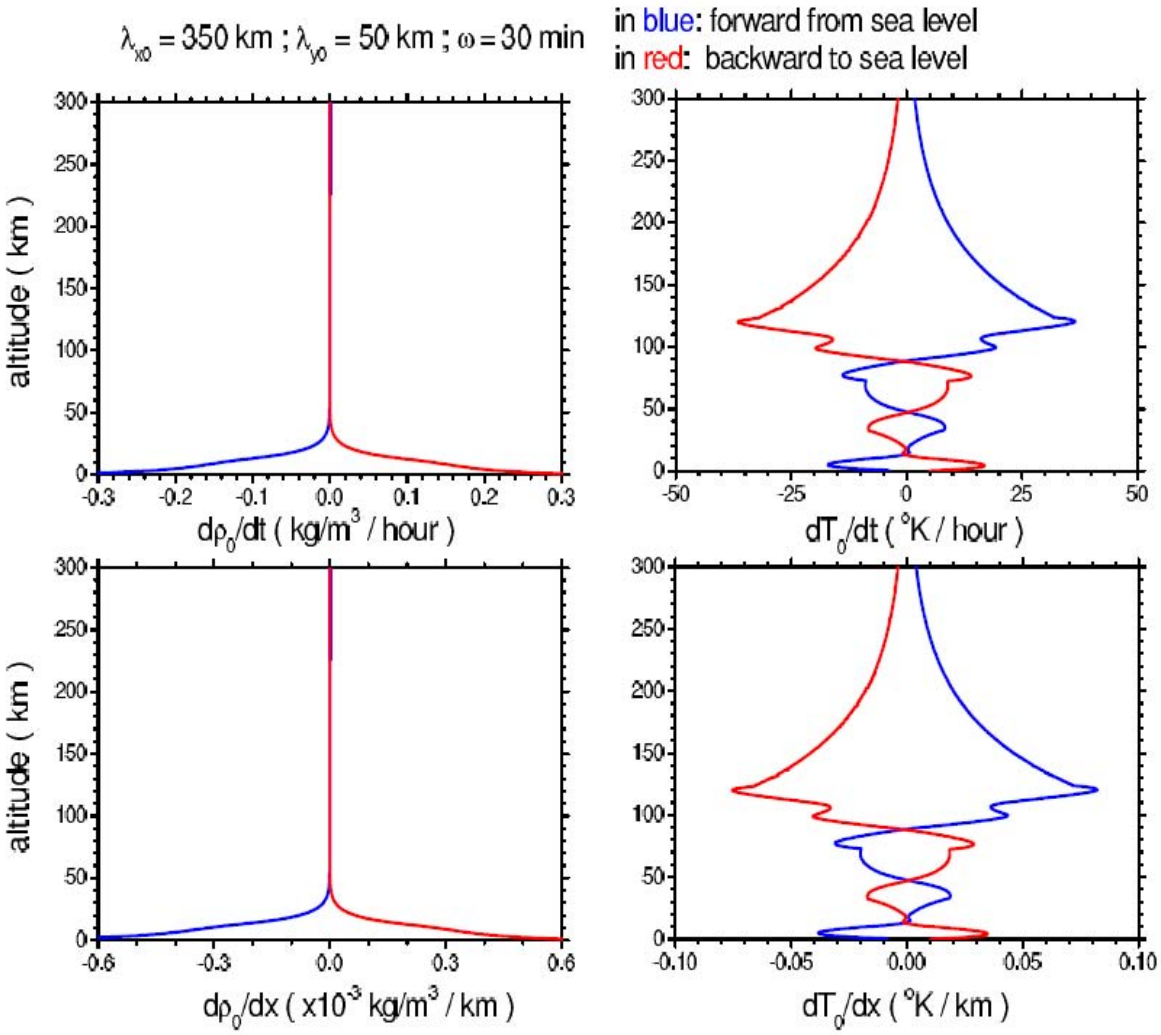

Figure 14 : Case 5-3: Altitude profiles of density gradients (LHS two panels) and temperature gradients (RHS two panels) in t (upper two panels) and x (lower two panels) in nonisothermal and wind-shearing atmosphere

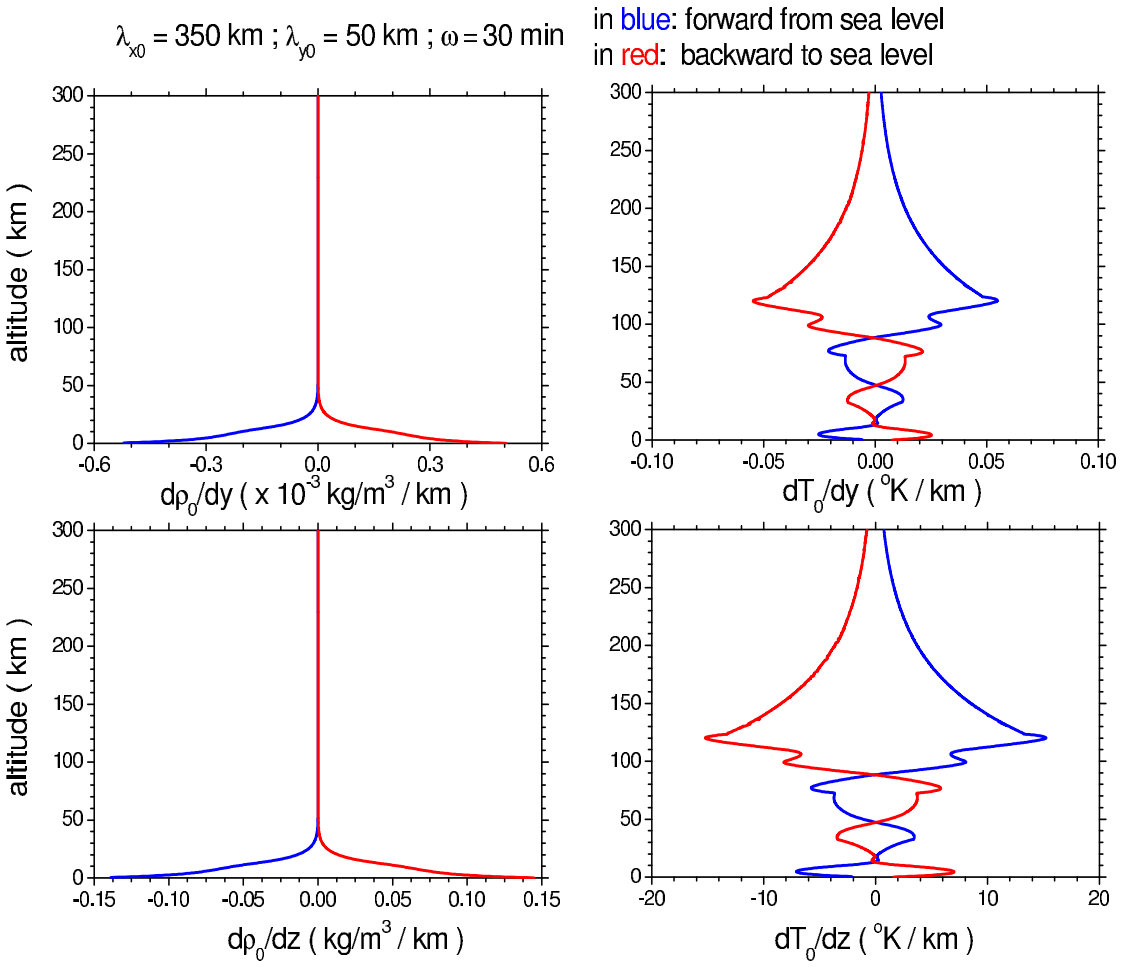

Figure 15 : Case 5-4: Altitude profiles of density gradients (LHS two panels) and temperature gradients (RHS two panels) in y (upper two panels) and z (lower two panels) in nonisothermal and wind-shearing atmosphere

Notes

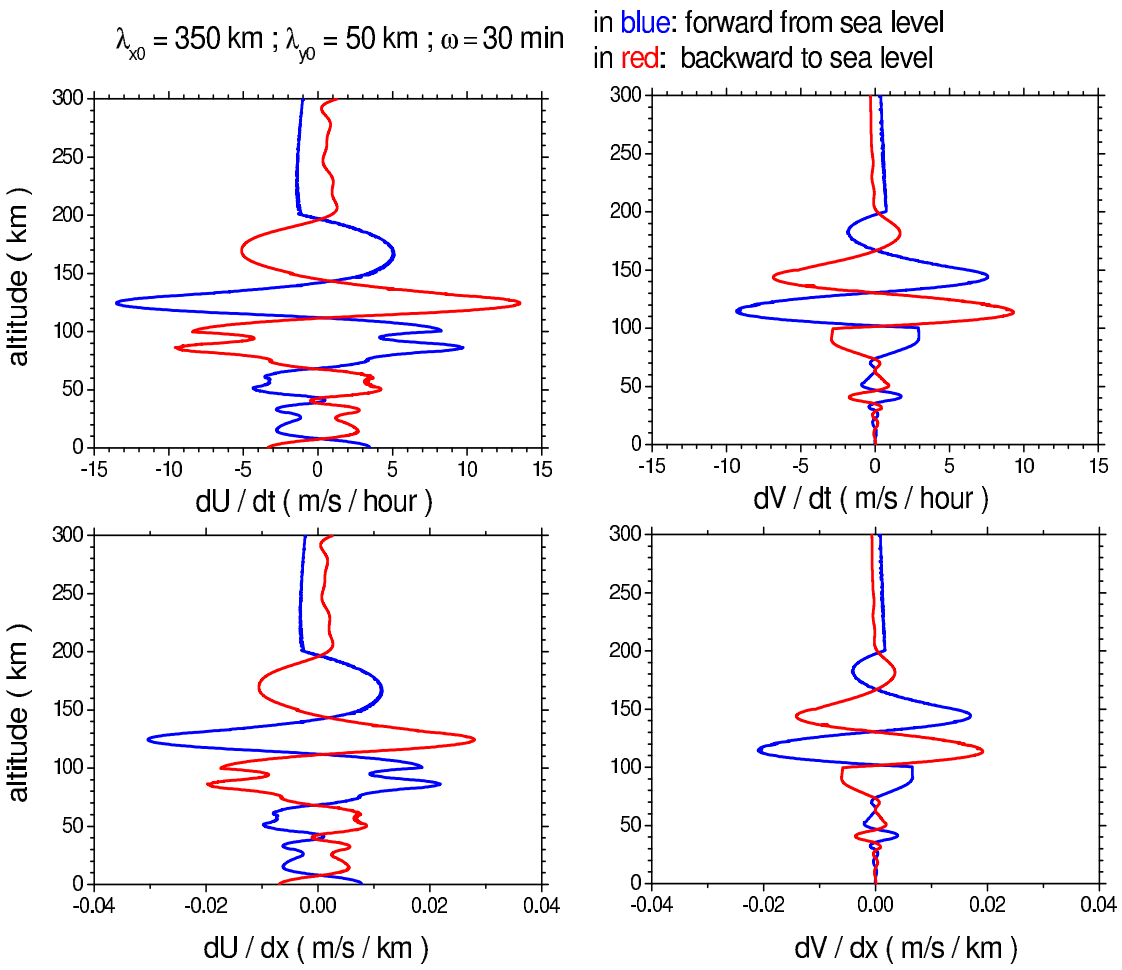

Figure 16 : Case 5-5: Altitude profiles of zonal wind gradients (LHS two panels) and meridional wind gradients (RHS two panels) in t (upper two panels) and x (lower two panels) in nonisothermal and wind-shearing atmosphere

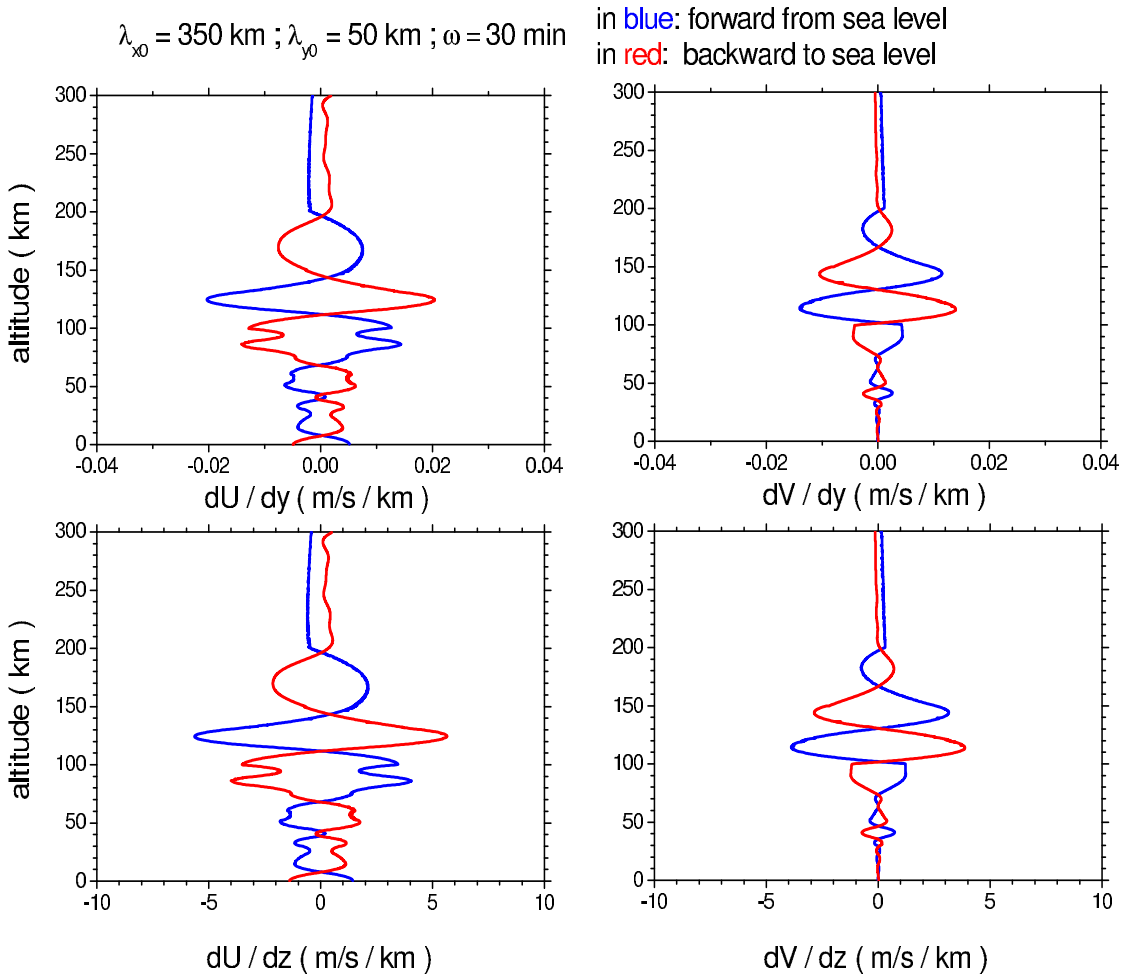

Figure 17 : Case 5-6: Altitude profiles of zonal wind gradients (LHS two panels) and meridional wind gradients (RHS two panels) in y (upper two panels) and z (lower two panels) in nonisothermal and wind-shearing atmosphere

Notes

Notes

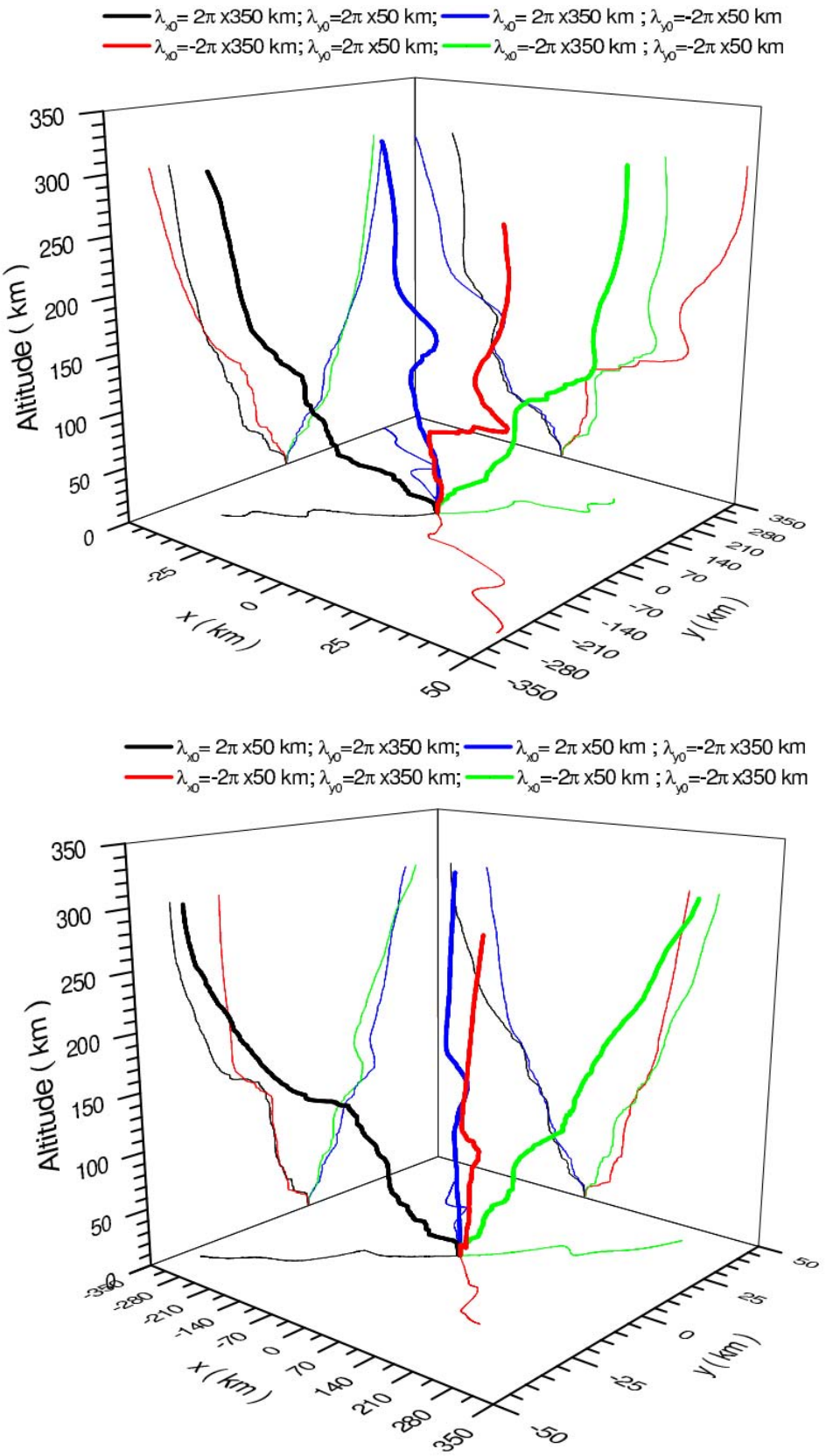

Figure 18 : Case 6-1: Propagating ray paths in space in nonisothermal and windshearing atmosphere under different initial wavelengths

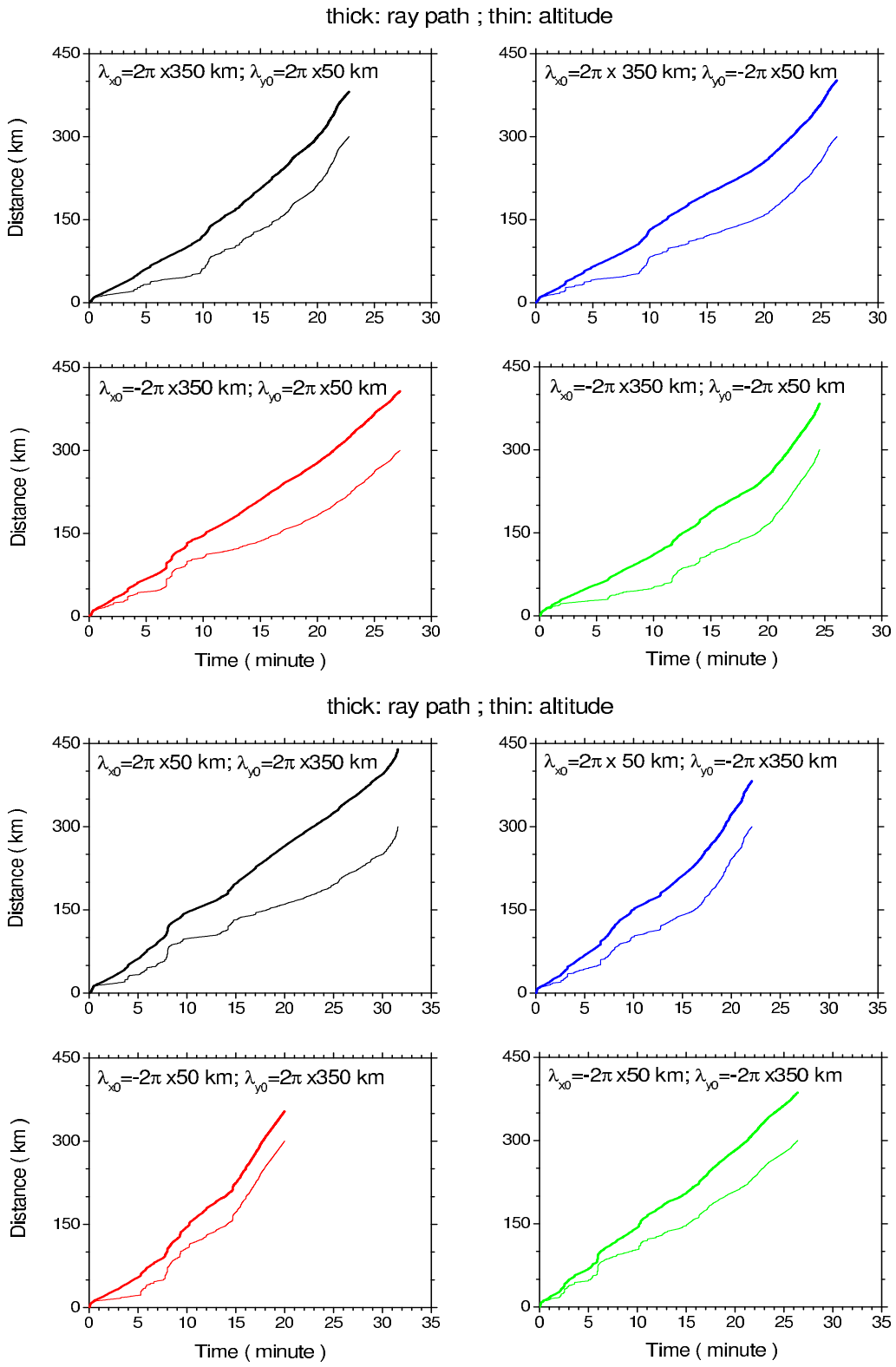

Figure 19 : Case 6-2: the same as Fig.18 but ray paths and vertical increments in time

Notes

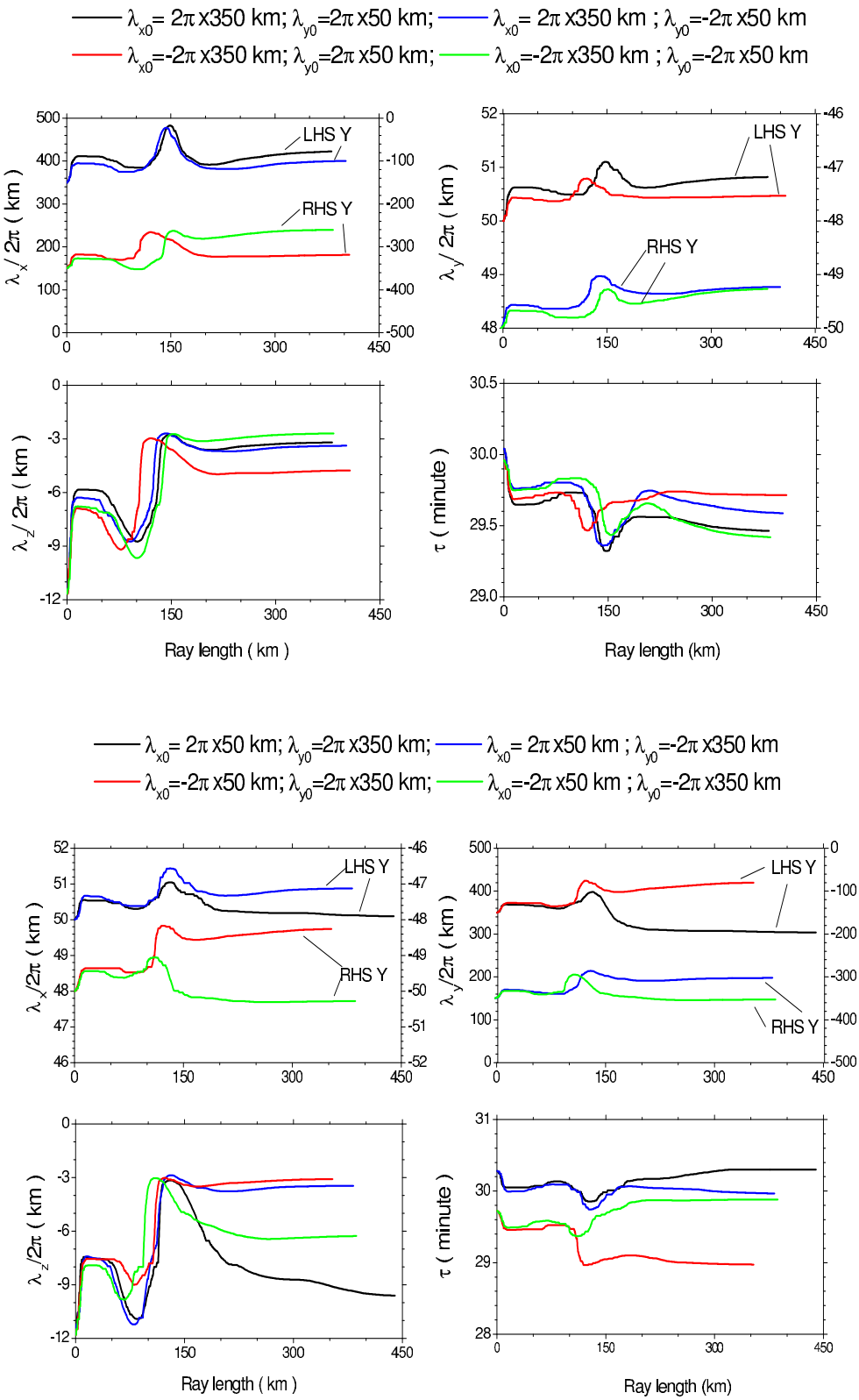

Figure 20 : Case 6-3: Development of $\lambda_{x,y,z}$ and τ versus ray path in wave propagation

This page is intentionally left blank

Global Journal of Science Frontier Research: F
Mathematics and Decision Sciences
Volume 16 Issue 3 Version 1.0 Year 2016
Type : Double Blind Peer Reviewed International Research Journal
Publisher: Global Journals Inc. (USA)
Online ISSN: 2249-4626 & Print ISSN: 0975-5896

A Semi-Symmetric Metric S-Connection in a Generalised Co-Symplectic Manifold

By Deepa Kandpal & J. Upreti
Kumaun University, India

Abstract- In the present paper, we define a new type of connection called semi-symmetric S-connection in a generalised co-symplectic manifold and studied some of its properties. The relation between the curvature tensor with respect to this connection and the curvature tensor with respect to the Riemannian connection is establised.

Keywords: *semi-symmetric s-connection, generalised co-symplectic manifold, curvature tensor.*

GJSFR-F Classification : *MSC 2010: 53C25*

Strictly as per the compliance and regulations of :

1. Mishra, R.S., Almost Contact Metric Manifold, Monograph (I), Tensor Society of India, Lucknow, (1991).

A Semi-Symmetric Metric S-Connection in a Generalised Co-Symplectic Manifold

Deepa Kandpal [α] & J. Upreti [σ]

Abstract- In the present paper, we define a new type of connection called semi-symmetric S-connection in a generalised co-symplectic manifold and studied some of its properties. The relation between the curvature tensor with respect to this connection and the curvature tensor with respect to the Riemannian connection is establised.

Keywords: *semi-symmetric s-connection, generalised co-symplectic manifold, curvature tensor.*

I. Introduction

An n-dimensional differentiable manifold M_n is an almost Contact manifold, if it admidts a tensor field F of type $(1,1)$, a vector field ξ and a 1-form η satisfying for arbitrary vector field X , such that

$$\overline{\overline{X}} + X = \eta(X)\xi \tag{1.1}$$

$$\overline{\xi} = 0 \tag{1.2}$$

where

$$\overline{X} = FX$$

Again equations (1.1) and (1.2) gives

$$\eta(\overline{X}) = 0 \tag{1.3}$$

$$\eta(\xi) = 1 \tag{1.4}$$

An almost contact manifold M_n in which a Riemannian metric tensor g of type (0,2) satisfies

$$g(\overline{X}, \overline{Y}) = g(X, Y) - \eta(X)\eta(Y) \tag{1.5}$$

$$g(X, \xi) = \eta(X) \tag{1.6}$$

for arbitrary vector field X, Y, is called an almost Contact Metric Manifold [1].

Author: *Dept. of Mathematics, S.S.J. Campus, Kumaun University, Almora. e-mails: kandpal.diya@gmail.com, prof.upreti@gmail.com*

Let us put

$$F^{'}(X,Y) = g(\overline{X},Y)$$

then we have

$$F^{'}(\overline{X},\overline{Y}) = F^{'}(X,Y) \tag{1.7}$$

$$F^{'}(X,Y) = g(\overline{X},Y) = -g(X,\overline{Y}) = -F^{'}(Y,X) \tag{1.8}$$

An almost contact metric manifold satisfying

$$(\bigtriangledown_X F^{'})(Y,Z) = \eta(Y)(\bigtriangledown_X \eta)(\overline{Z}) - \eta(Z)(\bigtriangledown_X \eta)\overline{Y} \tag{1.9}$$

and

$$(\bigtriangledown_X F^{'})(Y,Z) + (\bigtriangledown_Y F^{'})(Z,X) + (\bigtriangledown_Z F^{'})(X,Y) + \eta(X)[(\bigtriangledown_Y \eta)\overline{Z} - (\bigtriangledown_Z \eta)\overline{Y}]$$

$$+\eta(Y)[(\bigtriangledown_Z \eta)\overline{X} - (\bigtriangledown_X \eta)\overline{Z}] + \eta(Z)[(\bigtriangledown_X \eta)\overline{Y} - (\bigtriangledown_Y \eta)\overline{X}] = 0 \tag{1.10}$$

for arbitrary vector field X,Y, Z . Then M_n is called Generalised Co-Symplectic and Generalised Quasi-Ssasakian Manifold[2] .

If in M_n

$$(\bigtriangledown_X \eta)\overline{Y} = -(\bigtriangledown_{\overline{X}} \eta)Y = (\bigtriangledown_Y \eta)\overline{X} \tag{1.11}$$

$$(\bigtriangledown_X \eta)Y = (\bigtriangledown_{\overline{X}} \eta)\overline{Y} = -(\bigtriangledown_Y \eta)X \tag{1.12}$$

$$(\bigtriangledown_\xi F) = 0 \tag{1.13}$$

Then ξ is said to be of the first class and the manifold is said to be first class [2].

If in an almost Contact metric Manifold M_n , ξ satisfies

$$(\bigtriangledown_X \eta)\overline{Y} = (\bigtriangledown_{\overline{X}} \eta)Y = -(\bigtriangledown_Y \eta)\overline{X} \Leftrightarrow (\bigtriangledown_X \eta)Y = -(\bigtriangledown_{\overline{X}} \eta)\overline{Y} = (\bigtriangledown_Y \eta)X \tag{1.14}$$

$$(\bigtriangledown_\xi F) = 0. \tag{1.15}$$

Then ξ is said to be of the second class and the manifold M_n is said to be of the second class [2].

The Nijenhuis tensor in Generalised Co-Symplectic Manifold is given by

$$N(X,Y) = (\bigtriangledown_{\overline{X}} F)Y - (\bigtriangledown_{\overline{Y}} F)X - \overline{\bigtriangledown_X F)Y} + \overline{\bigtriangledown_Y F)X} \tag{1.16}$$

$$N^{'}(X,Y,Z) = (\bigtriangledown_{\overline{X}} F^{'})(Y,Z) - (\bigtriangledown_{\overline{Y}} F^{'})(X,Z) + (\bigtriangledown_X F^{'})(Y,\overline{Z}) - (\bigtriangledown_Y F^{'})(X,\overline{Z}) \tag{1.17}$$

Ref

2. Ojha , R.H. and Prasad S. , On Semi-Symmetric Metric s-Connextion in a Sasakian Manifold , Indian Jour. Pure and Appl. Math. , (Vol. 16(4), 341-344(1985).

II. A Semi-Symmetric Metric S-Connection

Let E be an affine connection and E is said to be metric if

$$(E_X g) = 0 \tag{2.1}$$

The metric connection satisfying

$$(E_X F)Y = \eta(Y)X - g(X,Y)\xi \tag{2.2}$$

is called S-connection [3].
A metric S-Connection E is called semi -symmetric metric S-Connection if

$$E_X Y = \nabla_X Y - \eta(X)\overline{Y} \tag{2.3}$$

which implies

$$S(X,Y) = \eta(Y)\overline{X} - \eta(X)\overline{Y} \tag{2.4}$$

where S is the torsion tensor of connection E. We know that

$$E_X(g(Y,Z)) = (E_X g)(Y,Z) + g(E_X Y, Z) + g(Y, E_X Z).$$

Using equation (2.3)

$$(E_X g)(Y,Z) = 0, where X, Y, Z \epsilon M_n. \tag{2.5}$$

Therefore , linear connection E defined by equation (2.3) and satisfying equations (2.4) and (2.5) is semi-symmetric metric connection ,we have

$$S(X,Y) = -S(Y,X)$$

This implies S is semi-symmetric. Now let E be a linear connection defined on a generalised Co-Symplectic manifold M_n by

$$E_X Y = \nabla_X Y + P(X,Y) \tag{2.6}$$

where P is a tensor of type (1,2) defined on M_n. Now , from equations (2.5) and (2.6) , we have

$$E_X(g(Y,Z)) = (E_X g)(Y,Z) + g(E_X Y, Z) + g(Y, E_X Z)$$

$$\Leftrightarrow g(P(X,Y),Z) + g(Y, P(X,Z)) = 0$$

$$g(P(X,Y),Z) + g(P(X,Z),Y) = 0 \tag{2.7}$$

from equation (2.6) , we get

$$S(X,Y) = P(X,Y) - P(Y,X). \tag{2.8}$$

Using equation (2.8), we get

$$g(S(X,Y),Z) + g(S(Z,X),Y) + g(S(Z,Y),X) = 2g(P(X,Y),Z) \tag{2.9}$$

Ref

3. Sasaki, S., Almost Contact Manifold, I, II, III, A lecture Note, Tohoku University, (1967),(1967),(1968).

and

$$P(X,Y) = \frac{1}{2}[\eta(Y)\overline{X} - \eta(X)\overline{Y}] \tag{2.10}$$

Now from equations (2.6) and (2.10), we get

$$E_X Y = \bigtriangledown_X Y + \frac{1}{2}[\eta(Y)\overline{X} - \eta(X)\overline{Y}] \tag{2.11}$$

Further for a 1-form η on a generalised Co-Symplectic manifold M_n, we have,

Theorem 2.1. *A Generalised Co-Symplectic Manifold M_n admitting a connection E , is uniquely determined by the contact form η and tensor field F satisfies*

$$(E_X\eta)Y = (\bigtriangledown_X\eta)Y \tag{2.12}$$

$$(E_X\eta)(FY) = (\bigtriangledown_X\eta)(FY) \tag{2.13}$$

$$E_X(FY) = \eta(Y)X - g(X,Y)\xi + \overline{\bigtriangledown_X Y} - \frac{1}{2}[\eta(Y)X - \eta(X)Y] \tag{2.14}$$

$$E_X(FY) - E_Y(FX) = \overline{\bigtriangledown_X Y} - \overline{\bigtriangledown_Y X} \tag{2.15}$$

Proof: Using equations (2.6), (2.10) and (2.11) , we have the results (2.12),(2.13),(2.14) and (2.15).

Again covariant differentiation of the torsion tensor S is given by

$$E_X(S(Y,Z)) = (E_X S)(Y,Z) + S(E_X Y, Z) + S(Y, E_X Z).$$

Using equation (2.4) , we have

$$(E_X S)(Y,Z) = ((E_X\eta)Z)Y - ((E_X\eta)Y)Z \tag{2.16}$$

Let us define

$$\overline{S}(X,Y,Z) = g(S(X,Y),Z) \tag{2.17}$$

Then from the equations (2.4) and (2.17), we get

$$\overline{S}(X,Y,Z) + \overline{S}(Y,Z,X) + \overline{S}(Z,X,Y) = 0 \tag{2.18}$$

and

$$g(P(X,Y),Z) + g(P(X,Z),Y) = 0 \tag{2.19}$$

The torsion tensor S of the connection E satisfies the following relations

(a) $S(\overline{X},\overline{Y}) = 0$
(b) $S(X,\xi) = \overline{\overline{X}}$
(c) $S(\overline{X},\xi) = \overline{X}$,
(d) $S(X,\xi) - S(\overline{\overline{X}},\xi) = 2X - 2\eta(X)\xi$
(e) $S(\overline{\overline{X}},Y) = \eta(X)\eta(Y)\xi - \eta(Y)X$
(f) $S(X,Y) = \eta(Y)\overline{X}$
(g) $\eta(S(X,Y) = 0$

Theorem 2.2. *A generalised Co-symplectic Manifold M_n satisfies the following relations i.e. (a),(b),(c),(d),(e),(f) and (g)defined above.*

Notes

Notes

Theorem 2.3. *In a Generalised Co-Symplectic manifold M_n with connection E ,we have*
(a) $\tilde{P}(X,Y,Z) = \frac{1}{2}[\eta(Y)F'(X,Y) - \eta(X)F'(Y,Z)]$
(b) $\tilde{P}(X,\overline{Y},\overline{Z}) = 1/2[\eta(X)g(Y,Z) - \eta(X)\eta(Y)\eta(Z)]$
(c) $\tilde{P}(\overline{X},\overline{Y},\overline{Z}) = 0$
(d) $\tilde{P}(\overline{X},\overline{Y},Z) = 0 = \tilde{S}(\overline{X},\overline{Y},\overline{Z}) = 0$
(e) $\tilde{P}(X,Y,\overline{Z}) = \frac{1}{2}[\eta(Y)F'(X,\overline{Z}) - \eta(X)F'(Y,\overline{Z})]$
where $\tilde{P}(X,Y,Z) = g(P(X,Y),Z)$

Theorem 2.4. *In a Generalised Co-Symplectic Manifold M_n admitting connection E satisfied the following properties:*
(a) $(E_X F')(Y,Z) = (\bigtriangledown_X F')(Y,Z) - \frac{1}{2}[\eta(Y)F'(\overline{X},Z) + \eta(Z)F'(Y,\overline{X})]$
(b) $E_{FX}F'(\overline{Y},\overline{Z}) = (\bigtriangledown_{FX}F')(\overline{Y},\overline{Z})$

Proof: (a) We have

$$X(F'(Y,Z)) = (E_X F')(Y,Z) + F'(E_X Y,Z) + F'(Y,E_X Z)$$

$$X(F'(Y,Z)) = (\bigtriangledown_X F')(Y,Z) + F'(\bigtriangledown_X Y,Z) + F'(Y,\bigtriangledown_X Z)$$

which implies

$$(E_X F')(Y,Z) = (\bigtriangledown_X F')(Y,Z) + F'(\bigtriangledown_X Y,Z) + F'(Y,\bigtriangledown_X Z) - F'(E_X Y,Z) - F(Y,E_X Z)$$
$$= (\bigtriangledown_X F')(Y,Z) - 1/2[\eta(Y)F'(\overline{X},Z) + \eta(Z)F'(Y,\overline{X})]$$

Using equation (2.10) , we get (a). Again baring (a), we get (b) and (c).

III. Curvature Tensor of M_n with Respect to Connection E

Let $\tilde{R}$ be the curvature tensor with respect to the semi -symmetric metric connection E on a generalised co-symplectic manifold M_n. Then

$$\tilde{R}(X,Y,Z) = E_X E_Y Z - E_Y E_X Z - E_{[X,Y]}Z \tag{3.1}$$

We have the following results:

Theorem 3.1. *In a Generalised Co-Symplectic Manifold M_n curvature tensor $\tilde{R}$ is given by*

$$\tilde{R}(X,Y,Z) = R(X,Y,Z) + \frac{1}{2}[S(X,\bigtriangledown_Y Z) + S(\bigtriangledown_X Z,Y)] + \frac{1}{2}\eta(Z)S'(X,Y)$$
$$+\frac{1}{2}\eta(Z)[\bigtriangledown_X \overline{Y} - \bigtriangledown_Y \overline{X}] + \frac{1}{2}[\eta(Y)\bigtriangledown_X \overline{Z} - \eta(X)\bigtriangledown_Y \overline{Z}]$$
$$-\frac{1}{2}(\bigtriangledown_Y \eta(Z))\overline{X} - \frac{1}{2}\eta(Z)\overline{[X,Y]} + \frac{1}{2}\eta([X,Y])\overline{Z} - ((\bigtriangledown_X \eta)Y)\overline{Z} \tag{3.2}$$

where

$$S'(X,Y) = \eta(X)Y - \eta(Y)X$$

$$R(X,Y,Z) = \bigtriangledown_X \bigtriangledown_Y Z - \bigtriangledown_Y \bigtriangledown_X Z - \bigtriangledown_{[X,Y]}Z$$

Proof: Let $\tilde{R}(X,Y,Z)$ be the curvature tensor for generalised co-symplectic manifold with respect the semi-symmetric metric S-connection E , then

$$\tilde{R}(X,Y,Z) = E_X E_Y Z - E_Y E_X Z - E_{[X,Y]} Z$$

By using equations (1.1),(1.2),(1.11),(1.12),(1.13) ,(2.9) and (2.12), we get equation (3.1), where R(X,Y,Z) is curvature tensor of M_n with respect to the Riemannian Curvature $\bigtriangledown$.

Let K and $\tilde{K}$ be curvature tensor of type (0,4) given by

$$K(X,Y,Z) = g(R(X,Y,Z),U)$$

$$\tilde{K}(X,Y,Z,U) = g(\tilde{K}(X,Y,Z),U)$$

Theorem 3.2. In a Generalised Co-Symplectic Manifold M_n,we have

$$\tilde{R}(X,Y,Z) + \tilde{R}(Y,Z,X) + \tilde{R}(Z,X,Y) = 0 \tag{3.3}$$

If

$$2[((\bigtriangledown_X \eta)Z)\overline{Y} + ((\bigtriangledown_Y \eta)X)\overline{Z} + ((\bigtriangledown_Z \eta)Y)\overline{X}]$$

$$+\eta([X,Z])\overline{Y} + \eta([Y,X])\overline{Z} + \eta([Z,Y])\overline{X} = 0 \tag{3.4}$$

and

$$\tilde{K}(X,Y,Z,U) + \tilde{K}(Y,X,Z,U) = 0 \tag{3.5}$$

If and only if

$$g((\bigtriangledown_Y \eta(Z))\overline{X}, U) + g((\bigtriangledown_X \eta(Z))\overline{Y}, U) = 0 \tag{3.6}$$

and

$$(\bigtriangledown_Y \eta)X + (\bigtriangledown_X \eta)Y = 0 \tag{3.7}$$

Proof: Using equation (3.2) and the first Bianchi identity

$$R(X,Y,Z) + R(Y,Z,X) + R(Z,X,Y) = 0$$

with respect to Riemannian Connection $\bigtriangledown$, we get eq.(3.3) and (3.4).

We have

$$\tilde{K}(X,Y,Z) = g(\tilde{R}(X,Y,Z),U)$$

$$= g(R(X,Y,Z),U) + \frac{1}{2}g(S(X,\bigtriangledown_Y Z),U) + \frac{1}{2}g(S(\bigtriangledown_X Z,Y),U)$$

$$+\frac{1}{2}g(\eta(Z)[\bigtriangledown_X \overline{Y} - \bigtriangledown_Y \overline{X}],U) + \frac{1}{4}g(\eta(Z)[\eta(X)Y - \eta(Y)X]$$

$$-g(((\bigtriangledown_X \eta)Y)\overline{Z},U) + \frac{1}{2}g((\eta(Y)\bigtriangledown_X \overline{Z} - \eta(X)\bigtriangledown_Y \overline{Z}),U)$$

$$-\frac{1}{2}g((\bigtriangledown_Y\eta(Z)\overline{X},U)-\frac{1}{2}g(\eta(Z)\overline{[X,Y]},U)+\frac{1}{2}g(\eta([X,Y])\overline{Z},U)$$

We get

$$\tilde{K}(X,Y,Z,U)=-\tilde{K}(Y,X,Z,U) \tag{3.8}$$

If

$$g(\bigtriangledown_Y\eta(Z)\overline{X},U)=-g(\bigtriangledown_X\eta(Z)\overline{Y},U) \tag{3.9}$$

and

$$(\bigtriangledown_Y\eta)X+(\bigtriangledown_X\eta)Y=0 \tag{3.10}$$

IV. Nijenhuis Tensor of M_n with Respect to New Connection E

The Nijenhuis tensor with respect to E of F in a generalised Co-symplectic manifold M_n is a vector valued bilinear scalar function N_E , is given by

$$N_E(X,Y)=(\bigtriangledown_{\overline{X}}F)Y+S(X,Y)-(\bigtriangledown_{\overline{Y}}F)X+\overline{\bigtriangledown_XF)Y}+\overline{\bigtriangledown_YF)X} \tag{4.1}$$

Using equation (1.16) , we get

$$N_E(X,Y)=N(X,Y)+S(X,Y)+2\overline{\bigtriangledown_XF)Y} \tag{4.2}$$

where N is Nijenhuis tensor with respect to Riemannian connection and S is the Torsion tensor of connection E.

Again by using equation (1.17) ,we get

$$N_E(X,Y,Z)=(E_{\overline{X}}F')(Y,Z)-(E_{\overline{Y}}F')(X,Z)-(E_YF')(X,\overline{Z})+\frac{1}{2}\eta(Y)[F'(X,\overline{Z})+F'(X,Z)] \tag{4.3}$$

and

$$N_E(X,Y,Z)=N(X,Y,Z) \tag{4.4}$$

If and only if

$$(\bigtriangledown_XF')(Y,\overline{Z})+(\bigtriangledown_YF')(X,Z)-(\bigtriangledown_YF')(X,\overline{Z})=\frac{1}{2}\eta(X)[F'(Y,Z)+F'(\overline{Y},Z)]+\frac{1}{2}\eta(Y)F'(X,\overline{Z}) \tag{4.5}$$

References Références Referencias

1. Mishra, R.S., Almost Contact Metric Manifold, Monograph (I), Tensor Society of India, Lucknow, (1991).
2. Ojha , R.H. and Prasad S. , On Semi-Symmetric Metric s-Connextion in a Sasakian Manifold , Indian Jour. Pure and Appl. Math. , (Vol. 16(4), 341-344(1985).
3. Sasaki, S., Almost Contact Manifold, I, II, III, A lecture Note, Tohoku University, (1967),(1967),(1968).

This page is intentionally left blank

Global Journal of Science Frontier Research: F
Mathematics and Decision Sciences
Volume 16 Issue 3 Version 1.0 Year 2016
Type : Double Blind Peer Reviewed International Research Journal
Publisher: Global Journals Inc. (USA)
Online ISSN: 2249-4626 & Print ISSN: 0975-5896

Numerical Solutions for the Improved Korteweg De Vries and the Two Dimension Korteweg De Vries (2D Kdv) Equations

By K. Raslan & Z. AbuShaeir
Al-Azhar University, Egypt

Abstract- In this paper we established a traveling wave solution by the $(\frac{G'}{G})$-expansion method for nonlinear partial differential equations (PDEs).The proposed method gives more general exact solutions for two different types of nonlinear partial differential equations such as the improved Korteweg de Vries equation and the two dimension Korteweg de Vries (2D KdV) equations.

Keywords: the $(\frac{G'}{G})$- expansion method, the improved korteweg de vries equation and the two dimension korteweg de vries (2D kdv).

GJSFR-F Classification : MSC 2010: 35Q53

Strictly as per the compliance and regulations of :

4. Fan, E. Extended tanh-function method and its applications to nonlinear equations. Phys. Lett. 2000;A (277) 212–218

Numerical Solutions for the Improved Korteweg De Vries and the Two Dimension Korteweg De Vries (2D KdV) Equations

K. Raslan [α] & Z. AbuShaeir [σ]

Abstract- In this paper we established a traveling wave solution by the $(\frac{G'}{G})$-expansion method for nonlinear partial differential equations (PDEs).The proposed method gives more general exact solutions for two different types of nonlinear partial differential equations such as the improved Korteweg de Vries equation and the two dimension Korteweg de Vries (2D KdV) equations.

Keywords: the $(\frac{G'}{G})$-expansion method, the improved korteweg de vries equation and the two dimension korteweg de vries (2D kdv).

I. Introduction

The nonlinear partial differential equations (NPDEs) are widely used to describe many important phenomena and dynamic processes in physics, chemistry, biology, fluid dynamics, plasma, optical fibers and other areas of engineering. Many efforts have been made to study NPDEs. One of the most exciting advances of nonlinear science and theoretical physics has been a development of methods that look for exact solutions for nonlinear evolution equations. The availability of symbolic computations such as Mathematica, has popularized direct seeking for exact solutions of nonlinear equations. Therefore, exact solution methods of nonlinear evolution equations have become more and more important resulting in methods like the tanh method [1–3], extended tanh function method [4, 5], the modified extended tanh function method [6], the generalized hyperbolic function [7]. Most of exact solutions have been obtained by these methods, including the solitary wave solutions, shock wave solutions, periodic wave solutions, and the like. In this paper, we propose the extended $(\frac{G'(\xi)}{G(\xi)})$-expansion method to find the exact solutions of the improved Korteweg de Vries (IKdV) equation and the two dimension Korteweg de Vries (2D KdV) equation. Our main goal in this study is to present the improved $(\frac{G'(\xi)}{G(\xi)})$-expansion method [12-15] for constructing the travelling wave solutions. In section 2, we describe the $(\frac{G'(\xi)}{G(\xi)})$-expansion method. In section 3, we apply the method to two physically important nonlinear evolution equations.,

Author α σ: Department of Mathematics, Faculty of Science, Al-Azhar University, Egypt. e-mail: kamal_raslan@yahoo.com

II. Outline of the $(\frac{G'(\xi)}{G(\xi)})$-Expansion Method

The $(\frac{G'(\xi)}{G(\xi)})$-expansion method will be introduced as presented by A.Hendi [8] and by [12–15].The method is applied to find out an exact solution of a nonlinear ordinary differential equation. Consider the nonlinear partial differential equation in the form

$$N(u, u_t, u_x, u_{tx}, u_{xx}, \dots.) = 0 \tag{2.1}$$

Where $u(x,t)$ is the solution of nonlinear partial differential equation Eq. (1). We use the transformation, $\xi = (x - c\,t)$, to transform $u(x,t)$ to $u(\xi)$ give :

$$\frac{\partial}{\partial t} = -c\frac{d}{d\xi}, \frac{\partial}{\partial x} = \frac{d}{d\xi}, \frac{\partial^2}{\partial x^2} = \frac{d^2}{d\xi^2}, \frac{\partial^3}{\partial x^3} = \frac{d^3}{d\xi^3}, \tag{2.2}$$

and so on, then Eq. (1) becomes an ordinary differential equation

$$N(u, -c\,u',\ u'\ , c^2\,u'', -c\,u'', \dots\dots.) = 0, \tag{2.3}$$

The solution of Eq.(3) can be expressed by a polynomial in $\frac{G'(\xi)}{G(\xi)}$

$$u(\xi) = \sum_{i=-N}^{N} a_i \left(\frac{G'(\xi)}{G(\xi)}\right)^i, \tag{2.4}$$

Where $G = G(\xi)$ satisfies,

$$G''(\xi) + \lambda\, G'(\xi) + \mu\, G(\xi) = 0, \tag{2.5}$$

Where $G'(\xi) = \frac{d\,G(\xi)}{d\xi}$, $G''(\xi) = \frac{d^2\,G(\xi)}{d\xi}$,a_i, λ and μ are constants to be determined later,$a_i \neq 0$, the unwritten part in (4) is also a polynomial in $\frac{G'(\xi)}{G(\xi)}$),but the degree of which is generally equal to or less than $m-1$,the positive integer m can be determined by balancing the highest order derivative terms with nonlinear term appearing in Eq.(3). The solutions of Eq.(5) for ($\frac{G'}{G}$) can be written in the form of hyperbolic, trigonometric and rational functions as given below[8].

$$\frac{G'(\xi)}{G(\xi)} = \begin{cases} \frac{\sqrt{\lambda^2-4\mu}}{2}\left(\frac{C_1 \sinh(\frac{\sqrt{\lambda^2-4\mu}}{2}\xi)+C_2 \cosh(\frac{\sqrt{\lambda^2-4\mu}}{2}\xi)}{C_1 \cosh(\frac{\sqrt{\lambda^2-4\mu}}{2}\xi)+C_2 \sinh(\frac{\sqrt{\lambda^2-4\mu}}{2}\xi)}\right) - \frac{\lambda}{2}, \text{when } \lambda^2-4\mu > 0, \\ \frac{\sqrt{4\mu-\lambda^2}}{2}\left(\frac{-C_1 \sin(\frac{\sqrt{4\mu-\lambda^2}}{2}\xi)+C_2 \cos(\frac{\sqrt{4\mu-\lambda^2}}{2}\xi)}{C_1 \cos(\frac{\sqrt{4\mu-\lambda^2}}{2}\xi)+C_2 \sin(\frac{\sqrt{4\mu-\lambda^2}}{2}\xi)}\right) - \frac{\lambda}{2}, \text{when } \lambda^2-4\mu > 0, \\ \frac{C2}{C1+C2\,\xi} - \frac{\lambda}{2}, \qquad \text{when } \lambda^2-4\mu = 0, \end{cases} \tag{2.6}$$

Where C_1 and C_2 are integration constants. Inserting Eq.(4) into (3) and using Eq.(5), collecting all terms with the same order $\frac{G'(\xi)}{G(\xi)}$ together, the left hand side of Eq.(3) is converted into another

Ref
8. M A Abdou, A.Hendi, Mirvet Al-Zumaie. On the extended $(\frac{G'}{G})$-expansion method and its applications Int. J. Comput. Math.(2011) 3(3): 193-199.

polynomial in $(\frac{G'(\xi)}{G(\xi)})$. Equating each coefficients of this polynomial to zero, yields a set of algebraic equations for a_i, λ, and μ.with the knowledge of the coefficients a_i and general solution of Eq.(5) we have more travelling wave solutions of the nonlinear evolution Eq.(1).

III. Applications

In order to illustrate the effectiveness of the proposed method two examples in mathematical are chosen as follows

a) The improved Korteweg de Vries (IKdV) equation

We Consider the IKdV equation in the form [11]

$$u_t + \epsilon\, u\, u_x + \beta u_{xxx} - \delta u_{xxt} = 0, \tag{3.1}$$

We make the transformation

$$u(x,t) = u(\xi),\ \xi = x - c\,t, \tag{3.2}$$

Eq. (3.1) becomes

$$-c\,u' + \epsilon\, u\, u' + \beta\, u''' + \delta\, c\, u''' = 0\,, \tag{3.3}$$

Integrating the above equation with respect to ξ, we get

$$-c\,u + \tfrac{\epsilon}{2}u^2 + (\beta + \delta c\,)u'' = 0, \tag{3.4}$$

Balancing u^2 with u''gives $m = 2$. thus we suppose solutions of Eq. (3.3) can be expressed by

$$u(\xi) = a_0 + a_1(\tfrac{G'(\xi)}{G(\xi)}) + a_2(\tfrac{G'(\xi)}{G(\xi)})^2, \tag{3.5}$$

Where a_0, a_1, a_2 are constants, Substituting Eq.(3.5) into Eq.(3.4),collecting the coefficients of $(\frac{G\,(\xi)}{G(\xi)})$ we obtain a set of algebraic equations for a_0, a_1, a_2 and c ,and solving this system we obtain the two sets of solutions as

Case (1)

$$a_0 = -\tfrac{2\beta(\lambda^2+2\mu)}{\epsilon(1+\delta(\lambda^2-4\mu))}, a_1 = -\tfrac{12\beta\,\lambda}{\epsilon(1+\delta(\lambda^2-4\mu))},\ a_2 = -\tfrac{12\beta}{\epsilon(1+\delta(\lambda^2-4\mu))}, \text{ and } c = \tfrac{-\beta(\lambda^2-4\mu)}{1+\delta(\lambda^2-4\mu)} \tag{3.6}$$

Case (2)

$$a_0 = \tfrac{12\beta\mu}{\epsilon(-1+\delta(\lambda^2-4\mu))}, a_1 = \tfrac{12\beta\lambda}{\epsilon(-1+\delta(\lambda^2-4\mu))}, a_2 = \tfrac{12\beta}{\epsilon(-1+\delta(\lambda^2-4\mu))}, \text{ and } c = \tfrac{-\beta(\lambda^2-4\mu)}{-1+\delta(\lambda^2-4\mu)} \tag{3.7}$$

By using Eq.(21) , Eq.(20)can written as

$$u(\xi) = -\tfrac{2\beta(\lambda^2+2\mu)}{\epsilon(1+\delta(\lambda^2-4\mu))} - \tfrac{12\beta\lambda}{\epsilon(1+\delta(\lambda^2-4\mu))}(\tfrac{G'(\xi)}{G(\xi)}) - \tfrac{12\,\beta}{\epsilon(1+\delta(\lambda^2-4\mu))}(\tfrac{G'(\xi)}{G(\xi)})^2, \tag{3.8}$$

or by using Eq.(3.7),Eq.(3.6)can written as

$$u(\xi) = \tfrac{12\beta\mu}{\epsilon(-1+\delta(\lambda^2-4\mu))} + \tfrac{12\beta\lambda}{\epsilon(-1+\delta(\lambda^2-4\mu))}\left(\tfrac{G'(\xi)}{G(\xi)}\right) + \tfrac{12\beta}{\epsilon(-1+\delta(\lambda^2-4\mu))}(\tfrac{G'(\xi)}{G(\xi)})^2 \tag{3.9}$$

We have three types of travelling wave solutions of the IKdV equation as

Ref

11. K. R. Raslan. Exact solitary wave solutions of equal width wave and related equations using a direct algebraic method. I.J. N. Science (2008) 6(3):246-254.

The first type: when $\lambda^2 - 4\,\mu > 0$,

$$u_1(\xi) = \left(\frac{3\beta(4\mu-\lambda^2)}{\epsilon(1+\delta(\lambda^2-4\mu))}\right)\left(\left(\frac{C_1 \sinh\left(\frac{\sqrt{\lambda^2-4\mu}}{2}\xi\right)+C_2 \cosh\left(\frac{\sqrt{\lambda^2-4\mu}}{2}\xi\right)}{C_1 \cosh\left(\frac{\sqrt{\lambda^2-4\mu}}{2}\xi\right)+C_2 \sinh\left(\frac{\sqrt{\lambda^2-4\mu}}{2}\xi\right)}\right)^2 - \frac{1}{3}\right), \tag{3.10}$$

Where $\xi = x + \frac{\beta(\lambda^2-4\mu)}{1+\delta(\lambda^2-4\mu)}t$, or

$$u_2(\xi) = \left(\frac{3\beta(4\mu-\lambda^2)}{\epsilon(-1+\delta(\lambda^2-4\mu))}\right)\left(1 - \left(\frac{C_1 \sinh\left(\frac{\sqrt{\lambda^2-4\mu}}{2}\xi\right)+C_2 \cosh\left(\frac{\sqrt{\lambda^2-4\mu}}{2}\xi\right)}{C_1 \cosh\left(\frac{\sqrt{\lambda^2-4\mu}}{2}\xi\right)+C_2 \sinh\left(\frac{\sqrt{\lambda^2-4\mu}}{2}\xi\right)}\right)^2\right) \tag{3.11}$$

Where $\xi = x + \frac{\beta(\lambda^2-4\mu)}{1-\delta(\lambda^2-4\mu)}t$,

The second type: when $\lambda^2 - 4\,\mu < 0$,

$$u_3(\xi) = \left(\frac{-3\beta(4\mu-\lambda^2)}{\epsilon(1+\delta(\lambda^2-4\mu))}\right)\left(\left(\frac{-C_1 \sin\left(\frac{\sqrt{4\mu-\lambda^2}}{2}\xi\right)+C_2 \cos\left(\frac{\sqrt{4\mu-\lambda^2}}{2}\xi\right)}{C_1 \cos\left(\frac{\sqrt{4\mu-\lambda^2}}{2}\xi\right)+C_2 \sin\left(\frac{\sqrt{4\mu-\lambda^2}}{2}\xi\right)}\right)^2 + \frac{1}{3}\right) \tag{3.12}$$

Where $\xi = x + \frac{\beta(\lambda^2-4\mu)}{1+\delta(\lambda^2-4\mu)}t$, or

$$u_4(\xi) = \left(\frac{3\beta(4\mu-\lambda^2)}{\epsilon(-1+\delta(\lambda^2-4\mu))}\right)\left(\left(\frac{-C_1 \sin\left(\frac{\sqrt{4\mu-\lambda^2}}{2}\xi\right)+C_2 \cos\left(\frac{\sqrt{4\mu-\lambda^2}}{2}\xi\right)}{C_1 \cos\left(\frac{\sqrt{4\mu-\lambda^2}}{2}\xi\right)+C_2 \sin\left(\frac{\sqrt{4\mu-\lambda^2}}{2}\xi\right)}\right)^2 + 1\right) \tag{3.13}$$

Where $\xi = x - \frac{\beta(\lambda^2-4\mu)}{1-\delta(\lambda^2-4\mu)}\,t$,

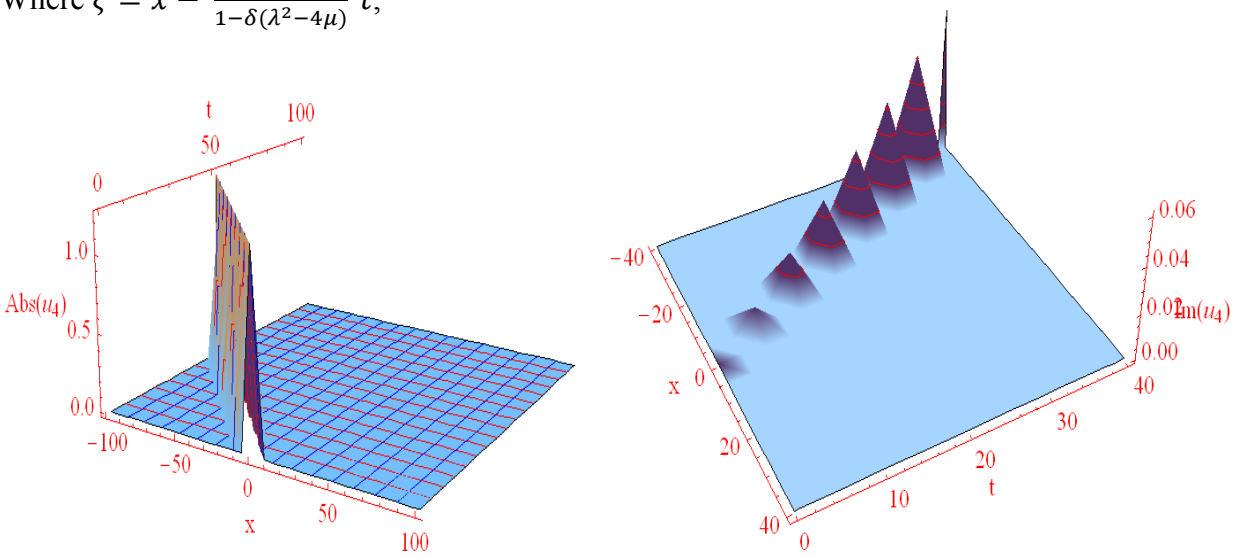

Figure 1 : for IKdV equation where $C_1 = 2, C_2 = 4, \lambda = 150$, and $\mu = 1, \beta = 2, \beta = 1$

The Third type: when $\lambda^2 - 4\,\mu = 0$

$$u_5(\xi) = \frac{-12\beta}{\epsilon}\left(\frac{C2}{C1+C2\xi}\right)^2, \quad \text{Where } \xi = x - \frac{\beta(\lambda^2-4\mu)}{1-\delta(\lambda^2-4\mu)}\,t, \tag{3.14}$$

b) The two dimension Korteweg de Vries (2D KdV) equation

Consider the two dimensions Korteweg de Vries in the form, [11]

$$(u_t - \epsilon u\, u_x + u_{xxx})_x + 3u_{yy} = 0, \tag{3.15}$$

Put $u(x,t) = u(\xi),\ \xi = x + \beta\, y - c\, t$, Eq. (3.15) become

$$(3\beta^2 - c)u'' - \epsilon(u\, u')' + u'''' = 0\,, \tag{3.16}$$

Integrating the above equation with respect to ξ, we get

$$(3\beta^2 - c)u - \frac{\epsilon}{2}u^2 + u'' = 0\,, \tag{3.17}$$

Balancing u^2 with u''gives $m = 2$. thus the solution of Eq. (3.15) can be expressed by

$$u(\xi) = a_0 + a_1\left(\frac{G'(\xi)}{G(\xi)}\right) + a_2\left(\frac{G'(\ \xi)}{G(\ \xi)}\right)^2, \tag{3.18}$$

By solving this system we obtain $a_0, a_1, a_2$and , we have two sets of solutions as

Case (1)

$$a_0 = \frac{12\mu}{\epsilon}\,, a_1 = \frac{12\lambda}{\epsilon}\,, a_2 = \frac{12}{\epsilon} \text{ and } c = 3\beta^2, + \lambda^2 - 4\mu \tag{3.19}$$

Case (2)

$$a_0 = \frac{2(\lambda^2+2\mu)}{\epsilon},\ \ a_1 = \frac{12\lambda}{\epsilon},\ \ a_2 = \frac{12}{\epsilon},\ c = 3\beta^2, - \lambda^2 + 4\mu \tag{3.20}$$

By using Eq.(34)and Eq(35),Eq.(33) can written as

$$u_1(\xi) = \frac{12\mu}{\epsilon} + \frac{12\lambda}{\epsilon}\left(\frac{G'(\xi)}{G(\xi)}\right) + \frac{12}{\epsilon}\left(\frac{G'(\ \xi)}{G(\ \xi)}\right)^2, \text{ or} \tag{3.21}$$

$$u_2(\xi) = \frac{2(\lambda^2+2\mu)}{\epsilon} + \frac{12\,\lambda}{\epsilon,}\left(\frac{G'(\xi)}{G(\xi)}\right) + \frac{12}{\epsilon}\left(\frac{G'(\ \xi)}{G(\ \xi)}\right)^2 \tag{3.22}$$

With the knowledge of the solution of Eq.(5) and Eqs.(21-22),we have three types of travelling wave solutions of the Eq.(3.15) as

The first type: when $\lambda^2 - 4\,\mu > 0$,

$$u_1(\xi) = -\frac{3(C_1^2 - C_2^2)(\lambda^2 - 4\mu)}{\epsilon\left(C_1 \text{Cosh}\left(\frac{\sqrt{\lambda^2-4\mu}}{2}\xi\right) + C_2\, \text{Sinh}\left(\frac{\sqrt{\lambda^2-4\mu}}{2}\xi\right)\right)^2}\,, \tag{3.23}$$

Where $\xi = x + \beta\, y - (3\beta^2 + \lambda^2 - 4\mu)t$, or

$$u_2(\xi) = \frac{(\lambda^2-4\mu)}{\epsilon}\left(2 - \frac{3(C_1^2 - C_2^2)}{\left(C_1 \text{Cosh}\left(\frac{\sqrt{\lambda^2-4\mu}}{2}\xi\right) + C_2\, \text{Sinh}\left(\frac{\sqrt{\lambda^2-4\mu}}{2}\xi\right)\right)^2}\right)\,, \tag{3.24}$$

Where $\xi = x + \beta\, y - (3\beta^2 - \lambda^2 + 4\mu)t$

The second type: when $\lambda^2 - 4\,\mu < 0$

Ref
11. K. R. Raslan. Exact solitary wave solutions of equal width wave and related equations using a direct algebraic method. I.J. N. Science (2008) 6(3):246-254

$$u_3(\xi) = \frac{(\lambda^2-4\mu)}{\epsilon}\left(2 - \frac{3(C_1^2+C_2^2)}{(C_1 Cos(\frac{1}{2}\sqrt{-\lambda^2+4\mu}\xi)+C_2 Sin(\frac{1}{2}\sqrt{-\lambda^2+4\mu}\xi))^2}\right), \quad (3.25)$$

Where $\xi = x + \beta\, y - (3\beta^2 + \lambda^2 - 4\mu)t$, or

$$u_4(\xi) = -\frac{3(C_1^2+C_2^2)(\lambda^2-4\mu)}{\epsilon(C_1 Cos(\frac{1}{2}\sqrt{-\lambda^2+4\mu}\xi)+C_2 Sin(\frac{1}{2}\sqrt{-\lambda^2+4\mu}\xi))^2}\ , \quad (3.26)$$

Where $\xi = x + \beta\, y - (3\beta^2 - \lambda^2 + 4\mu)t$

The Third type: when $\lambda^2 - 4\,\mu = 0$,

$$u_5(\xi) = \frac{12C_2^2}{\epsilon(C_2+C_2\xi)^2}, \quad (3.27)$$

Where $\xi = x + \beta\, y - 3\beta^2 t$,

The behavior of the solutions $u_3(x,t)$ and $iu_3(x,t)$ for 2DKdV equation are shown in Figure(2)

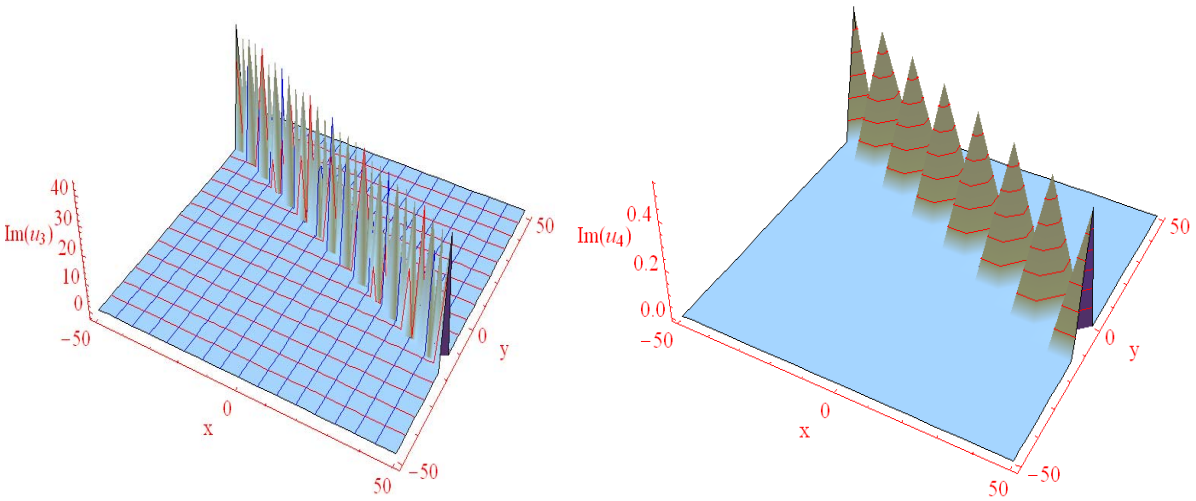

Figure 2 : $C_1 = 2, C_2 = 4, \lambda = 3,$ and $\mu = 1$

IV. Conclusion

In this work the $(\frac{G'(\xi)}{G(\xi)})$- expansion method was applied successfully for solving some solitary wave equations in one and two dimensions. Two equations which are the IKdV and 2D KdV have been solved exactly. As a result, many exact solutions are obtained which include the hyperbolic functions, trigonometric functions and rational functions. It is worthwhile to mention that the proposed method is reliable and effective and gives more solutions. The method can also be efficiently used to construct new and more exact solutions for some other generalized nonlinear wave equations arising in mathematical physics.

References Références Referencias

1. Abdul-Majid Wazwaz. Solitary wave solutions of the generalized shallow water wave (GSWW) equation by Hirota's method, tanh–coth method and Exp-function method, Appl. Math. Comput. (2008) 202: 275–286.

Ref

2. Khater, A.H., Malfiet, W., Callebaut, D.K., Kamel, E.S. The tanh method, a simple transformation and exact analytical solutions for nonlinear reaction–diffusion equations.Chaos Solitons Fractals. (2002)1(4): 513–522.
3. Evans, D.J., Raslan, K.R. The tanh function method for solving some important nonlinear partial differential equation.Int. J. Comput. Math. (2005) 82(7): 897–905.
4. Fan, E. Extended tanh-function method and its applications to nonlinear equations. Phys. Lett. 2000;A (277) 212–218.
5. Fan, E.Traveling wave solutions for generalized Hirota–Satsuma coupled KdV systems. Z. Naturforsch. (2001) A 56: 312–318.
6. Elwakil, S.A., El-Labany, S.K., Zahran, M.A., Sabry, R. Modified extended tanh-function method for solving nonlinear partial differential equations. Phys. Lett. 2002; A(299) 179–188.
7. Gao, Y.T., Tian, B. Generalized hyperbolic-function method with computerized symbolic computation to construct the solitonic solutions to nonlinear equations of mathematical physics. Comput. Phys. Commun.(2001) 133: 158–164.
8. M A Abdou, A.Hendi, Mirvet Al-Zumaie. On the extended $(\frac{G'}{G})$-expansion method and its applications Int. J. Comput. Math.(2011) 3(3): 193-199.
9. A. K. Khalifa, K. R. Raslan, H. M. Alzubaidi. A finite difference scheme for the MRLW and solitary wave interactions. Appl. Math. Comput. (2007)189 : 346-354.
10. D. Kaya. A numerical simulation of solitary-wave solutions of the generalized long-wave equation. Appl. Math. Comput. (2004)149(3) 833-841.
11. K. R. Raslan. Exact solitary wave solutions of equal width wave and related equations using a direct algebraic method. I.J. N. Science (2008) 6(3):246-254.
12. M.Ali, S. Tauseef. An alternative $(\frac{G'}{G})$-expansion method with generalized Riccati equation: Application to fifth order (1+1)-dimensional Caudrey-Dodd-Gibbon equation, open Journal of Mathematical Modeling. (2013)1(5):173-183.
13. Xiaohua Liu,Weiguo Zhang and Zhengming Li. Application of improved $(\frac{G'}{G})$-expansion method to traveling wave solutions of two nonlinear evolution equations. Advances in Applied Mathematics and Mechanics.(2012)4(1):122-130
14. M. Shakeel and S. Tauseef-Din. Improved $(\frac{G'}{G})$-expansion method for Burger's, Zakharov– Kuznetsov (ZK) and Boussinesq equations, Int. J. M. Math. Sci. (2013) 6(3): 160-173.

Global Journals Inc. (US) Guidelines Handbook 2016

www.GlobalJournals.org

FELLOWS

FELLOW OF ASSOCIATION OF RESEARCH SOCIETY IN SCIENCE (FARSS)

Global Journals Incorporate (USA) is accredited by Open Association of Research Society (OARS), U.S.A and in turn, awards "FARSS" title to individuals. The 'FARSS' title is accorded to a selected professional after the approval of the Editor-in-Chief/Editorial Board Members/Dean.

- The "FARSS" is a dignified title which is accorded to a person's name viz. Dr. John E. Hall, Ph.D., FARSS or William Walldroff, M.S., FARSS.

FARSS accrediting is an honor. It authenticates your research activities. After recognition as FARSB, you can add 'FARSS' title with your name as you use this recognition as additional suffix to your status. This will definitely enhance and add more value and repute to your name. You may use it on your professional Counseling Materials such as CV, Resume, and Visiting Card etc.

The following benefits can be availed by you only for next three years from the date of certification:

FARSS designated members are entitled to avail a 40% discount while publishing their research papers (of a single author) with Global Journals Incorporation (USA), if the same is accepted by Editorial Board/Peer Reviewers. If you are a main author or co-author in case of multiple authors, you will be entitled to avail discount of 10%.

Once FARSB title is accorded, the Fellow is authorized to organize a symposium/seminar/conference on behalf of Global Journal Incorporation (USA). The Fellow can also participate in conference/seminar/symposium organized by another institution as representative of Global Journal. In both the cases, it is mandatory for him to discuss with us and obtain our consent.

You may join as member of the Editorial Board of Global Journals Incorporation (USA) after successful completion of three years as Fellow and as Peer Reviewer. In addition, it is also desirable that you should organize seminar/symposium/conference at least once.

We shall provide you intimation regarding launching of e-version of journal of your stream time to time.This may be utilized in your library for the enrichment of knowledge of your students as well as it can also be helpful for the concerned faculty members.

The FARSS can go through standards of OARS. You can also play vital role if you have any suggestions so that proper amendment can take place to improve the same for the benefit of entire research community.

As FARSS, you will be given a renowned, secure and free professional email address with 100 GB of space e.g. johnhall@globaljournals.org. This will include Webmail, Spam Assassin, Email Forwarders,Auto-Responders, Email Delivery Route tracing, etc.

The FARSS will be eligible for a free application of standardization of their researches. Standardization of research will be subject to acceptability within stipulated norms as the next step after publishing in a journal. We shall depute a team of specialized research professionals who will render their services for elevating your researches to next higher level, which is worldwide open standardization.

The FARSS member can apply for grading and certification of standards of their educational and Institutional Degrees to Open Association of Research, Society U.S.A.
Once you are designated as FARSS, you may send us a scanned copy of all of your credentials. OARS will verify, grade and certify them. This will be based on your academic records, quality of research papers published by you, and some more criteria. After certification of all your credentials by OARS, they will be published on your Fellow Profile link on website https://associationofresearch.org which will be helpful to upgrade the dignity.

The FARSS members can avail the benefits of free research podcasting in Global Research Radio with their research documents. After publishing the work, (including published elsewhere worldwide with proper authorization) you can upload your research paper with your recorded voice or you can utilize chargeable services of our professional RJs to record your paper in their voice on request.

The FARSS member also entitled to get the benefits of free research podcasting of their research documents through video clips. We can also streamline your conference videos and display your slides/ online slides and online research video clips at reasonable charges, on request.

The FARSS is eligible to earn from sales proceeds of his/her researches/reference/review Books or literature, while publishing with Global Journals. The FARSS can decide whether he/she would like to publish his/her research in a closed manner. In this case, whenever readers purchase that individual research paper for reading, maximum 60% of its profit earned as royalty by Global Journals, will be credited to his/her bank account. The entire entitled amount will be credited to his/her bank account exceeding limit of minimum fixed balance. There is no minimum time limit for collection. The FARSS member can decide its price and we can help in making the right decision.

The FARSS member is eligible to join as a paid peer reviewer at Global Journals Incorporation (USA) and can get remuneration of 15% of author fees, taken from the author of a respective paper. After reviewing 5 or more papers you can request to transfer the amount to your bank account.

MEMBER OF ASSOCIATION OF RESEARCH SOCIETY IN SCIENCE (MARSS)

The ' MARSS ' title is accorded to a selected professional after the approval of the Editor-in-Chief / Editorial Board Members/Dean.

The "MARSS" is a dignified ornament which is accorded to a person's name viz. Dr. John E. Hall, Ph.D., MARSS or William Walldroff, M.S., MARSS.

MARSS accrediting is an honor. It authenticates your research activities. After becoming MARSS, you can add 'MARSS' title with your name as you use this recognition as additional suffix to your status. This will definitely enhance and add more value and repute to your name. You may use it on your professional Counseling Materials such as CV, Resume, Visiting Card and Name Plate etc.

The following benefitscan be availed by you only for next three years from the date of certification.

MARSS designated members are entitled to avail a 25% discount while publishing their research papers (of a single author) in Global Journals Inc., if the same is accepted by our Editorial Board and Peer Reviewers. If you are a main author or co-author of a group of authors, you will get discount of 10%.

As MARSS, you will be given a renowned, secure and free professional email address with 30 GB of space e.g. johnhall@globaljournals.org. This will include Webmail, Spam Assassin, Email Forwarders,Auto-Responders, Email Delivery Route tracing, etc.

We shall provide you intimation regarding launching of e-version of journal of your stream time to time.This may be utilized in your library for the enrichment of knowledge of your students as well as it can also be helpful for the concerned faculty members.

The MARSS member can apply for approval, grading and certification of standards of their educational and Institutional Degrees to Open Association of Research, Society U.S.A.

Once you are designated as MARSS, you may send us a scanned copy of all of your credentials. OARS will verify, grade and certify them. This will be based on your academic records, quality of research papers published by you, and some more criteria.

It is mandatory to read all terms and conditions carefully.

AUXILIARY MEMBERSHIPS

Institutional Fellow of Global Journals Incorporation (USA)-OARS (USA)

Global Journals Incorporation (USA) is accredited by Open Association of Research Society, U.S.A (OARS) and in turn, affiliates research institutions as "Institutional Fellow of Open Association of Research Society" (IFOARS).

The "FARSC" is a dignified title which is accorded to a person's name viz. Dr. John E. Hall, Ph.D., FARSC or William Walldroff, M.S., FARSC.

The IFOARS institution is entitled to form a Board comprised of one Chairperson and three to five board members preferably from different streams. The Board will be recognized as "Institutional Board of Open Association of Research Society"-(IBOARS).

The Institute will be entitled to following benefits:

The IBOARS can initially review research papers of their institute and recommend them to publish with respective journal of Global Journals. It can also review the papers of other institutions after obtaining our consent. The second review will be done by peer reviewer of Global Journals Incorporation (USA) The Board is at liberty to appoint a peer reviewer with the approval of chairperson after consulting us.

The author fees of such paper may be waived off up to 40%.

The Global Journals Incorporation (USA) at its discretion can also refer double blind peer reviewed paper at their end to the board for the verification and to get recommendation for final stage of acceptance of publication.

The IBOARS can organize symposium/seminar/conference in their country on behalf of Global Journals Incorporation (USA)-OARS (USA). The terms and conditions can be discussed separately.

The Board can also play vital role by exploring and giving valuable suggestions regarding the Standards of "Open Association of Research Society, U.S.A (OARS)" so that proper amendment can take place for the benefit of entire research community. We shall provide details of particular standard only on receipt of request from the Board.

The board members can also join us as Individual Fellow with 40% discount on total fees applicable to Individual Fellow. They will be entitled to avail all the benefits as declared. Please visit Individual Fellow-sub menu of GlobalJournals.org to have more relevant details.

We shall provide you intimation regarding launching of e-version of journal of your stream time to time. This may be utilized in your library for the enrichment of knowledge of your students as well as it can also be helpful for the concerned faculty members.

After nomination of your institution as "Institutional Fellow" and constantly functioning successfully for one year, we can consider giving recognition to your institute to function as Regional/Zonal office on our behalf.
The board can also take up the additional allied activities for betterment after our consultation.

The following entitlements are applicable to individual Fellows:

Open Association of Research Society, U.S.A (OARS) By-laws states that an individual Fellow may use the designations as applicable, or the corresponding initials. The Credentials of individual Fellow and Associate designations signify that the individual has gained knowledge of the fundamental concepts. One is magnanimous and proficient in an expertise course covering the professional code of conduct, and follows recognized standards of practice.

Open Association of Research Society (US)/ Global Journals Incorporation (USA), as described in Corporate Statements, are educational, research publishing and professional membership organizations. Achieving our individual Fellow or Associate status is based mainly on meeting stated educational research requirements.

Disbursement of 40% Royalty earned through Global Journals : Researcher = 50%, Peer Reviewer = 37.50%, Institution = 12.50% E.g. Out of 40%, the 20% benefit should be passed on to researcher, 15 % benefit towards remuneration should be given to a reviewer and remaining 5% is to be retained by the institution.

We shall provide print version of 12 issues of any three journals [as per your requirement] out of our 38 journals worth $ 2376 USD.

Other:

The individual Fellow and Associate designations accredited by Open Association of Research Society (US) credentials signify guarantees following achievements:

- The professional accredited with Fellow honor, is entitled to various benefits viz. name, fame, honor, regular flow of income, secured bright future, social status etc.

- In addition to above, if one is single author, then entitled to 40% discount on publishing research paper and can get 10%discount if one is co-author or main author among group of authors.
- The Fellow can organize symposium/seminar/conference on behalf of Global Journals Incorporation (USA) and he/she can also attend the same organized by other institutes on behalf of Global Journals.
- The Fellow can become member of Editorial Board Member after completing 3yrs.
- The Fellow can earn 60% of sales proceeds from the sale of reference/review books/literature/publishing of research paper.
- Fellow can also join as paid peer reviewer and earn 15% remuneration of author charges and can also get an opportunity to join as member of the Editorial Board of Global Journals Incorporation (USA)
- • This individual has learned the basic methods of applying those concepts and techniques to common challenging situations. This individual has further demonstrated an in–depth understanding of the application of suitable techniques to a particular area of research practice.

Note :

"

- In future, if the board feels the necessity to change any board member, the same can be done with the consent of the chairperson along with anyone board member without our approval.
- In case, the chairperson needs to be replaced then consent of 2/3rd board members are required and they are also required to jointly pass the resolution copy of which should be sent to us. In such case, it will be compulsory to obtain our approval before replacement.
- In case of "Difference of Opinion [if any]" among the Board members, our decision will be final and binding to everyone.

"

Process of submission of Research Paper

The Area or field of specialization may or may not be of any category as mentioned in 'Scope of Journal' menu of the GlobalJournals.org website. There are 37 Research Journal categorized with Six parental Journals GJCST, GJMR, GJRE, GJMBR, GJSFR, GJHSS. For Authors should prefer the mentioned categories. There are three widely used systems UDC, DDC and LCC. The details are available as 'Knowledge Abstract' at Home page. The major advantage of this coding is that, the research work will be exposed to and shared with all over the world as we are being abstracted and indexed worldwide.

The paper should be in proper format. The format can be downloaded from first page of 'Author Guideline' Menu. The Author is expected to follow the general rules as mentioned in this menu. The paper should be written in MS-Word Format (*.DOC,*.DOCX).

The Author can submit the paper either online or offline. The authors should prefer online submission.Online Submission: There are three ways to submit your paper:

(A) (I) First, register yourself using top right corner of Home page then Login. If you are already registered, then login using your username and password.

(II) Choose corresponding Journal.

(III) Click 'Submit Manuscript'. Fill required information and Upload the paper.

(B) If you are using Internet Explorer, then Direct Submission through Homepage is also available.

(C) If these two are not conveninet , and then email the paper directly to dean@globaljournals.org.

Offline Submission: Author can send the typed form of paper by Post. However, online submission should be preferred.

Preferred Author Guidelines

MANUSCRIPT STYLE INSTRUCTION (Must be strictly followed)

Page Size: 8.27" X 11'"

- Left Margin: 0.65
- Right Margin: 0.65
- Top Margin: 0.75
- Bottom Margin: 0.75
- Font type of all text should be Swis 721 Lt BT.
- Paper Title should be of Font Size 24 with one Column section.
- Author Name in Font Size of 11 with one column as of Title.
- Abstract Font size of 9 Bold, "Abstract" word in Italic Bold.
- Main Text: Font size 10 with justified two columns section
- Two Column with Equal Column with of 3.38 and Gaping of .2
- First Character must be three lines Drop capped.
- Paragraph before Spacing of 1 pt and After of 0 pt.
- Line Spacing of 1 pt
- Large Images must be in One Column
- Numbering of First Main Headings (Heading 1) must be in Roman Letters, Capital Letter, and Font Size of 10.
- Numbering of Second Main Headings (Heading 2) must be in Alphabets, Italic, and Font Size of 10.

You can use your own standard format also.
Author Guidelines:

1. General,

2. Ethical Guidelines,

3. Submission of Manuscripts,

4. Manuscript's Category,

5. Structure and Format of Manuscript,

6. After Acceptance.

1. GENERAL

Before submitting your research paper, one is advised to go through the details as mentioned in following heads. It will be beneficial, while peer reviewer justify your paper for publication.

Scope

The Global Journals Inc. (US) welcome the submission of original paper, review paper, survey article relevant to the all the streams of Philosophy and knowledge. The Global Journals Inc. (US) is parental platform for Global Journal of Computer Science and Technology, Researches in Engineering, Medical Research, Science Frontier Research, Human Social Science, Management, and Business organization. The choice of specific field can be done otherwise as following in Abstracting and Indexing Page on this Website. As the all Global

Journals Inc. (US) are being abstracted and indexed (in process) by most of the reputed organizations. Topics of only narrow interest will not be accepted unless they have wider potential or consequences.

2. ETHICAL GUIDELINES

Authors should follow the ethical guidelines as mentioned below for publication of research paper and research activities.

Papers are accepted on strict understanding that the material in whole or in part has not been, nor is being, considered for publication elsewhere. If the paper once accepted by Global Journals Inc. (US) and Editorial Board, will become the copyright of the Global Journals Inc. (US).

Authorship: The authors and coauthors should have active contribution to conception design, analysis and interpretation of findings. They should critically review the contents and drafting of the paper. All should approve the final version of the paper before submission

The Global Journals Inc. (US) follows the definition of authorship set up by the Global Academy of Research and Development. According to the Global Academy of R&D authorship, criteria must be based on:

1) Substantial contributions to conception and acquisition of data, analysis and interpretation of the findings.

2) Drafting the paper and revising it critically regarding important academic content.

3) Final approval of the version of the paper to be published.

All authors should have been credited according to their appropriate contribution in research activity and preparing paper. Contributors who do not match the criteria as authors may be mentioned under Acknowledgement.

Acknowledgements: Contributors to the research other than authors credited should be mentioned under acknowledgement. The specifications of the source of funding for the research if appropriate can be included. Suppliers of resources may be mentioned along with address.

Appeal of Decision: The Editorial Board's decision on publication of the paper is final and cannot be appealed elsewhere.

Permissions: It is the author's responsibility to have prior permission if all or parts of earlier published illustrations are used in this paper.

Please mention proper reference and appropriate acknowledgements wherever expected.

If all or parts of previously published illustrations are used, permission must be taken from the copyright holder concerned. It is the author's responsibility to take these in writing.

Approval for reproduction/modification of any information (including figures and tables) published elsewhere must be obtained by the authors/copyright holders before submission of the manuscript. Contributors (Authors) are responsible for any copyright fee involved.

3. SUBMISSION OF MANUSCRIPTS

Manuscripts should be uploaded via this online submission page. The online submission is most efficient method for submission of papers, as it enables rapid distribution of manuscripts and consequently speeds up the review procedure. It also enables authors to know the status of their own manuscripts by emailing us. Complete instructions for submitting a paper is available below.

Manuscript submission is a systematic procedure and little preparation is required beyond having all parts of your manuscript in a given format and a computer with an Internet connection and a Web browser. Full help and instructions are provided on-screen. As an author, you will be prompted for login and manuscript details as Field of Paper and then to upload your manuscript file(s) according to the instructions.

To avoid postal delays, all transaction is preferred by e-mail. A finished manuscript submission is confirmed by e-mail immediately and your paper enters the editorial process with no postal delays. When a conclusion is made about the publication of your paper by our Editorial Board, revisions can be submitted online with the same procedure, with an occasion to view and respond to all comments.

Complete support for both authors and co-author is provided.

4. MANUSCRIPT'S CATEGORY

Based on potential and nature, the manuscript can be categorized under the following heads:

Original research paper: Such papers are reports of high-level significant original research work.

Review papers: These are concise, significant but helpful and decisive topics for young researchers.

Research articles: These are handled with small investigation and applications

Research letters: The letters are small and concise comments on previously published matters.

5.STRUCTURE AND FORMAT OF MANUSCRIPT

The recommended size of original research paper is less than seven thousand words, review papers fewer than seven thousands words also.Preparation of research paper or how to write research paper, are major hurdle, while writing manuscript. The research articles and research letters should be fewer than three thousand words, the structure original research paper; sometime review paper should be as follows:

Papers: These are reports of significant research (typically less than 7000 words equivalent, including tables, figures, references), and comprise:

(a)Title should be relevant and commensurate with the theme of the paper.

(b) A brief Summary, "Abstract" (less than 150 words) containing the major results and conclusions.

(c) Up to ten keywords, that precisely identifies the paper's subject, purpose, and focus.

(d) An Introduction, giving necessary background excluding subheadings; objectives must be clearly declared.

(e) Resources and techniques with sufficient complete experimental details (wherever possible by reference) to permit repetition; sources of information must be given and numerical methods must be specified by reference, unless non-standard.

(f) Results should be presented concisely, by well-designed tables and/or figures; the same data may not be used in both; suitable statistical data should be given. All data must be obtained with attention to numerical detail in the planning stage. As reproduced design has been recognized to be important to experiments for a considerable time, the Editor has decided that any paper that appears not to have adequate numerical treatments of the data will be returned un-refereed;

(g) Discussion should cover the implications and consequences, not just recapitulating the results; conclusions should be summarizing.

(h) Brief Acknowledgements.

(i) References in the proper form.

Authors should very cautiously consider the preparation of papers to ensure that they communicate efficiently. Papers are much more likely to be accepted, if they are cautiously designed and laid out, contain few or no errors, are summarizing, and be conventional to the approach and instructions. They will in addition, be published with much less delays than those that require much technical and editorial correction.

The Editorial Board reserves the right to make literary corrections and to make suggestions to improve briefness.

It is vital, that authors take care in submitting a manuscript that is written in simple language and adheres to published guidelines.

Format

Language: The language of publication is UK English. Authors, for whom English is a second language, must have their manuscript efficiently edited by an English-speaking person before submission to make sure that, the English is of high excellence. It is preferable, that manuscripts should be professionally edited.

Standard Usage, Abbreviations, and Units: Spelling and hyphenation should be conventional to The Concise Oxford English Dictionary. Statistics and measurements should at all times be given in figures, e.g. 16 min, except for when the number begins a sentence. When the number does not refer to a unit of measurement it should be spelt in full unless, it is 160 or greater.

Abbreviations supposed to be used carefully. The abbreviated name or expression is supposed to be cited in full at first usage, followed by the conventional abbreviation in parentheses.

Metric SI units are supposed to generally be used excluding where they conflict with current practice or are confusing. For illustration, 1.4 l rather than 1.4 × 10-3 m3, or 4 mm somewhat than 4 × 10-3 m. Chemical formula and solutions must identify the form used, e.g. anhydrous or hydrated, and the concentration must be in clearly defined units. Common species names should be followed by underlines at the first mention. For following use the generic name should be constricted to a single letter, if it is clear.

Structure

All manuscripts submitted to Global Journals Inc. (US), ought to include:

Title: The title page must carry an instructive title that reflects the content, a running title (less than 45 characters together with spaces), names of the authors and co-authors, and the place(s) wherever the work was carried out. The full postal address in addition with the e-mail address of related author must be given. Up to eleven keywords or very brief phrases have to be given to help data retrieval, mining and indexing.

Abstract, used in Original Papers and Reviews:

Optimizing Abstract for Search Engines

Many researchers searching for information online will use search engines such as Google, Yahoo or similar. By optimizing your paper for search engines, you will amplify the chance of someone finding it. This in turn will make it more likely to be viewed and/or cited in a further work. Global Journals Inc. (US) have compiled these guidelines to facilitate you to maximize the web-friendliness of the most public part of your paper.

Key Words

A major linchpin in research work for the writing research paper is the keyword search, which one will employ to find both library and Internet resources.

One must be persistent and creative in using keywords. An effective keyword search requires a strategy and planning a list of possible keywords and phrases to try.

Search engines for most searches, use Boolean searching, which is somewhat different from Internet searches. The Boolean search uses "operators," words (and, or, not, and near) that enable you to expand or narrow your affords. Tips for research paper while preparing research paper are very helpful guideline of research paper.

Choice of key words is first tool of tips to write research paper. Research paper writing is an art.A few tips for deciding as strategically as possible about keyword search:

- One should start brainstorming lists of possible keywords before even begin searching. Think about the most important concepts related to research work. Ask, "What words would a source have to include to be truly valuable in research paper?" Then consider synonyms for the important words.
- It may take the discovery of only one relevant paper to let steer in the right keyword direction because in most databases, the keywords under which a research paper is abstracted are listed with the paper.
- One should avoid outdated words.

Keywords are the key that opens a door to research work sources. Keyword searching is an art in which researcher's skills are bound to improve with experience and time.

Numerical Methods: Numerical methods used should be clear and, where appropriate, supported by references.

Acknowledgements: Please make these as concise as possible.

References

References follow the Harvard scheme of referencing. References in the text should cite the authors' names followed by the time of their publication, unless there are three or more authors when simply the first author's name is quoted followed by et al. unpublished work has to only be cited where necessary, and only in the text. Copies of references in press in other journals have to be supplied with submitted typescripts. It is necessary that all citations and references be carefully checked before submission, as mistakes or omissions will cause delays.

References to information on the World Wide Web can be given, but only if the information is available without charge to readers on an official site. Wikipedia and Similar websites are not allowed where anyone can change the information. Authors will be asked to make available electronic copies of the cited information for inclusion on the Global Journals Inc. (US) homepage at the judgment of the Editorial Board.

The Editorial Board and Global Journals Inc. (US) recommend that, citation of online-published papers and other material should be done via a DOI (digital object identifier). If an author cites anything, which does not have a DOI, they run the risk of the cited material not being noticeable.

The Editorial Board and Global Journals Inc. (US) recommend the use of a tool such as Reference Manager for reference management and formatting.

Tables, Figures and Figure Legends

Tables: Tables should be few in number, cautiously designed, uncrowned, and include only essential data. Each must have an Arabic number, e.g. Table 4, a self-explanatory caption and be on a separate sheet. Vertical lines should not be used.

Figures: Figures are supposed to be submitted as separate files. Always take in a citation in the text for each figure using Arabic numbers, e.g. Fig. 4. Artwork must be submitted online in electronic form by e-mailing them.

Preparation of Electronic Figures for Publication

Even though low quality images are sufficient for review purposes, print publication requires high quality images to prevent the final product being blurred or fuzzy. Submit (or e-mail) EPS (line art) or TIFF (halftone/photographs) files only. MS PowerPoint and Word Graphics are unsuitable for printed pictures. Do not use pixel-oriented software. Scans (TIFF only) should have a resolution of at least 350 dpi (halftone) or 700 to 1100 dpi (line drawings) in relation to the imitation size. Please give the data for figures in black and white or submit a Color Work Agreement Form. EPS files must be saved with fonts embedded (and with a TIFF preview, if possible).

For scanned images, the scanning resolution (at final image size) ought to be as follows to ensure good reproduction: line art: >650 dpi; halftones (including gel photographs) : >350 dpi; figures containing both halftone and line images: >650 dpi.

Color Charges: It is the rule of the Global Journals Inc. (US) for authors to pay the full cost for the reproduction of their color artwork. Hence, please note that, if there is color artwork in your manuscript when it is accepted for publication, we would require you to complete and return a color work agreement form before your paper can be published.

Figure Legends: Self-explanatory legends of all figures should be incorporated separately under the heading 'Legends to Figures'. In the full-text online edition of the journal, figure legends may possibly be truncated in abbreviated links to the full screen version. Therefore, the first 100 characters of any legend should notify the reader, about the key aspects of the figure.

6. AFTER ACCEPTANCE

Upon approval of a paper for publication, the manuscript will be forwarded to the dean, who is responsible for the publication of the Global Journals Inc. (US).

6.1 Proof Corrections

The corresponding author will receive an e-mail alert containing a link to a website or will be attached. A working e-mail address must therefore be provided for the related author.

Acrobat Reader will be required in order to read this file. This software can be downloaded

(Free of charge) from the following website:

www.adobe.com/products/acrobat/readstep2.html. This will facilitate the file to be opened, read on screen, and printed out in order for any corrections to be added. Further instructions will be sent with the proof.

Proofs must be returned to the dean at dean@globaljournals.org within three days of receipt.

As changes to proofs are costly, we inquire that you only correct typesetting errors. All illustrations are retained by the publisher. Please note that the authors are responsible for all statements made in their work, including changes made by the copy editor.

6.2 Early View of Global Journals Inc. (US) (Publication Prior to Print)

The Global Journals Inc. (US) are enclosed by our publishing's Early View service. Early View articles are complete full-text articles sent in advance of their publication. Early View articles are absolute and final. They have been completely reviewed, revised and edited for publication, and the authors' final corrections have been incorporated. Because they are in final form, no changes can be made after sending them. The nature of Early View articles means that they do not yet have volume, issue or page numbers, so Early View articles cannot be cited in the conventional way.

6.3 Author Services

Online production tracking is available for your article through Author Services. Author Services enables authors to track their article - once it has been accepted - through the production process to publication online and in print. Authors can check the status of their articles online and choose to receive automated e-mails at key stages of production. The authors will receive an e-mail with a unique link that enables them to register and have their article automatically added to the system. Please ensure that a complete e-mail address is provided when submitting the manuscript.

6.4 Author Material Archive Policy

Please note that if not specifically requested, publisher will dispose off hardcopy & electronic information submitted, after the two months of publication. If you require the return of any information submitted, please inform the Editorial Board or dean as soon as possible.

6.5 Offprint and Extra Copies

A PDF offprint of the online-published article will be provided free of charge to the related author, and may be distributed according to the Publisher's terms and conditions. Additional paper offprint may be ordered by emailing us at: editor@globaljournals.org .

Before start writing a good quality Computer Science Research Paper, let us first understand what is Computer Science Research Paper? So, Computer Science Research Paper is the paper which is written by professionals or scientists who are associated to Computer Science and Information Technology, or doing research study in these areas. If you are novel to this field then you can consult about this field from your supervisor or guide.

TECHNIQUES FOR WRITING A GOOD QUALITY RESEARCH PAPER:

1. Choosing the topic: In most cases, the topic is searched by the interest of author but it can be also suggested by the guides. You can have several topics and then you can judge that in which topic or subject you are finding yourself most comfortable. This can be done by asking several questions to yourself, like Will I be able to carry our search in this area? Will I find all necessary recourses to accomplish the search? Will I be able to find all information in this field area? If the answer of these types of questions will be "Yes" then you can choose that topic. In most of the cases, you may have to conduct the surveys and have to visit several places because this field is related to Computer Science and Information Technology. Also, you may have to do a lot of work to find all rise and falls regarding the various data of that subject. Sometimes, detailed information plays a vital role, instead of short information.

2. Evaluators are human: First thing to remember that evaluators are also human being. They are not only meant for rejecting a paper. They are here to evaluate your paper. So, present your Best.

3. Think Like Evaluators: If you are in a confusion or getting demotivated that your paper will be accepted by evaluators or not, then think and try to evaluate your paper like an Evaluator. Try to understand that what an evaluator wants in your research paper and automatically you will have your answer.

4. Make blueprints of paper: The outline is the plan or framework that will help you to arrange your thoughts. It will make your paper logical. But remember that all points of your outline must be related to the topic you have chosen.

5. Ask your Guides: If you are having any difficulty in your research, then do not hesitate to share your difficulty to your guide (if you have any). They will surely help you out and resolve your doubts. If you can't clarify what exactly you require for your work then ask the supervisor to help you with the alternative. He might also provide you the list of essential readings.

6. Use of computer is recommended: As you are doing research in the field of Computer Science, then this point is quite obvious.

7. Use right software: Always use good quality software packages. If you are not capable to judge good software then you can lose quality of your paper unknowingly. There are various software programs available to help you, which you can get through Internet.

8. Use the Internet for help: An excellent start for your paper can be by using the Google. It is an excellent search engine, where you can have your doubts resolved. You may also read some answers for the frequent question how to write my research paper or find model research paper. From the internet library you can download books. If you have all required books make important reading selecting and analyzing the specified information. Then put together research paper sketch out.

9. Use and get big pictures: Always use encyclopedias, Wikipedia to get pictures so that you can go into the depth.

10. Bookmarks are useful: When you read any book or magazine, you generally use bookmarks, right! It is a good habit, which helps to not to lose your continuity. You should always use bookmarks while searching on Internet also, which will make your search easier.

11. Revise what you wrote: When you write anything, always read it, summarize it and then finalize it.

12. Make all efforts: Make all efforts to mention what you are going to write in your paper. That means always have a good start. Try to mention everything in introduction, that what is the need of a particular research paper. Polish your work by good skill of writing and always give an evaluator, what he wants.

13. Have backups: When you are going to do any important thing like making research paper, you should always have backup copies of it either in your computer or in paper. This will help you to not to lose any of your important.

14. Produce good diagrams of your own: Always try to include good charts or diagrams in your paper to improve quality. Using several and unnecessary diagrams will degrade the quality of your paper by creating "hotchpotch." So always, try to make and include those diagrams, which are made by your own to improve readability and understandability of your paper.

15. Use of direct quotes: When you do research relevant to literature, history or current affairs then use of quotes become essential but if study is relevant to science then use of quotes is not preferable.

16. Use proper verb tense: Use proper verb tenses in your paper. Use past tense, to present those events that happened. Use present tense to indicate events that are going on. Use future tense to indicate future happening events. Use of improper and wrong tenses will confuse the evaluator. Avoid the sentences that are incomplete.

17. Never use online paper: If you are getting any paper on Internet, then never use it as your research paper because it might be possible that evaluator has already seen it or maybe it is outdated version.

18. Pick a good study spot: To do your research studies always try to pick a spot, which is quiet. Every spot is not for studies. Spot that suits you choose it and proceed further.

19. Know what you know: Always try to know, what you know by making objectives. Else, you will be confused and cannot achieve your target.

20. Use good quality grammar: Always use a good quality grammar and use words that will throw positive impact on evaluator. Use of good quality grammar does not mean to use tough words, that for each word the evaluator has to go through dictionary. Do not start sentence with a conjunction. Do not fragment sentences. Eliminate one-word sentences. Ignore passive voice. Do not ever use a big word when a diminutive one would suffice. Verbs have to be in agreement with their subjects. Prepositions are not expressions to finish sentences with. It is incorrect to ever divide an infinitive. Avoid clichés like the disease. Also, always shun irritating alliteration. Use language that is simple and straight forward. put together a neat summary.

21. Arrangement of information: Each section of the main body should start with an opening sentence and there should be a changeover at the end of the section. Give only valid and powerful arguments to your topic. You may also maintain your arguments with records.

22. Never start in last minute: Always start at right time and give enough time to research work. Leaving everything to the last minute will degrade your paper and spoil your work.

23. Multitasking in research is not good: Doing several things at the same time proves bad habit in case of research activity. Research is an area, where everything has a particular time slot. Divide your research work in parts and do particular part in particular time slot.

24. Never copy others' work: Never copy others' work and give it your name because if evaluator has seen it anywhere you will be in trouble.

25. Take proper rest and food: No matter how many hours you spend for your research activity, if you are not taking care of your health then all your efforts will be in vain. For a quality research, study is must, and this can be done by taking proper rest and food.

26. Go for seminars: Attend seminars if the topic is relevant to your research area. Utilize all your resources.

27. Refresh your mind after intervals: Try to give rest to your mind by listening to soft music or by sleeping in intervals. This will also improve your memory.

28. Make colleagues: Always try to make colleagues. No matter how sharper or intelligent you are, if you make colleagues you can have several ideas, which will be helpful for your research.

29. Think technically: Always think technically. If anything happens, then search its reasons, its benefits, and demerits.

30. Think and then print: When you will go to print your paper, notice that tables are not be split, headings are not detached from their descriptions, and page sequence is maintained.

31. Adding unnecessary information: Do not add unnecessary information, like, I have used MS Excel to draw graph. Do not add irrelevant and inappropriate material. These all will create superfluous. Foreign terminology and phrases are not apropos. One should NEVER take a broad view. Analogy in script is like feathers on a snake. Not at all use a large word when a very small one would be sufficient. Use words properly, regardless of how others use them. Remove quotations. Puns are for kids, not grunt readers. Amplification is a billion times of inferior quality than sarcasm.

32. Never oversimplify everything: To add material in your research paper, never go for oversimplification. This will definitely irritate the evaluator. Be more or less specific. Also too, by no means, ever use rhythmic redundancies. Contractions aren't essential and shouldn't be there used. Comparisons are as terrible as clichés. Give up ampersands and abbreviations, and so on. Remove commas, that are, not necessary. Parenthetical words however should be together with this in commas. Understatement is all the time the complete best way to put onward earth-shaking thoughts. Give a detailed literary review.

33. Report concluded results: Use concluded results. From raw data, filter the results and then conclude your studies based on measurements and observations taken. Significant figures and appropriate number of decimal places should be used. Parenthetical remarks are prohibitive. Proofread carefully at final stage. In the end give outline to your arguments. Spot out perspectives of further study of this subject. Justify your conclusion by at the bottom of them with sufficient justifications and examples.

34. After conclusion: Once you have concluded your research, the next most important step is to present your findings. Presentation is extremely important as it is the definite medium though which your research is going to be in print to the rest of the crowd. Care should be taken to categorize your thoughts well and present them in a logical and neat manner. A good quality research paper format is essential because it serves to highlight your research paper and bring to light all necessary aspects in your research.

Informal Guidelines of Research Paper Writing

Key points to remember:

- Submit all work in its final form.
- Write your paper in the form, which is presented in the guidelines using the template.
- Please note the criterion for grading the final paper by peer-reviewers.

Final Points:

A purpose of organizing a research paper is to let people to interpret your effort selectively. The journal requires the following sections, submitted in the order listed, each section to start on a new page.

The introduction will be compiled from reference matter and will reflect the design processes or outline of basis that direct you to make study. As you will carry out the process of study, the method and process section will be constructed as like that. The result segment will show related statistics in nearly sequential order and will direct the reviewers next to the similar intellectual paths throughout the data that you took to carry out your study. The discussion section will provide understanding of the data and projections as to the implication of the results. The use of good quality references all through the paper will give the effort trustworthiness by representing an alertness of prior workings.

Writing a research paper is not an easy job no matter how trouble-free the actual research or concept. Practice, excellent preparation, and controlled record keeping are the only means to make straightforward the progression.

General style:

Specific editorial column necessities for compliance of a manuscript will always take over from directions in these general guidelines.

To make a paper clear

· Adhere to recommended page limits

Mistakes to evade

- Insertion a title at the foot of a page with the subsequent text on the next page
- Separating a table/chart or figure - impound each figure/table to a single page
- Submitting a manuscript with pages out of sequence

In every sections of your document

· Use standard writing style including articles ("a", "the," etc.)

· Keep on paying attention on the research topic of the paper

· Use paragraphs to split each significant point (excluding for the abstract)

· Align the primary line of each section

· Present your points in sound order

· Use present tense to report well accepted

· Use past tense to describe specific results

· Shun familiar wording, don't address the reviewer directly, and don't use slang, slang language, or superlatives

· Shun use of extra pictures - include only those figures essential to presenting results

Title Page:

Choose a revealing title. It should be short. It should not have non-standard acronyms or abbreviations. It should not exceed two printed lines. It should include the name(s) and address (es) of all authors.

Abstract:

The summary should be two hundred words or less. It should briefly and clearly explain the key findings reported in the manuscript--must have precise statistics. It should not have abnormal acronyms or abbreviations. It should be logical in itself. Shun citing references at this point.

An abstract is a brief distinct paragraph summary of finished work or work in development. In a minute or less a reviewer can be taught the foundation behind the study, common approach to the problem, relevant results, and significant conclusions or new questions.

Write your summary when your paper is completed because how can you write the summary of anything which is not yet written? Wealth of terminology is very essential in abstract. Yet, use comprehensive sentences and do not let go readability for briefness. You can maintain it succinct by phrasing sentences so that they provide more than lone rationale. The author can at this moment go straight to shortening the outcome. Sum up the study, with the subsequent elements in any summary. Try to maintain the initial two items to no more than one ruling each.

- Reason of the study - theory, overall issue, purpose
- Fundamental goal
- To the point depiction of the research
- Consequences, including definite statistics - if the consequences are quantitative in nature, account quantitative data; results of any numerical analysis should be reported
- Significant conclusions or questions that track from the research(es)

Approach:

- Single section, and succinct
- As a outline of job done, it is always written in past tense
- A conceptual should situate on its own, and not submit to any other part of the paper such as a form or table
- Center on shortening results - bound background information to a verdict or two, if completely necessary
- What you account in an conceptual must be regular with what you reported in the manuscript
- Exact spelling, clearness of sentences and phrases, and appropriate reporting of quantities (proper units, important statistics) are just as significant in an abstract as they are anywhere else

Introduction:

The **Introduction** should "introduce" the manuscript. The reviewer should be presented with sufficient background information to be capable to comprehend and calculate the purpose of your study without having to submit to other works. The basis for the study should be offered. Give most important references but shun difficult to make a comprehensive appraisal of the topic. In the introduction, describe the problem visibly. If the problem is not acknowledged in a logical, reasonable way, the reviewer will have no attention in your result. Speak in common terms about techniques used to explain the problem, if needed, but do not present any particulars about the protocols here. Following approach can create a valuable beginning:

- Explain the value (significance) of the study
- Shield the model - why did you employ this particular system or method? What is its compensation? You strength remark on its appropriateness from a abstract point of vision as well as point out sensible reasons for using it.
- Present a justification. Status your particular theory (es) or aim(s), and describe the logic that led you to choose them.
- Very for a short time explain the tentative propose and how it skilled the declared objectives.

Approach:

- Use past tense except for when referring to recognized facts. After all, the manuscript will be submitted after the entire job is done.
- Sort out your thoughts; manufacture one key point with every section. If you make the four points listed above, you will need a least of four paragraphs.

- Present surroundings information only as desirable in order hold up a situation. The reviewer does not desire to read the whole thing you know about a topic.
- Shape the theory/purpose specifically - do not take a broad view.
- As always, give awareness to spelling, simplicity and correctness of sentences and phrases.

Procedures (Methods and Materials):

This part is supposed to be the easiest to carve if you have good skills. A sound written Procedures segment allows a capable scientist to replacement your results. Present precise information about your supplies. The suppliers and clarity of reagents can be helpful bits of information. Present methods in sequential order but linked methodologies can be grouped as a segment. Be concise when relating the protocols. Attempt for the least amount of information that would permit another capable scientist to spare your outcome but be cautious that vital information is integrated. The use of subheadings is suggested and ought to be synchronized with the results section. When a technique is used that has been well described in another object, mention the specific item describing a way but draw the basic principle while stating the situation. The purpose is to text all particular resources and broad procedures, so that another person may use some or all of the methods in one more study or referee the scientific value of your work. It is not to be a step by step report of the whole thing you did, nor is a methods section a set of orders.

Materials:

- Explain materials individually only if the study is so complex that it saves liberty this way.
- Embrace particular materials, and any tools or provisions that are not frequently found in laboratories.
- Do not take in frequently found.
- If use of a definite type of tools.
- Materials may be reported in a part section or else they may be recognized along with your measures.

Methods:

- Report the method (not particulars of each process that engaged the same methodology)
- Describe the method entirely
- To be succinct, present methods under headings dedicated to specific dealings or groups of measures
- Simplify - details how procedures were completed not how they were exclusively performed on a particular day.
- If well known procedures were used, account the procedure by name, possibly with reference, and that's all.

Approach:

- It is embarrassed or not possible to use vigorous voice when documenting methods with no using first person, which would focus the reviewer's interest on the researcher rather than the job. As a result when script up the methods most authors use third person passive voice.
- Use standard style in this and in every other part of the paper - avoid familiar lists, and use full sentences.

What to keep away from

- Resources and methods are not a set of information.
- Skip all descriptive information and surroundings - save it for the argument.
- Leave out information that is immaterial to a third party.

Results:

The principle of a results segment is to present and demonstrate your conclusion. Create this part a entirely objective details of the outcome, and save all understanding for the discussion.

The page length of this segment is set by the sum and types of data to be reported. Carry on to be to the point, by means of statistics and tables, if suitable, to present consequences most efficiently.You must obviously differentiate material that would usually be incorporated in a study editorial from any unprocessed data or additional appendix matter that would not be available. In fact, such matter should not be submitted at all except requested by the instructor.

Content

- Sum up your conclusion in text and demonstrate them, if suitable, with figures and tables.
- In manuscript, explain each of your consequences, point the reader to remarks that are most appropriate.
- Present a background, such as by describing the question that was addressed by creation an exacting study.
- Explain results of control experiments and comprise remarks that are not accessible in a prescribed figure or table, if appropriate.
- Examine your data, then prepare the analyzed (transformed) data in the form of a figure (graph), table, or in manuscript form.

What to stay away from

- Do not discuss or infer your outcome, report surroundings information, or try to explain anything.
- Not at all, take in raw data or intermediate calculations in a research manuscript.
- Do not present the similar data more than once.
- Manuscript should complement any figures or tables, not duplicate the identical information.
- Never confuse figures with tables - there is a difference.

Approach

- As forever, use past tense when you submit to your results, and put the whole thing in a reasonable order.
- Put figures and tables, appropriately numbered, in order at the end of the report
- If you desire, you may place your figures and tables properly within the text of your results part.

Figures and tables

- If you put figures and tables at the end of the details, make certain that they are visibly distinguished from any attach appendix materials, such as raw facts
- Despite of position, each figure must be numbered one after the other and complete with subtitle
- In spite of position, each table must be titled, numbered one after the other and complete with heading
- All figure and table must be adequately complete that it could situate on its own, divide from text

Discussion:

The Discussion is expected the trickiest segment to write and describe. A lot of papers submitted for journal are discarded based on problems with the Discussion. There is no head of state for how long a argument should be. Position your understanding of the outcome visibly to lead the reviewer through your conclusions, and then finish the paper with a summing up of the implication of the study. The purpose here is to offer an understanding of your results and hold up for all of your conclusions, using facts from your research and generally accepted information, if suitable. The implication of result should be visibly described. Infer your data in the conversation in suitable depth. This means that when you clarify an observable fact you must explain mechanisms that may account for the observation. If your results vary from your prospect, make clear why that may have happened. If your results agree, then explain the theory that the proof supported. It is never suitable to just state that the data approved with prospect, and let it drop at that.

- Make a decision if each premise is supported, discarded, or if you cannot make a conclusion with assurance. Do not just dismiss a study or part of a study as "uncertain."
- Research papers are not acknowledged if the work is imperfect. Draw what conclusions you can based upon the results that you have, and take care of the study as a finished work
- You may propose future guidelines, such as how the experiment might be personalized to accomplish a new idea.
- Give details all of your remarks as much as possible, focus on mechanisms.
- Make a decision if the tentative design sufficiently addressed the theory, and whether or not it was correctly restricted.
- Try to present substitute explanations if sensible alternatives be present.
- One research will not counter an overall question, so maintain the large picture in mind, where do you go next? The best studies unlock new avenues of study. What questions remain?
- Recommendations for detailed papers will offer supplementary suggestions.

Approach:

- When you refer to information, differentiate data generated by your own studies from available information
- Submit to work done by specific persons (including you) in past tense.
- Submit to generally acknowledged facts and main beliefs in present tense.

Please carefully note down following rules and regulation before submitting your Research Paper to Global Journals Inc. (US):

Segment Draft and Final Research Paper: You have to strictly follow the template of research paper. If it is not done your paper may get rejected.

- The **major constraint** is that you must independently make all content, tables, graphs, and facts that are offered in the paper. You must write each part of the paper wholly on your own. The Peer-reviewers need to identify your own perceptive of the concepts in your own terms. NEVER extract straight from any foundation, and never rephrase someone else's analysis.

- Do not give permission to anyone else to "PROOFREAD" your manuscript.

- Methods to avoid Plagiarism is applied by us on every paper, if found guilty, you will be blacklisted by all of our collaborated research groups, your institution will be informed for this and strict legal actions will be taken immediately.)
- To guard yourself and others from possible illegal use please do not permit anyone right to use to your paper and files.

Criterion for Grading a Research Paper (Compilation) by Global Journals Inc. (US)

Please note that following table is only a Grading of "Paper Compilation" and not on "Performed/Stated Research" whose grading solely depends on Individual Assigned Peer Reviewer and Editorial Board Member. These can be available only on request and after decision of Paper. This report will be the property of Global Journals Inc. (US).

Topics	Grades		
	A-B	**C-D**	**E-F**
Abstract	Clear and concise with appropriate content, Correct format. 200 words or below	Unclear summary and no specific data, Incorrect form Above 200 words	No specific data with ambiguous information Above 250 words
Introduction	Containing all background details with clear goal and appropriate details, flow specification, no grammar and spelling mistake, well organized sentence and paragraph, reference cited	Unclear and confusing data, appropriate format, grammar and spelling errors with unorganized matter	Out of place depth and content, hazy format
Methods and Procedures	Clear and to the point with well arranged paragraph, precision and accuracy of facts and figures, well organized subheads	Difficult to comprehend with embarrassed text, too much explanation but completed	Incorrect and unorganized structure with hazy meaning
Result	Well organized, Clear and specific, Correct units with precision, correct data, well structuring of paragraph, no grammar and spelling mistake	Complete and embarrassed text, difficult to comprehend	Irregular format with wrong facts and figures
Discussion	Well organized, meaningful specification, sound conclusion, logical and concise explanation, highly structured paragraph reference cited	Wordy, unclear conclusion, spurious	Conclusion is not cited, unorganized, difficult to comprehend
References	Complete and correct format, well organized	Beside the point, Incomplete	Wrong format and structuring

INDEX

Global Journal of Science Frontier Research

Visit us on the Web at www.GlobalJournals.org | www.JournalofScience.org
or email us at helpdesk@globaljournals.org

ISSN 9755896